THE SOLUBILITY OF ALUMINIUM IN MELTS CONTAINING ALUMINIUM HALIDES

A Thesis

presented for the degree of

Doctor of Philosophy

in the

University of London

by

John Dyson Usher

London, May 1965

ABSTRACT

A technique for measuring the solubility of aluminium in $NaF-AlF_3$ and $NaF-AlF_3+5\%Al_2O_3$ melts has been developed using a refractory titanium boride-carbide crucible and a gas volumetric method of analysis.

Experiments were conducted at 1020, 1100 and 1180°C; in both systems no change in solubility limit was detected over the experimental composition range of 25.6 - 36.6 and 25.8 - 31.9 mol % AlF_3 respectively.

The figures in the pure fluoride are 0.022 0.041 and 0.072 wt %; in the alumina melts 0.073, 0.121 and 0.169 wt %.

Solution mechanisms have been suggested which account for the observed behaviour, and an attempt has been made to interpret the current inefficiency process in the reduction cell in terms of the results.

CONTENTS

CHAPTER I

INTRODUCTION

1.1. ALUMINIUM REDUCTION CELL - BRIEF DESCRIPTION

The cell is a shallow carbon-lined container insulated at the sides and base and contained in a steel box structure. The cathodic connection is made by iron bars buried in the bottom, and the anodic connection is made by steel pins embedded in either a series of prebaked carbon blocks or 'Söderberg' self-baking blocks of carbon paste, which dip into bath.

In normal practice the electrolyte consists of molten cryolite containing 5-15% CaF_2 and 1-5% alumina. The bath is about 12 inches deep, and is covered by a crust of frozen electrolyte and alumina, which diminishes heat losses and protects the anode from atmospheric oxidation. At the operating temperature of 950-1000°C, aluminium is denser than the melt and forms a layer (or 'pad') of molten metal on the cell floor which acts as the cathode throughout the working life of the furnace. A gas mixture containing 70-90% CO_2 and 10-30% CO is evolved from the carbon anode. The anode-cathode distance is maintained at a constant value (1½-2 inches) by lowering the blocks steadily as carbon is consumed.

Because of a continuous back reaction, current efficiencies vary between 80-90% and because of lead and contact resistances the voltage efficiencies are no

more than 40-50%. The overall energy efficiency is about 35%. The remainder of the electrical input maintains the furnace at its operating temperature and is dissipated as heat.

As electrolysis proceeds the alumina content gradually falls to about 0.5%. At this concentration a small amount of fluorine begins to be deposited at the anode surface, producing an insulating film which forms quite suddenly and prevents the electrolyte from wetting the carbon blocks. The voltage of the furnace then rises immediately to 30-50v and the current is carried by numerous small arcs between the carbon block and the electrolyte. This is known as the "up" condition. Normal or 'down' running is resumed by stirring in part of the alumina crust. Times between 'ups' vary between 6-12 hours.

Metal accumulates in a 100kA furnace at the rate of 1600 lb per day, and portions of the pad are withdrawn by suction at regular intervals.

There are at the present time a number of unsolved problems regarding the cell process - one of the most important being the mechanism of the current inefficiency reaction. This study has been directed to achieve a greater understanding of the factors involved in this aspect of the process.

1.2 CURRENT EFFICIENCY

1.2.1. Measurement

The current efficiency of the reduction cell electrolysis is the ratio of the number of equivalents of aluminium metal produced to the number of equivalents calculated from Faraday's law. An average value can thus be obtained by recording the weight of metal tapped and the cell electrical consumption over a set period. In practice however, the weight of the daily tap is small compared to the reserve remaining in the bath and even over periods of up to several weeks the true metal yield may not be accurately obtained. For this reason it is desirable to know the metal content of the cell at the beginning and end of the measurement.

A method which has been successfully developed in a number of industrial plants has been described by Smart.(1) A small known weight of copper is added to the bath and the weight of metal present calculated from a determination, by chemical analysis, of the increase in copper content. The use of radio-active isotopes,(3) and a post-irradiation technique(2) for determining reserve metal have also been reported.

Pearson and Waddington(4) carried out a series of laboratory scale electrolyses on a cryolite melt containing

5% Al_2O_3 and 15% CaF_2. The anode material was well-baked dense carbon or graphite. It was found that the measured anode weight loss was approximately the same as that calculated from Faraday's law assuming the product to be exclusively CO_2. It was therefore concluded that CO_2 was the primary anode product and that the deficiency in CO_2 content of the anode gas was due to recombination of the original electrode products to give alumina and carbon monoxide according to the reaction.

$$2\ Al + 3\ CO_2 = Al_2O_3 + 3\ CO \quad \ldots \quad 1.2(i)$$

On this basis the oxygen in the gases passing out of the industrial furnace is equivalent to the actual metal yield, and it can be shown that

$$\text{current efficiency} = \tfrac{1}{2}(CO_2 \text{ per cent of anode gas}) + 50 \quad \ldots \quad 1.2(ii)$$

This expression enables instantaneous current efficiencies to be determined from an analysis of the anode gas and provides an independent check on current efficiencies determined directly. However in experiments on a 10 kA cell, Beck[5] showed that the per cent CO_2 increased with increasing anode bake

temperature whilst at the same time the current efficiency did not alter significantly. A modification of equation 1.2(ii) was presented which took into consideration losses without the involvement of CO_2 and the possible reaction of CO_2 with carbon, and which fitted the data more satisfactorily. A further refinement has been developed by Hamlin and Richards[6] who included a correction due to contamination by a small amount of atmospheric gases. These authors showed that the use of gas analysis in determining current efficiencies, and thus in the operational control of cells was justified.

1.2.2. Cell Variables and Current Efficiency

No quantitative expression relating the cell operating variables to current efficiency has yet been derived. However, it is well-known that current efficiency decreases with increasing temperature and also decreases with increasing sodium fluoride content and with decreasing distance between anode and the aluminium surface. It may also be adversely affected by a fall in current density and by a reduction in the bath alumina content. The absolute value at any one instance depends in addition on the thermal and composition history of the electrolyte and on design

factors of the cell.

1.2.3. Postulated Mechanisms of Metal Loss

Despite significant deviations from the Pearson Waddington equation under industrial conditions, it is generally accepted that the reaction 1.2(i) accounts for the major part of the metal loss. This assumption is supported by long-term metal and alumina inventories which show that 99% of the metal in alumina is recovered.(7) It should however be noted that the equation merely describes the overall re-oxidation process, and does not necessarily mean that the reacting species are aluminium metal and CO_2 gas.

In general terms there are two possible kinds of process which account for the fact that aluminium losses are equivalent to the CO_2 deficiency. The first arises from a reaction between the molten aluminium and the electrolyte at the cathode surface. This may take the form of dissolution of aluminium (or some product of a reaction between cryolite and aluminium) and its subsequent migration to and re-oxidation at the anode. It is also conceivable that a gaseous product might be formed, but this is unlikely to be a significant factor since escape from the furnace could occur without involvement in a reaction with CO_2.

The second possibility arises from an anode reaction. CO_2 might dissolve in the bath and be reduced to CO or carbon at the cathode. Indeed, both processes might occur simultaneously.

Many different mechanisms have in fact been suggested. These were critically reviewed by Grjotheim[8] in 1956 in the light of experimental and thermodynamic data then available. Since then additional information has been published and further discussion is included in section 1.6.

1.3. ORIGINS OF PRESENT WORK

1.3.1. Information Required

Despite the exclusive use of Hall-Héroult type cells in the aluminium industry for nearly eighty years, progress in understanding the reduction process has been slow and has largely been confined to the past decade. The major obstacle has been the unavailability (until recently) of container materials highly resistant to the action of molten cryolite and aluminium.

With regard to the solvent properties of cryolite a number of investigations have been reported. Førland, Storegraven and Urnes[9] measured the solubility of CO_2 in molten cryolite, and their figure was later confirmed by Haupin,[56] who found 21 µg. dissolved in a 10 g. sample

of molten electrolyte. It is shown later in Chapter 4 that this extent of CO_2 dissolution is very unlikely to be the sole cause of current inefficiency. Reliable information on the nature and extent of the metal-cryolite reaction is thus of great importance in understanding the cell inefficiency process and in achieving optimum working performance.

However, no systematic studies of this reaction have yet been made. Furthermore the results of independent experiments are widely discrepant and the interpretation thereof is in nearly all cases open to serious objections (see section 1.7). It has not therefore been possible to assess quantitatively the contribution to current inefficiency of metal dissolution in the electrolyte.

As mentioned above the current efficiency falls as the cell temperature rises, and this could be caused by an enhanced solubility of aluminium (or a product of an aluminium-cryolite reaction such as sodium) in the melt. In addition the low efficiencies noted in NaF - enriched melts could be explained in terms of increased sodium activity and dissolution. Variation of the alumina content might also affect the cryolite-aluminium equilibrium. Again an alteration of the

anode-cathode distance could cause a change in the effective rate of migration of dissolved species, and therefore of the re-oxidation process.

Data on the solubility of aluminium (or a product of an aluminium-cryolite reaction) in cryolite with respect to temperature, NaF/AlF_3 ratio and alumina content is therefore needed and is the aim of the experimental programme of this work.

1.3.A PRELIMINARY THEORETICAL APPROACH

It is possible to gain an insight into the process of aluminium dissolution in cryolite by a comparison with other systems whose nature and properties have been established. However, the majority of solutions examined have been of a metal dissolved in one of its own halides, and in the aluminium-cryolite system a novel situation could arise from the displacement equilibrium

$$Al + 3NaF \text{ (in melt)} = AlF_3 \text{ (in melt)} + 3Na \quad \ldots 1.3(i)$$

and the consequent possibility of sodium dissolution in the melt. Furthermore, cryolite has long been known to dissociate on fusion, and, unlike the single metal halides which in most cases can be considered to consist of short range ordered metal cations and halide

anions, speculation still continues on the nature and concentration of its ionic constituents.

In the presence of alumina a reaction of the type

$$4\ Al + Al_2O_3 = 3\ Al_2O \qquad \ldots\ \ldots\ 1.3(ii)$$

might occur to a significant extent, and the cryolite dissociation and thus equilibrium 1.3(i) might be disturbed through association or breakdown of the original ions.

Thus, in addition to a discussion of metal-molten salt solutions in Section 1.4, the present state of knowledge of the structure of pure cryolite and cryolite-alumina melts is reviewed in Section 1.5, and the significance of reaction 1.3(i) is assessed in the light of available thermodynamic data in Section 1.6. Previous attempts at measuring the solubility of aluminium in cryolite are then summarised and the techniques employed criticised in each case.

Because of the industrial application of this investigation it is profitable to estimate what magnitude of solubility could cause the current inefficiences normally encountered in the commercial cell. As a result considerations of heat and mass transport are dealt with in Chapter 4.

1.4. METAL - MOLTEN SALT SOLUTIONS

1.4.1. General

The phenomenon of true metal solutions in molten salts has long been recognised and systematic studies have been carried out on the metal groups I [11-15] and II [16-18], the rare earths [10, 28, 30, 33, 38], Cd [19-21] and Bi [22,23] and their halides. Data on other systems have also been published, and recently the whole field has been surveyed in detail independently by Bredig[26] and Corbett.[27]

Bredig et al. studied the solubility of the alkali metals in their halides, and reported the phase diagrams of the Na-NaX, [11, 12], K-KX [14], Rb-RbX [15] and Cs-CsX [13] systems (X=F, Cs, Br, I). Cooling curves and quenching techniques were used to detect the phase boundary compositions.

The phase diagram for the Na-NaF system (figure 1) is typical of all the Na, K and Rb systems (except for Rb-RbBr) in that there is a liquid miscibility gap and a monotectic on the salt rich side.

Rogers[17] determined the diagram of Ca-CaF_2 (figure 2). Again there is a miscibility gap and a monotectic. In fact the alkaline earth metal systems (Ca, Sr, Ba) are qualitatively similar to those of the

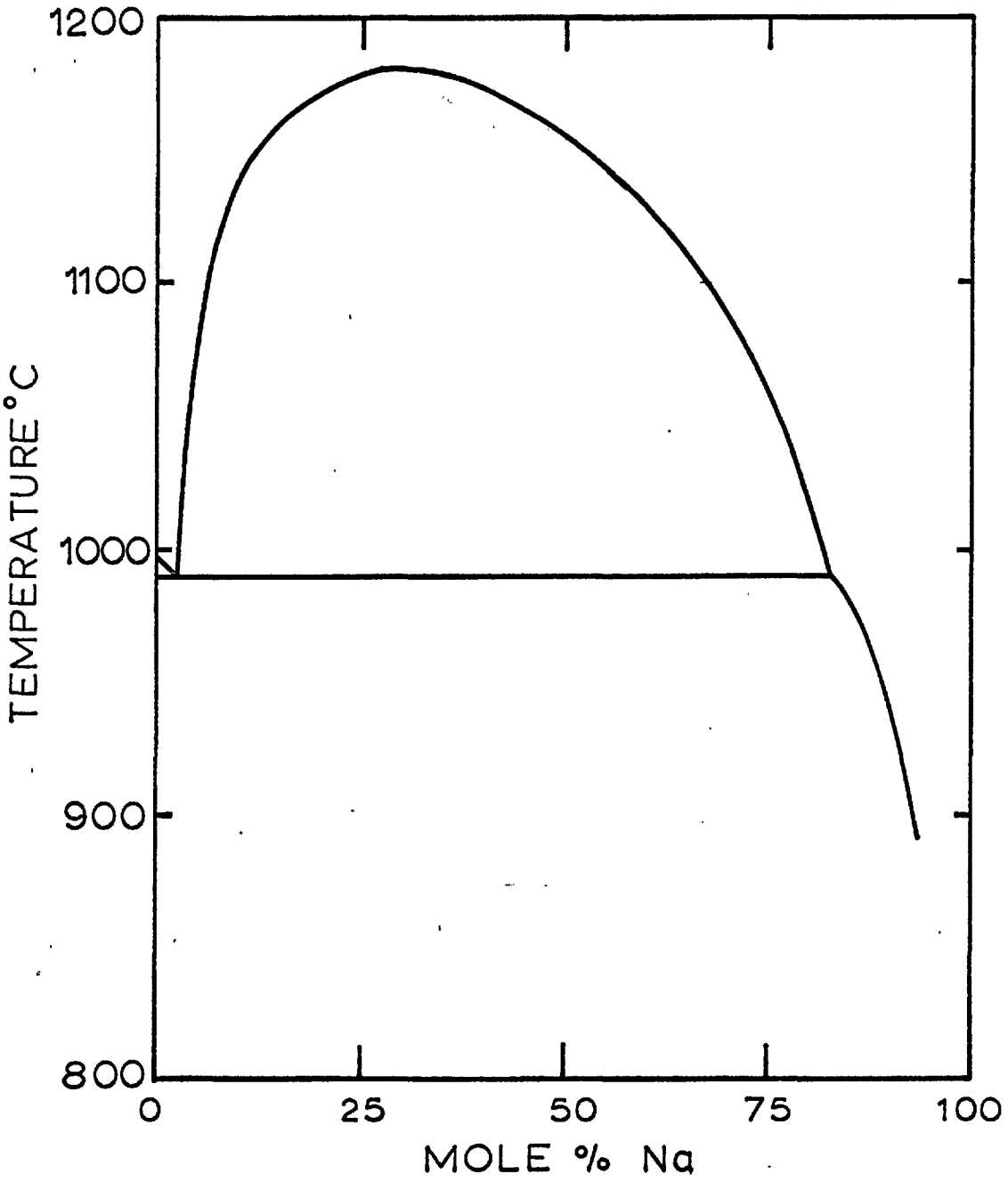

FIG. 1 PHASE DIAGRAM Na-NaF (Bredig [12]

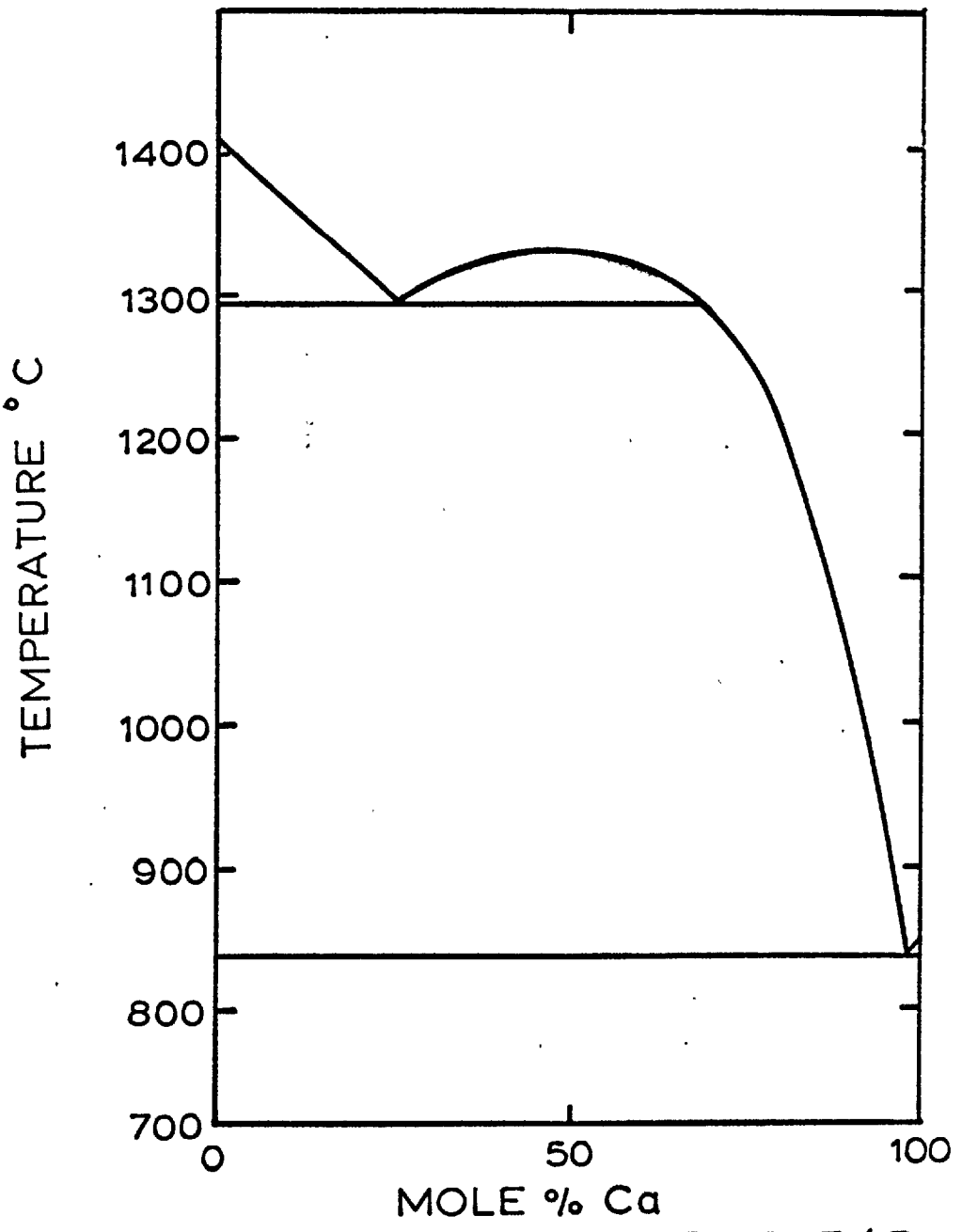

FIG. 2 PHASE DIAGRAM Ca-CaF_2 (Rogers [17])

alkali metals.

In group IIB, Zn, Cd and Hg solubilities in their respective chlorides have been investigated and are shown together with halide systems of a number of metals belonging to other groups of the periodic table (table 1, p. 15). Values vary from 10^{-7} mol % for Al in $AlCl_3$ at 230°C to complete miscibility in the Bi-BiI_3 system at 458°C.

Within each group the tendency towards miscibility increases with increasing atomic weight of the metal, and of the halogen

$$(F) < Cl < Br < I$$

for all halide systems except those of cadmium where $I < Cl \leq Br$ and the alkali metals for which the trend is $I \leq Cl < Br < F$. Apart from the alkali and alkaline earth metals, no data has been published on fluoride solutions.

The solution process is apparently specific; that is, dissolution of one metal in the salt of another and more reactive metal is very small indeed - in the case of Pb in $CaCl_2$ it cannot be detected. In the reverse system (Ca-$PbCl_2$) an oxidation reduction reaction is superimposed on the process of interest.[27] When two

TABLE I

Solubility of Metals in their Halides

Group	System	Temp. °C	Solubility Mol%	M.Pt Salt°C	B.Pt Salt°C	Reference
IB	Ag-AgCl	700	0.06	455	1564	24
IIB	Zn-$ZnCl_2$	500	0.18	326	732	29
		700	1.64			
	Cd-$CdCl_2$	550	14.0	568	960	19
	Hg-$HgCl_2$	280	7.0	277	304	25
		500	40.0			
IIIB	Al-$AlCl_3$	230	10^{-7}	subl.	180	31
	Al-AlI_3	230	0.02	191	383	29
		423	0.3			24
	Ga-$GaCl_2$	180	1.92	171		24
	In-$InCl_2$	230	50.0	235	485	29
	Tl-TlCl	550	0.009	429	816	24
IVB	Sn-$SnCl_2$	500	0.0032	247	652	24
	Sn-$SnBr_2$	500	0.068	232	640	24
	Pb-$PbCl_2$	700	0.020	498	954	32
	Pb-PbI_2	700	0.41	412	872	29
VB	Sb-SbI_3	200	1.69	170	400	24
	Bi-$BiCl_3$	202	28.0	230	441	22
	Bi-BiI_3	336	48.0	408		22
		458	100.0			

halides have similar standard free energies of formation ($Ca-BaCl_2$;[43] Na-KCl) a metal (alloy) rich phase and a mixed salt containing an excess of both metals may be formed. In such a case the metals at activities < 1 may be considered to be dissolved in their respective salts whose activities are also < 1.

1.4.2. Nature of Metal - Molten Salt Solutions

No generally accepted theory has yet been developed. The question as to why there is complete miscibility is some systems and only very slight miscibility in others is not fully understood. Even the superficially similar systems K-KCl and Na-NaCl exhibit such differences in conductance behaviour that it has been necessary to postulate quite different solution models to account for them.

Bredig[26] classifies metal solutions in molten halides according to two main types:

(a) 'metallic' solutions whose properties reflect the presence of mobile electrons and whose principal feature is an increase in specific conductance with dissolved metal content and a positive temperature coefficient of conductivity up to high metal concentrations. The alkaline earth and rare earth systems fall into this group, but the alkali metal

systems are the most typical. Here it has been suggested that the electrons are bound in anion vacancies analogous to F-centres in the solid state.

(b) "sub-halide" solutions where there is a strong interaction (i.e. oxidation - reduction reaction) between the metal and the salt; the metal assuming a lower than normal valency. The specific conductance of the salt is not increased, if altered at all, on the addition of metal. This group may be sub-divided into (i) systems in which the "sub-halide" is of high enough stability to crystallise as a separate phase and (ii) systems in which the lower valence state of the metal is only stable in the molten solution, which at saturation is in equilibrium with the metal itself. Bi in $BiCl_3$ and Cd in $CdCl_2$ are examples of these respective sub-groups.

The division between the two main types is not clear cut and both mechanisms of dissolution may apply to a single system. The distinction is that between relatively mobile electrons and electrons which attach themselves to, and become part of, ions of a lower valence state. Intermediate cases are likely in which the attachment of electrons may be a matter of degree only, rather than that of an equilibrium between two

distinctly different states.

Even in the alkali metal systems the discreet solute Na_2^+, K_2^+ has been postulated to explain the positive deviation from ideality of the freezing point depression of the halide by the metal. Bredig[11] et al. suggested the equilibrium

$$M_2^{\circ} + 2\ M^+ = 2\ M_2^+ \qquad \ldots\ \ldots\ 1.4(i)$$

for a very dilute solution of sodium in sodium chloride near the melting point of the salt. Such a species may be considered to arise from an F-centre paired with an adjacent anion vacancy; the interaction of the electron with the two interposed and less shielded cations amounting to a weakly bound M_2^+. The presence of Na_2 (which is known to exist in the vapour state) in the melt was suggested from conductivity measurements below the consolute temperature up to the metal saturation limit.[34] This dimer could result from a combination of F-centres to give electrons with spins paired, in adjacent holes. In a 1:2 salt MX_2, molecule ions such as Cd_2^{2+}, Ca_2^{2+} could arise from a similar combination of F-centres, but with one half the cation sites empty. Cryoscopic measurements on the alkaline earth metal halides can be interpreted in terms of these species,[17]

and the diamagnetism[40,39] of some solutions also indicates a preponderance of sites with paired electrons.

1.4.3. Extent of Solubility

In type (a) salt rich solutions the postulated model for the solvated metal electrons explains to a certain extent the electrical properties and freezing point depressions, but not the wide variations in the saturation limits between different systems.

An illuminating view point[45] can be obtained by considering the properties of the metal, or metal rich phase with which the salt rich phase in in equilibrium.

The dissolution process may be divided into three steps

metal → atoms 1.

atoms → ions + electrons 2.

electrons → electrons trapped in melt 3.

Neglecting the modification of the metal by the salt it dissolves, the energy for the first step is approximately the heat of evaporation of the metal. The energy of the second step is given by the ionization potential. The energy of the third step is unknown. The heats of vaporisation and ionization potentials of some metals

are compared with the solubilities or monotectic compositions in Table IIA. It is seen that in the alkali metal chlorides, as expected, the solubility increases as the heat of vaporisation of the metal decreases and as the ionization potential decreases. By comparison silver and thallium both have higher heats of vaporisation and ionisation potentials, and the solubilities are very much lower. Tin and lead have much higher heats of vaporisation than the alkaline earth metals and high ionisation potentials, and again have very low solubilities. Even neglecting the final step 3 of the process it is evident that a general pattern of behaviour is obtained simply by considering the differences in properties of the metals themselves.

If the same reasoning were applied to aluminium dissolution in aluminium fluoride then a very small solubility would be expected in view of the very high heat of evaporation of the metal (69.6 kcal/g. atom) and its high ionisation potential (5.95v).

In this system however it is much more likely that the solution would fall into category (b). Aluminium monofluoride is known to exist in the gaseous state, and an equilibrium of the form

TABLE IIA

Solubility of Metals in their Chlorides[45]

Metal	ΔH_v At T_b kcal/g.atm	1st Ionisation Pot[1]. volts	Metal Solubility or Monotectic Compn. mol per cent	T°C
Li	35.3	5.37	0.5	610
Na	23.7	5.12	2.1	795
K	18.9	4.32	10.5	751
Rb	18.1	4.16	18.0	696
Cs	15.9	3.88	miscible	-
Mg	30.5	7.61	0.2	714
Ca	39.9	6.09	2.7	820
Sr	36.9	5.87	5.5	839
Ba	(36.7)	5.19	15.0	878
Ag	60.0	7.54	0.06	700
Tl	39.7	6.07	0.009	600
Sn	64.7	7.37	0.003	500
Pb	42.5	7.39	0.02	700

$$2\ M + MX_3 = 3\ MX \quad \ldots \quad \ldots \quad 1.4(ii)$$

would be expected to describe the magnitude of solubility. The greater the stability of the condensed sub-halide relative to the tri-halide, the greater would be the dissolution of metal. As AlF is unknown in a condensed condition, its extent of solution in the liquid trifluoride is a matter of conjecture. A qualitatively useful comparison can however be made between the chlorides of group IIIB metals. Figures for the standard free energies of formation of the mono- and trivalent salts are shown in Table IIB. The monochlorides become increasingly stable with increase in atomic weight of the metal.

TABLE IIB

Stabilities of Chlorides of Group IIIB Metals

Metal	ΔG^{o}_{298} per $\frac{1}{2}$ mol chlorine			Solubility of metal in MCl_3 (mol %)	Temp°C
	MCl	MCl_2	MCl_3		
Al	-17(gas)		-45	10^{-7}	230
Ga	-5 (gas)		-37		
In	-43	-40	-37		
Tl	-45		-23	50.0	230

1.4.4. Effect of Foreign Ions on Metal Solubility

This is a phenomenon of great importance to the present study in which NaF could affect the Al-AlF_3 equilibrium and AlF_3 the Na-NaF equilibrium by altering the activity coefficients of the dissolved species. However the literature on the subject is relatively meagre and is limited to the effect of foreign cations.

Cubiciotti[35] studied the effect of adding KCl, $CaCl_2$, $MgCl_2$ and $CeCl_3$ on the solubility of cadmium in $CdCl_2$. It was suggested that the larger chloride ions were effectively close-packed, so that the cations of the salt (and any dissolved metal) occupied octahedral holes in the loose anion structure. Thus the bigger the numerical ratio of cations to anions in the foreign salt, the smaller would be the number of holes available to the dissolving metal, in agreement with the observed trend of

$$KCl > CaCl_2 > CeCl_3$$

in decreasing the solution of Cd in $CdCl_2$. The ratio of Cd to $CdCl_2$ in the salt phase actually increased on addition of $CeCl_3$, whilst an equimolar solution of KCl-$CdCl_2$ was found to dissolve only about 15% as much metal as the pure dichloride. Differences in the

effect of various divalent chlorides added ($Ca^{2+} > Mg^{2+} > Mn^{2+}$) were attributed to an increase in the energy of the band occupied by the electrons of the metal - the more electropositive metals having a greater depressing effect.

Ukshe[36] described the influence of foreign cations in terms of their polarising power*. Potassium and calcium ions have a lower polarising power than cadmium, and thus decrease the solubility essentially by increasing the energy of the Cd^{2+}-Cl^{-} bond. On the other hand magnesium and cerium, whose polarising powers are higher than cadmium, by weakening the Cd^{2+}-Cl^{-} bond decrease the solubility in the salt phase to a much lesser extent. Similar results were obtained in a study of Bi in $BiCl_3$ in the presence of NaCl and $CaCl_2$. Na^{+} with a lower polarising power than bismuth decreased the solubility to a greater extent than Ca^{2+}.[112]

Thus a marked depression of aluminium solution in aluminium fluoride could be expected on addition of sodium fluoride. On the other hand a much smaller depression of sodium dissolution in NaF by AlF_3 might

---

*The polarising powers of Cd^{2+}, K^{+}, Ca^{2+}, Mg^{2+}, Ce^{3+} are 1.9, 0.56, 1.76, 3.78 and 2.94 respectively.

be expected because of the high polarising power of Al^{3+}.

The mechanism and extent of aluminium solubility in cryolite is further discussed in Chapter 4.

1.5 STRUCTURE OF CRYOLITE AND CRYOLITE-ALUMINA MELTS

1.5.1 Pure Molten Cryolite

Cryolite has long been known to undergo some decomposition on melting. That this is so is immediately evident from the $NaF-AlF_3$ phase diagram (figure 3) in which the liquidus curve at the Na_3AlF_6 peak is somewhat flattened.

Pearson and Waddington[4] presented evidence for partial dissociation to sodium fluoride and aluminium fluoride (or their ions). The variation of density of sodium fluoride-aluminium fluoride melts indicated dissociation of 20% at 1000°C and 30% at 1100°C according to the proposed reaction

$$Na_3AlF_6 = 3\ NaF + AlF_3 \quad \ldots \quad \ldots \quad 1.5(i)$$

Additivity of molar volumes was assumed, and the densities of undissociated cryolite and pure aluminium fluoride were estimated by extrapolation.

However more recently Pearson[7] calculated equilibrium constants of 1.7×10^{-5} and 4.6×10^{-5} at

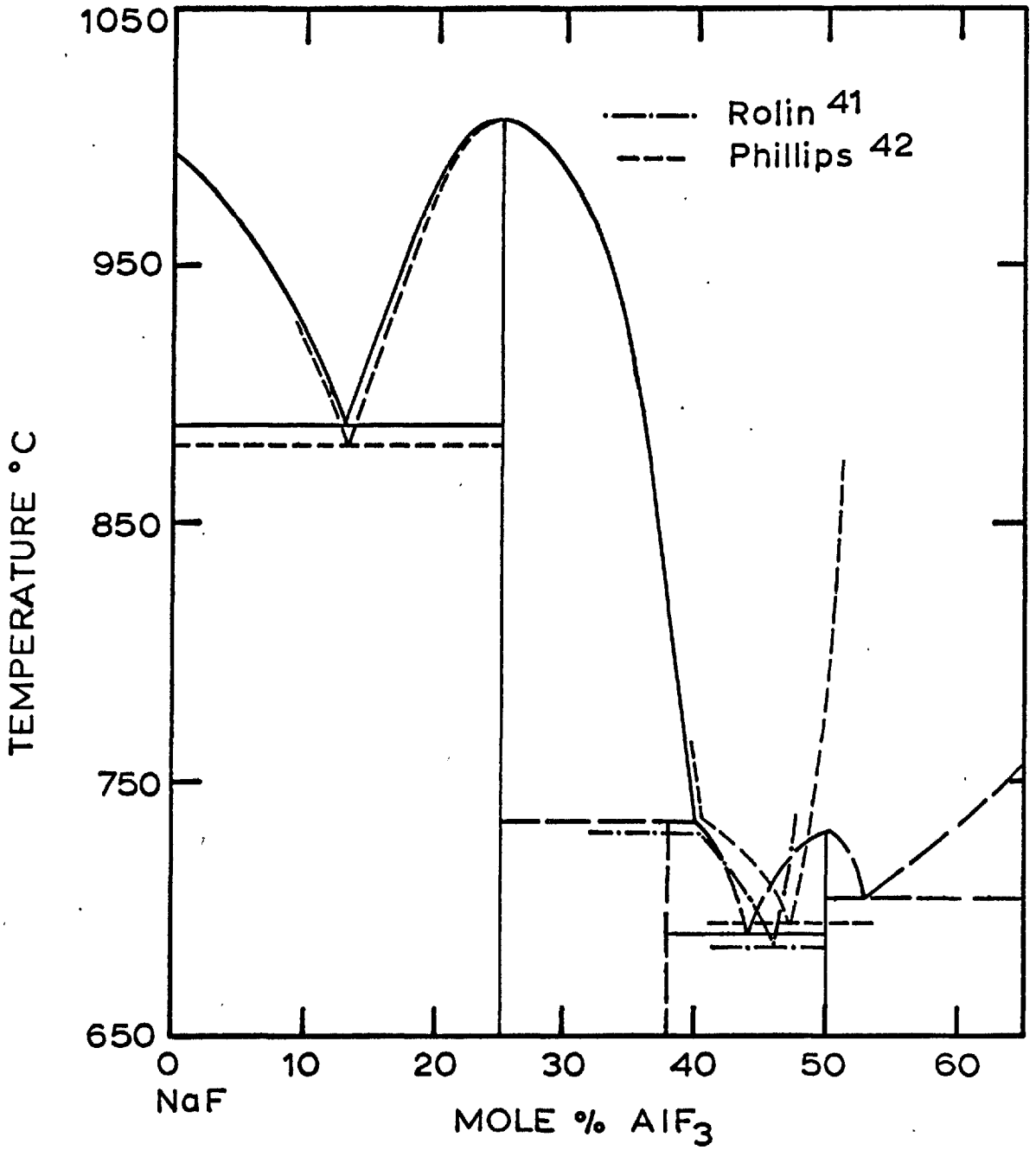

FIG. 3 PHASE DIAGRAM NaF-AlF_3 (Grjotheim 8)

1000°C and 1100°C respectively for reaction 1.5(i). These revised values were too low to account for the position and shape of the density maxima of the system. Pearson suggested that the discrepancy could be accounted for by complex formation which would effectively enhance the degree of dissociation of cryolite.

In 1953 Forland and associates[9] suggested complete dissociation of molten cryolite into its constituent ions thus

$$Na_3AlF_6 = 3\ Na^+ + AlF_6^{3-} \quad \ldots \quad \ldots \quad 1.5(ii)$$

and that breakdown of the AlF_6^{3-} ion occurred to a limited extent according to

$$AlF_6^{3-} = AlF_5^{2-} + F^- \quad \ldots \quad \ldots \quad 1.5(iii)$$

$$\text{or} \quad 2\ AlF_6^{3-} = AlF_5\text{-}F\text{-}AlF_5^{5-} + F^- \quad \ldots \quad 1.5(iv)$$

Grjotheim[8] on the other hand, from a structural interpretation of the liquidus curve around the cryolite composition showed that these forms of secondary dissociation were highly unlikely and suggested instead the reaction

$$AlF_6^{3-} = AlF_4^- + 2\ F^- \quad \ldots \quad \ldots \quad 1.5(v)$$

although the possibility of the earlier accepted

dissociation

$$AlF_6^{3-} = Al^{3+} + 6\ F^- \quad \ldots \quad \ldots \quad 1.5(vi)$$

was not ruled out.

The $NaF-AlF_3$ phase diagram was reinvestigated for the purpose of the calculations, which were performed on the basis of the four schemes 1.5(iii) - 1.5(vi). In all cases complete dissociation of cryolite into Na^+ and AlF_6^{3-} ions was assumed. The mixtures were regarded as ideal Temkin solutions, with the heat of dissociation of the AlF_6^{3-} ion taken to be zero - the dissociation constant thus being independent of temperature. Corrections due to different heat capacity of the solid and liquid over the temperature range considered were neglected, and it was assumed that there was no solid state dissociation of the cryolite anion just below the melting point.

Measurements were considered to be more reliable on the basic than on the acidic side of the cryolite composition, and the first step of the calculation was to assume a degree of dissociation α for the AlF_6^{3-} ion in pure cryolite, and from this derive a value of K, the dissociation constant. On addition of sodium fluoride the degree of dissociation was reduced to α_i and from the expressions relating the ion fractions of

the constituents (for each of the four schemes) to the dissociation constant the value of α_i was determined.

Assuming no solid solubility of NaF or AlF_3 in cryolite, the activity of cryolite in the liquid mixture is given by the product of the ion fractions

$$\ln a_{Na_3AlF_6} = \ln N^3_{Na^+} N_{AlF_6^{3-}} = \frac{-\Delta H_f}{R}\left[\frac{1}{T} - \frac{1}{T_o}\right] \quad \ldots \text{ 1.5(vii)}$$

T_o, the melting point of the hypothetical undissociated cryolite was calculated from the expression

$$\frac{1}{T_o} = \frac{1}{T_c} + \frac{R}{\Delta H_f} \ln N^3_{Na^+} . N_{AlF_6^{3-}} \quad \ldots \quad \ldots \quad \text{1.5 (viii)}$$

where T_c is the real melting point. By expressing $N_{AlF_6^{3-}}$ in terms of α_i, a value of T_o was calculated. In general this was different from the observed liquidus temperature for the same composition. Another value of α was then chosen and the calculations repeated until the best possible agreement between calculated and measured temperatures was obtained over the whole composition range.

Using a calorimetrically determined heat of fusion of cryolite = 20,850 cal/mol,[59] the best fitting curves corresponded to a value of T_o = 1152°C

and $\alpha = 0.3$ for scheme 1.5(v) and $T_o = 1082°C$ and $\alpha = 0.07$ for scheme 1.5(vi).

In a subsequent paper Grjotheim[61] employed a more recent calorimetric heat of fusion of cryolite = 27,640 cal/mol,[60] and took into consideration the heat of dissociation of the cryolite anion. A somewhat better fit for scheme 1.5(v) was obtained when α and $\Delta H_{dissociation}$ were taken as 0.25 and 10,000 cal/mol respectively. This scheme was preferred to that of 1.5(vi) as a result of determinations of the freezing point depression of sodium sulphate by cryolite. Fair agreement with the experimental curve was obtained only if partial dissociation of AlF_6^{3-} to AlF_4^- and $2F^-$ was assumed. Again the system was considered as a Temkin ionic solution and therefore that the SO_4^{2-} ion did not interfere with the cryolite dissociation. The same value of the dissociation constant, 0.06 ($\alpha = 0.3$), in the temperature range 800-880°C (m.p. of Na_2SO_4 = 884°C) was taken as that estimated in the original paper at 950-1010°C around the cryolite peak.

An alternative method was used by Rolin[62] to calculate the degree of dissociation and the structural entities in the melt, but which was based on the same

assumptions as were made by Grjotheim and which involved the same schemes. Because of some uncertainty in the location of the liquidus curve on the AlF_3 rich side of the cryolite composition, a thorough investigation of this region was carried out (figure 3). Grjotheim's liquidus near the Na_3AlF_6 peak was confirmed and the schemes 1.5(iii), 1.5(iv) and 1.5(vi) were rejected. Using a heat of fusion of cryolite = 16,640 cal/mol,[63] a T_o of 1302°C and α = 0.44 were derived at the melting point. More recently[64] the same calculations were republished using a cryometric heat of fusion = 26,600 cal/mol, which gave an α = 0.204 and T_o = 1082°C.

Further evidence for the credibility of scheme 1.5(v) was provided by conductivity measurements on cryolite-alumina melts,[44] in which no migration of aluminium towards the cathode was detected, thereby indicating the absence of the Al^{3+} ion; and also by the observations of Howard,[65] who found that the compound $NaAlF_4$ was stable at high temperature.

Frank and Foster[66] used a different approach to find the species present in liquid cryolite. Due to the limitations of the cryoscopic treatment, an attempt was made to correlate the shape of the experimentally determined density composition relationship

with the following dissociation models

$$Na_3AlF_6 = 3NaF + AlF_3 \quad \ldots \quad \ldots \quad 1.5(i)$$

$$3Na_3AlF_6 = 4NaF + 5NaF.3AlF_3 \quad \ldots \quad \ldots \quad 1.5(ix)$$

$$Na_3AlF_6 = 2NaF + NaAlF_4 \quad \ldots \quad \ldots \quad 1.5(x)$$

As in Pearson's calculations, additivity of molar volumes was assumed. By arbitrary but reasonable density assignment to the species present at equilibrium in each scheme, and by successive adjustment of the dissociation constant, good agreement with the experimental curve at four temperatures was obtained only for scheme 1.5(x). The dissociation constant at 1000°C was estimated to be 0.09 (α = 0.35) and its temperature dependence was given by a heat of dissociation of 22 kcal/mol. This value was later altered to 22.5 kcal/mol.[67]

Thus both density and cryoscopic calculations indicated the same model for dissolution; the former method giving a moderately higher value of α.

The above workers[67] replotted Grjotheim's graph of sodium sulphate activity as a function of temperature, allowing for the variation of K with temperature by extrapolation of values from the region 1000-1090°C, and obtained almost perfect agreement with a line representing the known calorimetric heat of fusion.

This was taken as confirming the values of the heat and degree of dissociation estimated from the density data.

Mashovets and Yudin[68] however came to a rather different view of cryolite dissociation. From measurements of the P_{HF}/P_{H_2O} ratio over melts of the stoichiometric composition $3NaF.AlF_3$ and $NaF.AlF_3$ by equilibration with steam, cryolite was found to be only 6% dissociated according to the reaction 1.5(x) at 1300°K. Furthermore breakdown of $NaAlF_4$ following the equation

$$3\ NaAlF_4 = Na_3AlF_6 + 2\ AlF_3 \quad \ldots \quad \ldots \quad 1.5(xi)$$

was evaluated to be 65% complete. Dissociation was thus considered in terms of the two simultaneous reactions 1.5(i) and 1.5(x).

1.5.2 Cryolite-Alumina Melts

The Na_3AlF_6 rich side of the cryolite alumina phase diagram from the most recent work is shown on p. 34 (figure 4).

Earlier investigators reported much lower eutectic temperatures and eutectic compositions of as such as 20 wt% Al_2O_3. No compound between the two components was found in the solid state and hence the phase diagram did not furnish any direct evidence of the

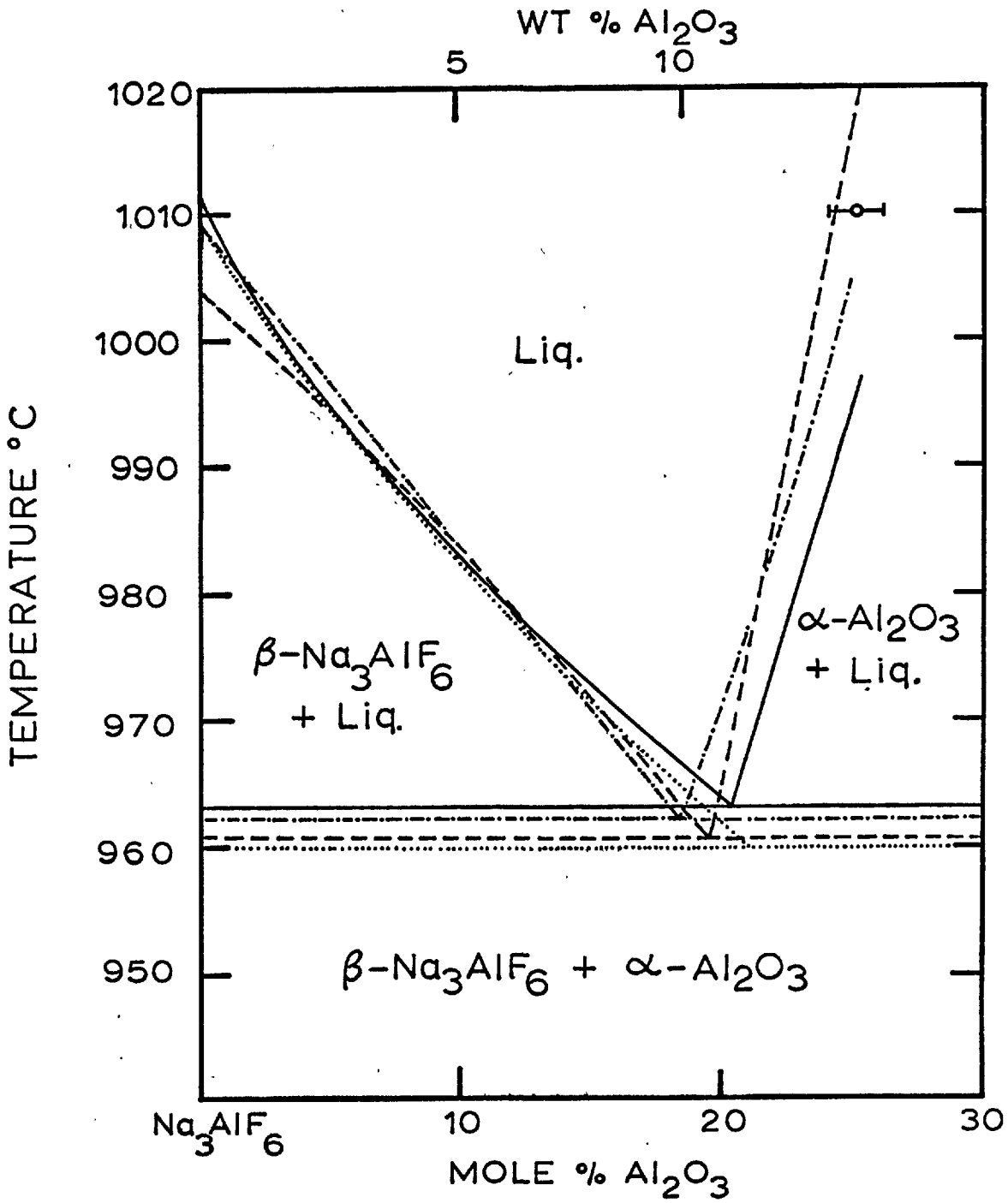

FIG. 4 PHASE DIAGRAM Na_3AlF_6–Al_2O_3.

—— Grjotheim[73] ····· Rolin[48] -·-·- Phillips et al[46] – – – Foster[49]
o Weill and Fyffe[47]

complexes formed by dissolved alumina. Some kind of reaction was however indicated by the relatively high solubility in comparison with other salts, and by the decrease in density of cryolite on adding alumina, despite the higher density of the solid oxide.

A number of complexes have been suggested by different workers

Treadwell[69]	$(F_2AlO_2AlF_2)^{2-}$
Grünert[70]	$AlOF_5^{4-}$ and $AlOF_3^{2-}$
Boner[71]	$AlOF_2^-$
Rolin[72]	AlO_2^- and AlO^+

Rolin's argument favouring the species AlO_2^- and AlO^+ was based on the observed three times ideal freezing point depression in very dilute solution and only one and a half times ideal depression at higher concentrations. Absence of solid solubility was assumed, and the dissolution mechanism at higher concentrations was considered to be

$$Al_2O_3 = AlO_2^- + AlO^+ \quad \ldots \quad \ldots \quad 1.5(xii)$$

In more dilute solutions the positive complex dissociated further

$$AlO^+ = Al^{3+} + O^{2-} \quad \ldots \quad \ldots \quad 1.5(xiii)$$

Through the independent investigations of Foster[49] and Grjotheim et al.[73], the absence of solid solubility in the system was subsequently confirmed and thus Rolin's cryoscopic calculations were justified. However diagreement arose as to the most likely species present in solution. Foster and Frank[67] calculated the freezing point depression according to various schemes and compared them with the observed liquidus. The results were plotted as log activity of cryolite against 1/T. Allowance was made for the temperature dependence of the cryolite dissociation [equation 1.5(x)] and the true heat of fusion of cryolite was evaluated at 19.9 cal/mol. (in a later paper Frank[74] reported the figure 18.76 kcal/mol.). After taking dissociation into account, the heat capacities of solid and the hypothetical undissociated liquid cryolite were judged to be almost identical. The method of calculation was similar to that adopted by Grjotheim and invoked the assumption of Temkin ionic solutions. From the graph the solution scheme which gave the heat of solution nearest 19.9 kcal was

$$3\ F^- + Al_2O_3 = 3/2\ AlO_2^- + 1/2\ AlF_6^{3-} \qquad \ldots\ \ldots\ 1.5(xiv)$$

Dewing[75] criticised this proposed mechanism, and pointed out that the reaction

$$Al_2O_3 + 3(x-1)NaF + AlF_3 = 3Na_{(x-1)}AlOF_x \quad \ldots \quad \ldots \quad 1.5(xv)$$

explained the insolubility of alumina in pure NaF and its maximum solubility in NaF enriched cryolite melts if the value of x lay between 2 and 4.

In reply Foster and Frank pointed out that sodium aluminate was very soluble in cryolite and that although alumina was insoluble in sodium fluoride a quantitative reaction occurred according to the equation

$$6NaF + Al_2O_3 = 3NaAlO_2 + Na_3AlF_6 \quad \ldots \quad \ldots \quad 1.5(xvi)$$

It was stated further that the AlO_2^- solubility was related to the activity of AlF_6^{3-}. In view of the suggested dissociation scheme [see equation 1.5(x)] the AlF_6^{3-} activity was a maximum in an NaF-enriched cryolite melt and thus a maximum solubility of alumina in this region was not unexpected.

The mechanism 1.5(xiv) however, contradicted Ivanova's statement[76] that the formation of sodium aluminate from alumina solution in cryolite was thermodynamically inconceivable. As a consequence Frank[74] repeated Ivanova's calculations using more recent values of the heat of formation of cryolite and

aluminium fluoride, and showed that sodium aluminate was in fact stable enough to be formed in a dilute alumina solution.

On the other hand Grjotheim[61] proposed a different dissolution model. After careful reinvestigation of the phase diagram, and again considering the freezing point depressions of several schemes, the following mechanism was favoured in the very dilute range

$$Al_2O_3 + AlF_6^{3-} + 3F^- = 3AlOF_3^- \quad \ldots \quad \ldots \quad 1.5(xvi)$$

Thus three foreign paricles were formed, in agreement with Rolin, and all complex ions containing more than one oxygen were excluded. The calorimetric heat of fusion of 27,640 cal/mol was used and as a result the correction arising from the heat of dissociation was ignored.

In a succeeding paper Grjotheim and co-workers[73] included the possible simultaneous existence of $AlOF_5^-$ and $Al_2OF_6^{3-}$ and ions containing even longer -Al-O-Al- chains. The phase diagrams of Kostiukov[77] for the ternary reciprocal system $NaF+AlF_3+Al_2O_3+Na_2O$ were cited as supporting the presence of these complexes as well as speculation on the structural properties of the melt. Because of the rapidly increasing solubility of Al_2O_3 in NaF on adding AlF_3 (or cryolite), the Al/O ratio

of the dissolved complexes was thought to be equal or greater than unity. From the greater solubility in NaF enriched melts, complexes rich in fluorine were considered to be more stable than complexes with little fluorine. Furthermore viscosity measurements and the decreasing liquidus slope indicated the occurrence of association at higher alumina contents.

Förland[78] considered that the Al/O ratio of the complexes should be at least two in order to form a species containing only one oxygen. A lower Al/O ratio would only be possible in a larger complex.

Holm[73] investigated the liquidus of the Na_3AlF_6 + $NaAlO_2$ system and found that the addition of one unit of $NaAlO_2$ created two units of foreign particles, thereby disproving the existence of the AlO_2^- ion. An entropy model which required that the oxygen ions were distributed among the aluminium ions in the melt gave a good correlation between the calculated and the experimental liquidus line. A similar model was proposed to explain the slope of the liquidus of the Al_2O_3-Na_3AlF_6 system,[80] and was consistent with the solubility maximum in NaF enriched cryolite.

1.6 THERMODYNAMICS OF ALUMINIUM + CRYOLITE

Aluminium dissolution in cryolite is most likely to be described by one or other or both of the following equilibria

$$Al + 6NaF = Na_3AlF_6 + 3Na \quad \ldots \quad \ldots \quad 1.6(i)$$

$$2Al + AlF_3 = 3AlF \quad \ldots \quad \ldots \quad 1.6(ii)$$

The respective equilibrium constants might thus indicate which reaction is of the greater significance and might also predict the order of magnitude and the temperature and composition dependence of the solubility.

1.6.1. Equilibrium 1.6(i): Experimental

The importance of this reaction has been widely recognised, and it is an old assumption that sodium is more noble than aluminium under the conditions of the commercial process. Grünert[70] gave the main support for this view and stated that metallic aluminium reacts with molten cryolite around 1000°C to produce sodium gas at one atmosphere pressure. This opinion was based on observations of cryolite and aluminium melted together. Gas bubbles form in the melt and burn at the surface with a yellow sodium flame, which was taken as proof that the bubbles consisted of sodium gas. However, it has since been shown that these bubbles

are hydrogen gas, arising from a reduction of hydroxyl ions in the melt by dissolved metal.

Grünert also pointed out that Piontelli,[81] when electrolizing molten cryolite with a lead cathode, obtained a lead-sodium alloy. However, Grjotheim[8] pointed out that this observation was hardly significant, since lead and aluminium are almost immiscible, while lead and sodium form a series of stable compounds.

The view that sodium gas was not produced at one atmosphere over cryolite and aluminium was demonstrated by Jander and Herrmann[82] who investigated the sodium content of aluminium equilibrated with fluoride melts at 1090°C. A continuous increase from 0.004 to 0.063 wt.% with increase in sodium fluoride content was observed, and nearly pure sodium fluoride caused an explosive reaction. Using this data, and extrapolating the sodium solubilities in liquid aluminium measured by Ransley and Neufeld[83] between 665 and 775° to 1090°C, Grjotheim estimated the sodium partial pressure at the cryolite composition to be 0.1 atm. The dilute sodium solution was assumed to obey Henry's law.

Grube and Hantlemann[84] examined the reaction between sodium and $NaF-AlF_3$ melts at 1000-1020°C. Despite differences in the initial composition the final

melt contained about 6 mol % aluminium fluoride, indicating that this was the composition in equilibrium with molten aluminium and sodium gas at one atmosphere. The pressure over pure cryolite would have been considerably lower.

Recently Stokes and Frank[85] measured the ultra-violet absorption by sodium gas over aluminium + cryolite mixtures as a function of temperature. The calibration curve relating absorption to sodium pressure was obtained from the data of Makansi et al.[86] who measured the vapour pressure in the range 0.047-6.5 atm. Mixtures of cryolite and aluminium were placed inside an open-ended graphite cell, which was held horizontally and heated by high frequency induction. The temperature control was $\pm$ 20°C. In each run absorption measurements were made first at 1100° and then at 50° intervals down to 750°C. The results are shown in figure 5 together with sodium pressures calculated by the authors from thermodynamic data.

1.6.2 Equilibrium 1.6(i): Calculations

Grjotheim[92] originally calculated the standard free energy change for reaction 1.6(i) at 1000°C as + 43 kcal. However the value of the heat of formation of cryolite then available (-761.6 kcal.)[4] was based

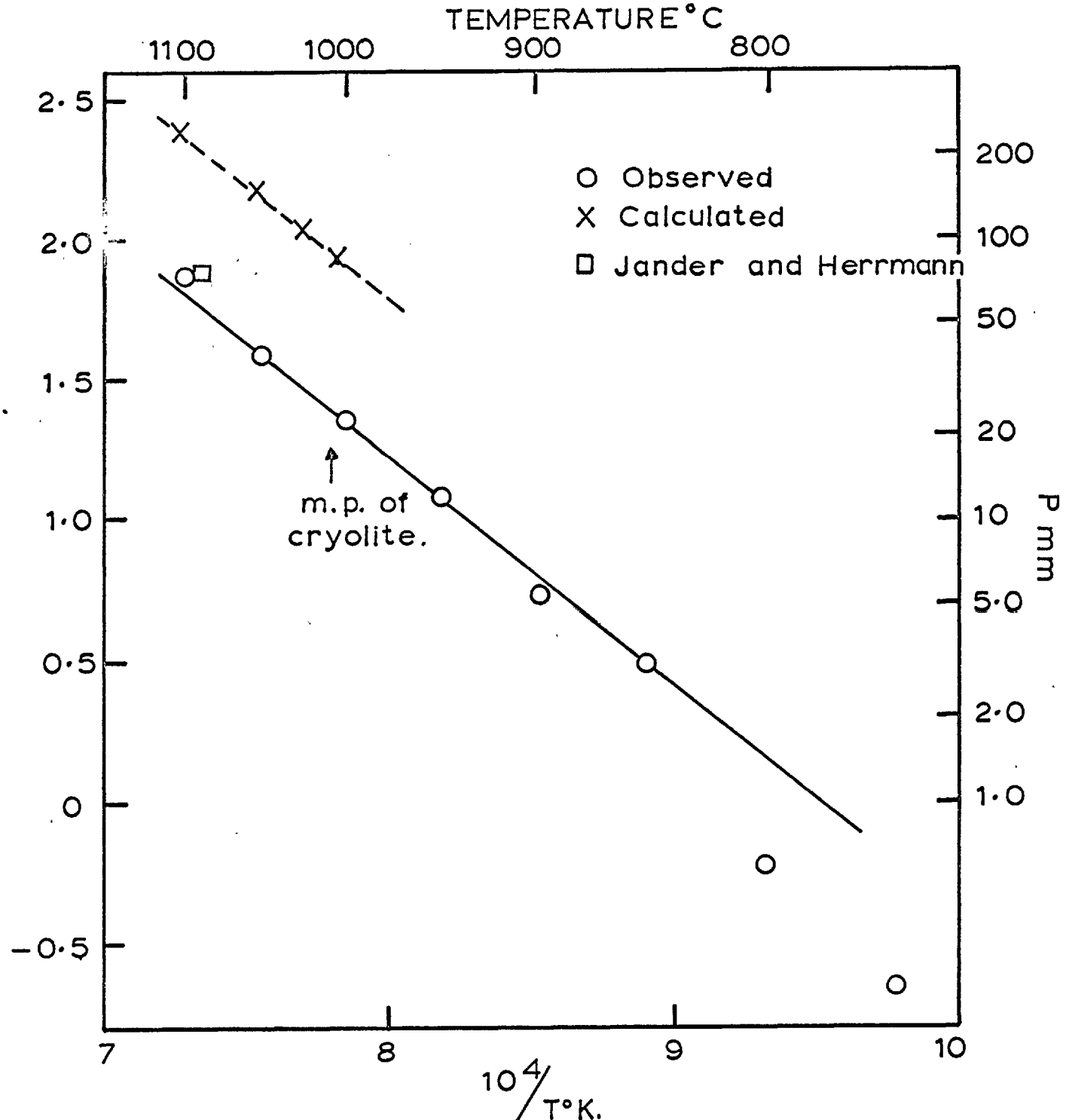

FIG. 5 PLOT OF LOG P_{Na} AGAINST $1/T$ FOR A CRYOLITE + ALUMINIUM MIXTURE. (Stokes and Frank[85])

on a heat of formation of aluminium fluoride of -331.5 kcal. which was later shown to be much too low. Using the figure published by Gross Hayman and Levi[88] (-355.7 kcal.) Grjotheim corrected the heat of formation of cryolite accordingly and obtained + 13 kcal for the free energy change. The ΔG° from the most reliable data at present available is -4.7 kcal. (see Appendix A). This is rather more negative than the figure of -3.1 kcal. derived from Stokes and Frank's data.

It is evident that the calculated sodium pressures will depend on the accepted degree and model of the cryolite dissociation. Table 3 shows the pressures derived on the basis of the dissociation equilibria of various investigations (Section 1.5) and the data in Appendix A (a correction due to partial dimerisation was neglected).

Table 3

Partial Pressure of Sodium
over Pure Cryolite + Aluminium

Author	Dissociation scheme	Temp. °C	P_{Na} mm Hg	Expt. P_{Na} (85)	Ref.
Grjotheim 1960	$AlF_6^{3-}=AlF_4^-+2F^-$	1009	46	23	61
Rolin 1962	"	1009	35	23	64
Frank & Foster 1960	"	1006	70	22	66
Mashovets & Yudin 1963	" and $AlF_6^{3-}= Al^{3+}+6F^-$	1027	13.3	28	87

1.6.3 Equilibrium 1.6(ii)

The possibility of this reaction accounting for aluminium solubility and thus current inefficiency has been suggested by a number of authors.(89,90)

Aluminium sub-fluoride is unknown in a condensed state and no measurements have been published on its partial pressure over the molten aluminium + cryolite system. Stokes however reported 0.4 mm Hg at 1000°C.(91)

Again the calculated value would depend on the chosen dissociation mechanism for cryolite. In Table 4 the sodium partial pressure measurements of Stokes and Frank have been used to calculate aluminium trifluoride activities in the melt, from which aluminium

sub-fluoride pressures were derived. These are compared with AlF partial pressures over the $Al+AlF_3$ system (Appendix A).

TABLE 4

Partial Pressure of Aluminium Sub-Fluoride

Temp. °K	P_{AlF} over melt mm Hg	P_{AlF} over AlF_3 + Al mm Hg
1000	.006	.96
1100	.09	≈1.09
1200	.79	7.9
1282	≈3.6	32.4

1.7 PREVIOUS EXPERIMENTAL WORK

The reported experiments on the solubility of aluminium in cryolite are summarised in Table 5 (p. 47) and may be profitably discussed according to the method of determining the excess metal in the melt.

These were (a) measurement of the weight loss of the metal phase after prolonged contact with the molten cryolite and (b) measurement of the gas evolved (hydrogen) on immersion of the quenched melt in hydrochloric acid.

SOLUBILITY OF ALUMINIUM IN CRYOLITE AND CRYOLITE-ALUMINA MELTS

TABLE 5

(a)	(b)	(c)	(d)	(e)	(f)	(g)	(h)
WORKER	NaF/AlF_3 Mol RATIO	TEMP. ^oC	CRUCIBLE	TIME OF EXPERIMENT	ANALYSIS	ATMOSPHERE	SOLY WT%
FEDOTIEV[50] and ILJINSKY (1912)	5:3 + 7.5% Al_2O_3	1000	C	5 min. agitation	WL	Air	0.771
	3:1 + 15% Al_2O_3	1000		5 min. settling			0.870
	3:1 + 15% Al_2O_3	1150		10 min. no agitation			0.806
	3:1 + 15% Al_2O_3	?		17 min. (agitated)			1.323
	eutectic+ 15% Al_2O_3	1050		10 min.			1.155
PRUVOT[51] (1934)	3:1 + 10% Al_2O_3	1000	C		WL	Air	1.5
	3:1 + 10% Al_2O_3	1200					2.93
	3:1 + 10% Al_2O_3	1400					6.22
	3:1 + 10% Al_2O_3	950					2.17
	5:3 + 10% Al_2O_3	950					0.62
	NaF	1000					13
ZHURIN[52] (a) (1937)	3:1	1050	C	20 min.	WL	S	0.62
	3:1	1050					0.61
	eutectic	1050					0.54
	3:1 + 10% AlF_3	1050			(GV)		0.45(.16)
(b)	3:1	1060				Air	2.8 (.14)
	3:1	1060					2.6 (.09)
	3:1	1080					2.8 (.11)
	3:1 + Al_2O_3	1060					2.2 (.15)
	5:3	1060					2.4 (.21)
	eutectic	1060					3.5 (.085)
	NaF	1020					2.1 (.062)
NOGUCHI[53] (1947)	85% cryolite 10% Al_2O_3 5% AlF_3	970-1070	C	10-30min.	WL	Air	0.1
ABRAMOV[54] and BROVMAN (1951)	85% cryolite 15% Al_2O_3	990	C	1 hour	WL	Air	0.38
		1050					0.75
		1110					0.92
GRJOTHEIM[8] (1956)	3:1	1004	SS		FP	A	0.2
MASHOVETS[55] and SVOBODA (1959)	5:3 to 3:1	1060 to 1060	C	3 hours	GV	A	0.44 to 0.05
		1060					
HAUPIN[56] (1960)	All melts 3:1 + 8% CaF_2+5% Al_2O_3	980	C	72 hours	GV	A	0.10
	+ 3.6% AlF_3	980					0.09
	+ 11.5% NaF	980					0.11
FERBER[57] (1960)	3:1	1040	BN	90 min agitation 15-30 min settling	WL	Air (A) (S)	2.6
FIRSANOVA[58] and BELYAEV (1961)	All melts + 10wt%$BaCl_2$	1050	Al_2O_3	7-9 hours	WL	S	0.56
	+ 10wt%MgF_2	1050					0.60
	2.6:1 + 10wt%NaCl	1050					0.85
	+ + 10mol%NaCl	1050					0.80
	6%Al_2O_3-10mol%KCl	1050					1.00

ABBREVIATIONS A = argon; C = graphite; BN = boron nitride; GV = gas volumetric; SS stainless steel; FP = freezing point depression; WL = weight loss; S =sealed

1.7.1 Analysis by Metal Weight Loss

From the considerations of the last chapter it is immediately evident that this method will only measure the true solubility if escape of sodium by volatilisation is prevented i.e. if the system is equilibrated in a hermetically sealed vessel and also if there is clean separation of the solidified phases. In experiments[50] to[54] [excluding[52](a)] in which the system was exposed to the atmosphere, aluminium losses would have been enhanced by the first and possibly the second of the following processes

(i) oxidation of sodium at the melt surface to give soluble Na_2O, which is then reduced by the successive steps

$$3\ Na_2O + 2\ AlF_3 = Al_2O_3 + 6\ NaF$$

$$Al + 3\ NaF = AlF_3 + 3\ Na$$

The overall reaction may be written as

$$4\ Al + 3\ O_2 = 2\ Al_2O_3$$

(ii) hydrolysis of the melt from attack by moisture in the air and reduction of the hydroxyl ions so formed according to the equation

$$3\ H_2O + 2\ Al = Al_2O_3 + 3\ H_2$$

The dissolved alumina content of the bath would have increased continuously until either the system was cooled or the saturation limit reached.

The solubility figures of [50], [51] and [52](b) [column (h) Table 5] were obtained directly from the measured weight loss and are therefore much too high. They merely indicate the rate of metal loss. Little meaning can be attached to Noguchi's[53] value because of the short duration of the experiment and the wide temperature fluctuation. However a negligible depression of the freezing point of the cryolite-alumina melt was observed in the presence of aluminium.

Both Abramov and Brovman[54] and Firsanova and Belyaev[58] appreciated that in the presence of air a substantial part of the metal losses were due to oxidation. Abramov and Brovman used a graphite crucible in which a pool of molten metal was covered by a cryolite bath of known height. They attempted to calculate the saturation concentration of aluminium in the bath from the weight loss against time relationship. It was assumed that the rate of oxidation was controlled by diffusion of metal through the bath, and thus that under steady state conditions the actual concentration was half the saturated value. With a bath depth

of 3.7 cm. it was found that the slope of the curve became constant after 80 minutes and the weight of excess metal in the bath was taken as the intercept of this slope on the weight loss axis.

However, the condition of steady state diffusion was not experimentally verified, nor was the graphical analysis shown to be mathematically valid. The calculated figures cannot therefore be taken to be reliable.

It is most unlikely that the technique used by Firsanova and Belyaev[58] was effective in eliminating non-solution metal losses. These workers used corundum crucibles which were packed in a bed of powdered alumina. It is well-known that alumina is strongly corroded in the presence of sodium, and in view of the extremely high melt losses which were reported (up to 50 g. of an initial charge of 100 g.) together with the fact that the time to reach saturation was not clearly defined, indicates that the true solubility was not measured.

Ferber[57] carried out two types of experiments. In the first which was similar to that of Abramov and Brovman, aluminium and cryolite were contained in a graphite crucible assembly with a boron nitride lining

at the bottom, so that the metal was not in contact with the graphite. The system was open to an atmosphere of either air or argon. In the second aluminium and cryolite were agitated for 90 minutes in an enclosed boron nitride container, and the metal loss determined after 15 and 30 minutes standing time.

The solubility was calculated in the first series by a refinement of the previous workers' method of graphical extrapolation. However it is difficult to see how the figures obtained bear any relation to the equilibrium quantity of excess metal in cryolite. Not only was Abramov and Brovman's solubility misquoted as 0.075 g/cm^3 in a comparison, but the chemical interpretation of the difference in metal loss rates under argon and air was not explained. Furthermore the rate of aluminium loss was found to be lower from a shallower bath (in contradiction to the earlier workers' experiments) and the metal saturation limit was arbitrarily assumed to be similar in melts of different compositions.

The results of the second technique can also be discounted. No attempt was made to show that the weight loss approached a well-defined constant value, thereby proving that equilibrium had been achieved.

Because of the vigorous nature of the agitation and the small difference in density between molten cryolite and aluminium, a dispersion of fine metal particles could conceivably have formed in the salt phase. A significantly lower solubility value was in fact reported for a run allowed to stand for half an hour than for one allowed to stand for only 15 minutes.

1.7.2 Gas Volumetric Method

Errors can arise in this method from

(i) non-equilibrium conditions in the melt i.e. the metal not dissolved to its saturation limit.

(ii) segregation of excess metal during quenching

(iii) poor separation of the solidified phases.

Solubility figures obtained by this technique are thus only reliable if the system is shown to be at equilibrium and if the analytical sample is representative of the whole melt.

Evidence for the absence of these sources of error was not presented by Zhurin[52](b) or Mashovets and Svoboda[55] and their solubilities are therefore uncertain.

In addition to the objections already raised, a further source of error arises in experiments using graphite, because of attack by aluminium to form

aluminium carbide. This reaction would cause positive errors in both methods of analysis; in the first by increasing the metal losses, and in the second - assuming the carbide to be soluble in the melt - through methane evolution. Thus with the exception of Haupin[56] who determined the actual volume of hydrogen, all data from experiments in graphite crucibles are unacceptable.

This applies to Ferber's diffusion technique, in which the formation of aluminium carbide cannot be dismissed because of a physical separation of aluminium and carbon.

Grjotheim[8] used a graphite stirrer in his freezing point depression determinations. Interpretation of the lowering is thus uncertain and the aluminium solubility value derived is likely to be too high.

In conclusion it is evident that with one exception[56], all the literature values of the solubiluty of aluminium in cryolite and cryolite+alumina melts are open to serious objection.

CHAPTER 2

EXPERIMENTAL METHODS

2.1 FOREWORD

The following pages of this chapter describe a procedure which enabled the solubility of aluminium in cryolite with respect to temperature, melt composition and added alumina to be measured. Its development is dealt with in Chapter 3 part A where the results of preliminary experiments are presented and discussed.

2.2 ORIGIN OF EXPERIMENTAL TECHNIQUE

2.2.1 Elimination of Errors

In view of the points raised in 1.7 a technique was required which avoided the objections to earlier measurements. These were

(a) attack of the container material by the molten cryolite + aluminium system

(b) atmospheric oxidation of metal and change in composition of melt through vaporisation losses.

(c) presence of a fine dispersion of aluminium in the molten salt phase from either mechanical agitation or from thermal fluctuations

(d) invalid method of analysis: (i) in the gas volumetric technique from segregation of metal on solidification and (ii) in the weight loss technique from oxidation or escape of sodium gas.

2.2.2 Container Material

Of the materials sufficiently inert to molten aluminium + cryolite, boron nitride was the only one commercially available which could be readily machined. However the pressed substance contained an appreciable amount (2.4%) of B_2O_3 which would have been soluble in the fluoride melt. Consequently a 70/30 (w/w) mixture of TiB_2/TiC was preferred. In industrial experiments this material had been found to be almost completely unattacked by the reduction bath electrolyte for periods of up to several weeks.(96) The author is indebted to the British Aluminium Company for the supply and fabrication of crucibles used throughout this work.

2.2.3 Method of Analysis for Excess Metal and Design of Crucible

The use of an extremely hard, refractory, and inexpendable material ruled out the possibility of achieving hermetic sealing of the volatile molten system and thus of determing the solubility by weight loss of metal. For this reason a method of avoiding errors due to segregation of metal in the quenched melt had to be devised.

The design of crucible which was chosen to achieve this is shown in figure 6. A small quantity of

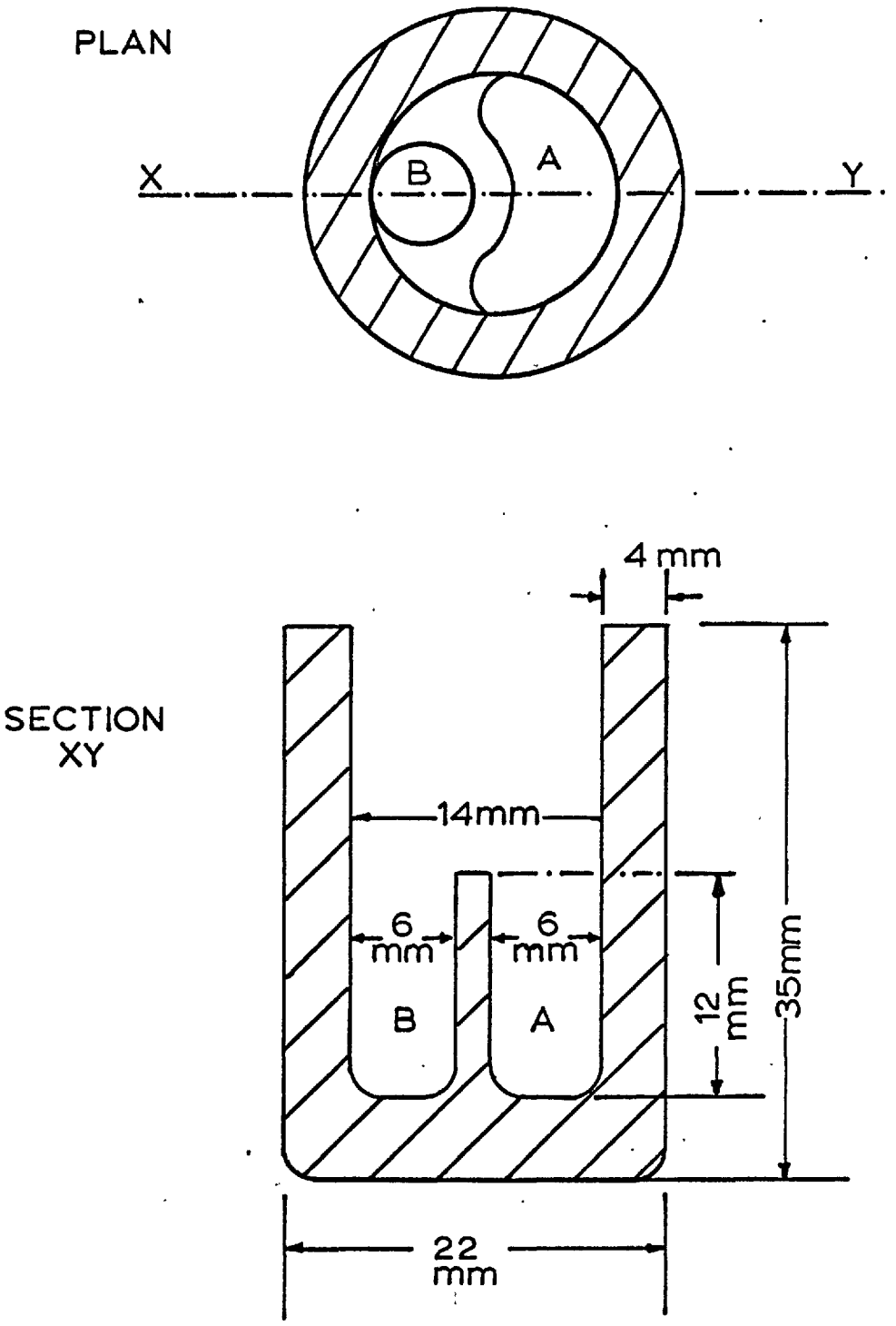

FIG. 6 TiB_2 / TiC Crucible

aluminium was to be charged only into the large well and enough cryolite added so that the melt surface would have just covered the ridge between the two wells. On cooling and solidification, precipitated metal could not escape from the small well, the whole contents of which could then be removed for analysis.

Crucibles were spark-eroded from solid rod and the surfaces cleaned by sand blasting and etching in a solution of HF and HNO_3.

2.2.4 Equilibration Technique

To reduce the time required for saturation an effective method of agitation was needed which at the same time precluded the possible formation of a dispersion of aluminium in the salt (the density difference between molten Al and cryolite at 1000°C is about 0.2 $g.cm^{-3}$).

This could be accomplished either by rocking the crucible slowly through a certain angle or else by slowly rotating it in a tilted position. Melt would then spill out of the large well into the small well and back again whilst the metal bead would remain stationary or move along the bottom of the large well from one end to the other.

2.3 PREPARATION AND PURITY OF MATERIALS

2.3.1 Aluminium

Aluminium in the form of 3 mm dia. wire was supplied by Koch Light Laboratories Ltd. The minimum purity was stated to be 99.999% Al, and a typical analysis gave the impurities in parts per million as

Ca	Cu	Fe	Mg	Mn	Si	C	H_2	N_2
< 1	1.0	2.2	< 1	< 1	1.0	< 1	0.2	< 1

The metal was treated in Tucker's etch (15 ml 40% HF, 45 ml conc. HCl, 15 ml conc. HNO_3, 25 ml water) to remove the oxide film before use.

2.3.2 Silver

Spec. pure 7 mm dia. rod (Johnson Matthey Ltd.) was used in making up aluminium-silver alloys.

2.3.3 Graphite

Crucibles for vacuum preparations were machined from EY9 grade solid rod (Morganite Carbon Ltd.) The impurity limits, determined from a spectrographic analysis, in wt% were

Fe	Si	Mg	V	Al	Ti	Cu	Ca	B
.02	.001	.001	.002	.001	.001	.001	.002	.002

2.3.4 Cryolite

In the final series of experiments, hand picked natural Greenland cryolite containing no visible impurities was used. The aluminium content was determined gravimetrically by the 8-hydroxyquinoline method and found to be 12.85 $\pm$ 0.04% (the value for stoichiometric cryolite is 12.86).

2.3.5 Alumina

"Analar" grade powder (Hopkin & Williams Ltd.) was fired at 1350°C for several hours and stored in a desiccator. The stated impurities were given as (wt.%).

SO_4	Cl	Fe	
0.01	0.05	0.01	loss on ignition 1%

2.36 Sodium Fluoride

"Analar" sodium fluoride of the following specification was supplied by Hopkin and Williams Ltd.

free acid	2 ml N/1		
free alkali	2 ml N/1		
Cl	0.002 (wt %)	NaF not less than 98%	
SO_4	0.01	Fe	0.002
PO_4	0.001	Pb	0.004
SiO_2	0.05	K	0.01

Up to 2% moisture could be present and this was removed by vacuum fusion in a nickel crucible (see figure 8).

2.3.7 Aluminium Fluoride

Commercial grade AlF_3 was obtained from Hopkin and Williams Ltd. The principal impurities were moisture (5%), Na(0.15%), Fe (0.01-0.02%) and K(0.005%). The suppliers gave the weight loss on ignition as 16%.

The moisture is present in part at least as the demihydrate $AlF_3.\frac{1}{2}H_2O$ which is stable at room temperature and is only decomposed completely at 600°C into alumina and hydrogen fluoride.

Purification was carried out under vacuum in two stages - exhaustive drying followed by sublimation.

Drying of AlF_3

The apparatus for this is shown in figure 7. A "Purox" recrystallised alumina crucible (60 x 35 mm) containing about 10 g. of the finely powdered material was loaded into the silica envelope which was then placed in the furnace and gradually evacuated. The electrical input was controlled by an 8A continuously variable auto-transformer which was initially adjusted to give a crucible temperature of 100°C. After 12 hours the temperature was raised to 250°C and then after another 12 hours to 450°C. A further 6 hours

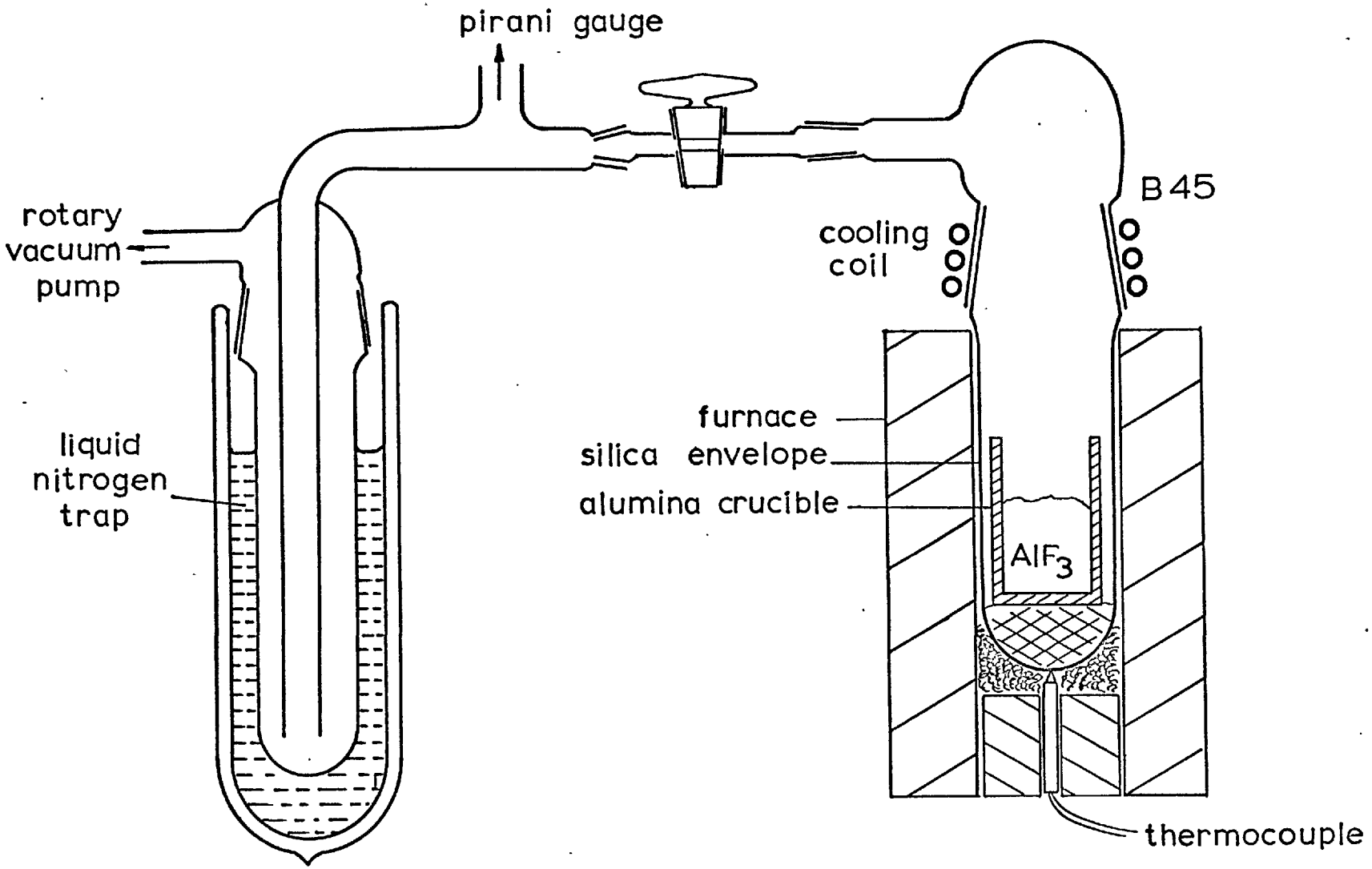

FIG. 7 APPARATUS FOR DRYING AlF_3

at 600°C was required to complete the drying operation.

Attempts to speed up the procedure resulted in excessive escape of material from the crucible and fouling up of the vacuum line.

Vacuum Sublimation of AlF_3

Several methods of preparing pure AlF_3 have been reported in the literature[113] and the technique used here was adapted from that of Henry and Dreisbach.[114]

The anhydrous material (now containing Al_2O_3 as the principal impurity) was charged into a graphite crucible (EY9 grade), over which a second crucible acting as a condenser lid was loosely fitted (the arrangement measured 3" by 1¼").

The sublimation was performed at 925 - 950°C in an evacuated glass envelope (figure 8) in which the graphite was heated by H.F. induction.

The diffusion pump was switched off as soon as degassing finished and the vacuum thereafter rose to a steady 0.05 torr.

The temperature was measured by a disappearing filament pyrometer and did not fluctuate by more than ± 10°. The H.F. coil was arranged so that the condenser lid was 150-200°C cooler than the crucible. The sublimation took 6-8 hours. The sublimate consisted of a mass of shiny translucent crystals (1-4mm)

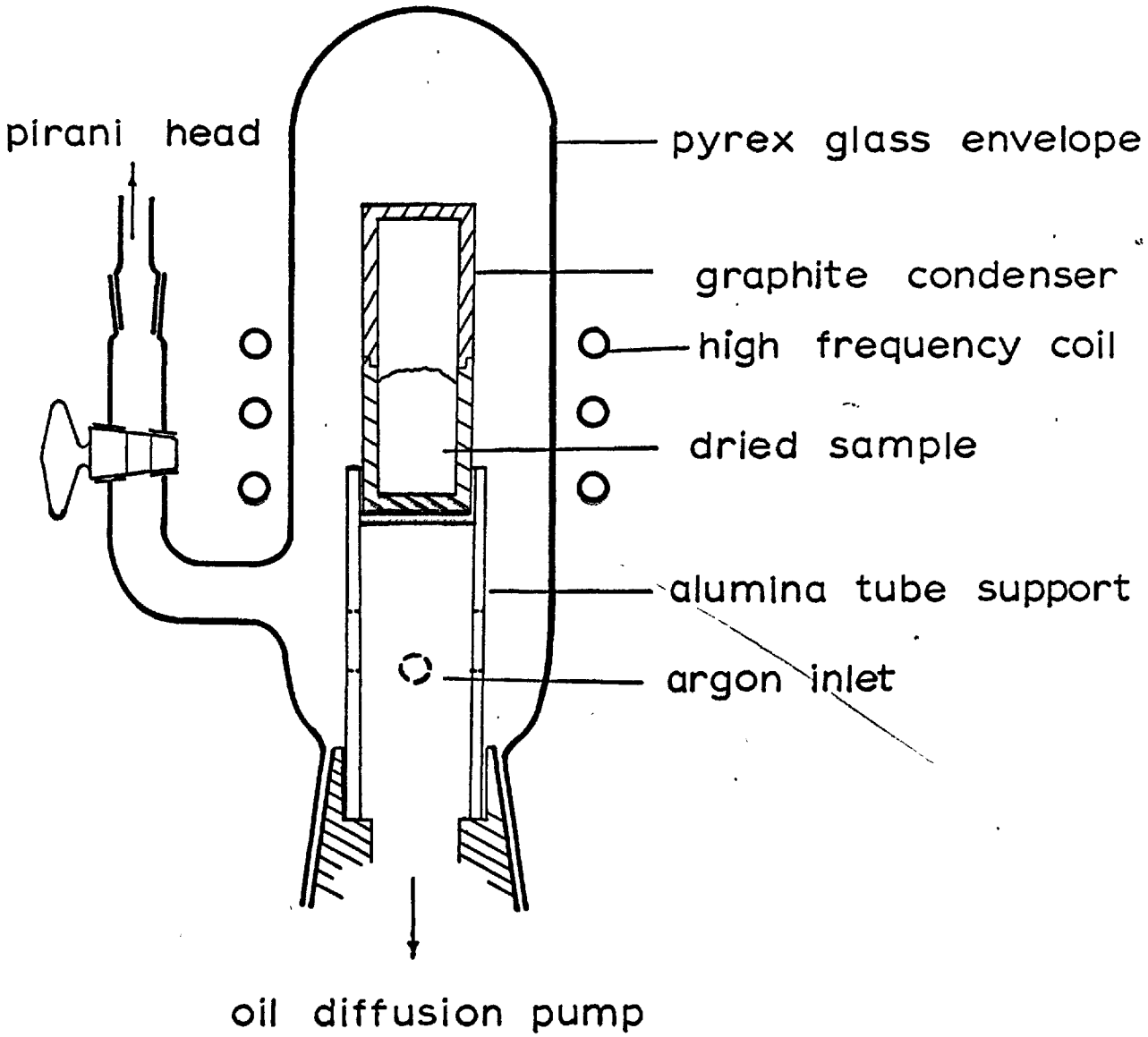

FIG. 8 APPARATUS FOR VACUUM SUBLIMATIOI OF AlF_3

embedded in a matrix of microcrystals. 2-3 g. of the larger crystals were removed with tweezers and retained, and the remainder re-sublimed in the next operation.

2.3.8 Preparation of Synthetic Cryolite

12 g. of purified NaF and 8 g. of purified AlF_3 were fused in a graphite crucible ($2\frac{1}{2}$" x $1\frac{1}{4}$") under a dry argon atmosphere. The apparatus of figure 8 was used. A white button of cryolite was formed and was readily removed from the crucible. The surface was scraped with a piece of recrystallised alumina before use to remove small particles of graphite.

2.4 FURNACE ASSEMBLY FOR SOLUBILITY MEASUREMENTS

Two vertical furnaces of identical size were used for the solubility experiments, the first of which is shown schematically in figure 9. This consisted of a recrystallised alumina furnace tube, 2" external diameter and 21" long, wound with a 22 s.w.g. platinum spiral kept in place by a coating of refractory cement. The tube was encased in a rectangular "sindanio" box, 9" x 9" x 21", packed with alumina powder as thermal insulator. The windings were spaced along the length of the tube in such a way that the turns were closer together nearer the ends than in the centre. This had the object of producing a larger zone of constant

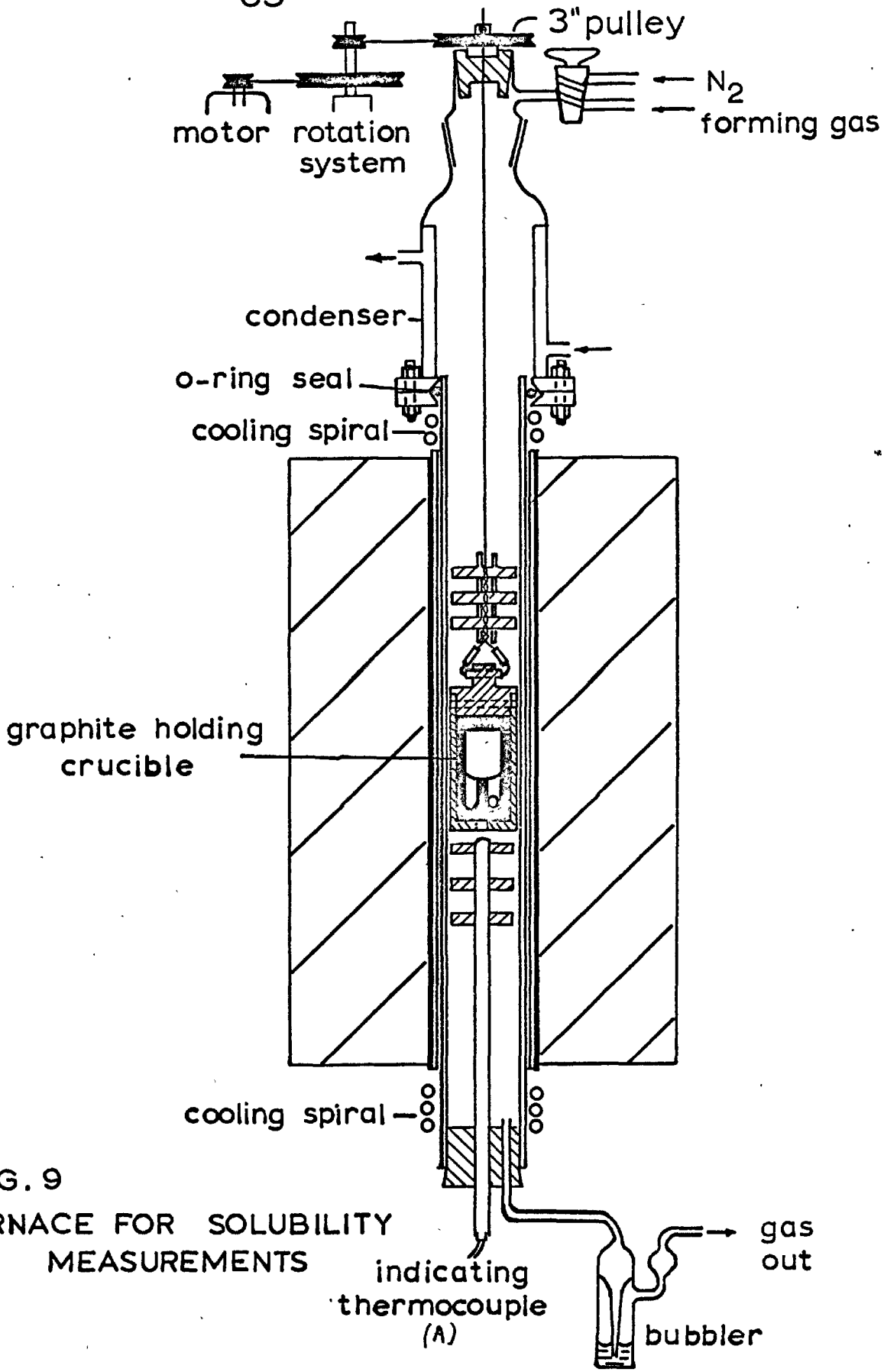

FIG. 9
FURNACE FOR SOLUBILITY MEASUREMENTS

temperature than would have been obtained with a uniform winding. The resistance was about 5 ohms.

A second recrystallised alumina tube, 650 mm long, 35.5 mm o.d., 28.5 mm. i.d., was placed inside the furnace tube and projected from either end. The rubber bung at the bottom was kept cool by means of a lead coil, wound over a strip of copper foil which was wrapped round the tube to improve heat transfer. A similar coil was placed at the top to promote cooling of the silicone rubber O-ring seal by which the copper condenser (6" x 2½") was fixed in position. A stream of cold water was maintained through the condenser and both coils. A section of pyrex glass tubing was connected by an "araldite" joint on to the top of the condenser and the system sealed by a rubber bung with a hollow top and base. The 3" pulley was supported by a brass washer 10 mm by 22 mm dia. which fitted into the top of the bung.

Current to the furnace came from the A.C. supply through a Variac continuously variable auto-transformer. The temperature was controlled by a Smiths Mark 4 proportional action controller which operated a mercury switch connected across the ends of a resistor in series with the furnace winding. When the temperature fell below the preset value the photo-resistor

became exposed to the exciter lamp and activated the micro-switch, thus magnetising the solenoid of the mercury switch and thereby causing current to bypass the resistor. The value of the resistor was such that it reduced the current to the furnace by 20% when in the circuit. E.m.f. was supplied to the controller by a platinum/13% rhodium-platinum thermocouple whose junction was placed between the reaction and furnace tubes in the hottest part of the furnace. The voltage input from the variac was adjusted until the on and off periods of the time cycle were both of 10 seconds duration. The degree of control as measured by the thermocouple (A) inside the reaction tube was better than $\pm$ 0.5°C.

In order to prevent condensation of volatile products around the crucible lid a positive temperature gradient was required up the length of the crucible. The most suitable position was found by suspending a dummy assembly containing a charge of molten silver and two thermocouples, one of which was immersed in the metal and the other such that the weld was level with the lower surface of the lid. The furnace was fully tilted to the 45° position for this operation as it was found that the location of the hot zone shifted by

more than 1" when tilted and took several hours to attain a steady position. There was a temperature difference of 3° between the lid and the metal and 26° between the metal and the indicating thermocouple (A) when this was 7½" from the furnace base, and the graphite assembly 1/8" above the tip of the probe in which it was inserted. This position was adopted for all experiments. The probe was an 5 mm i.d. x 8 mm o.d. alumina tube on which radiation shields of aluminous firebrick were cemented. Further shields separated by alumina washers were spaced on the assembly supporting wire.

An atmosphere of dry oxygen-free forming gas (90% N_2, 10%H_2) was maintained inside the reaction tube by feeding in and out through di-butylphthalate bubblers. Any oxygen was removed by a platinum gauze catalyst and water by two drying towers in series, the first of silica gel and the second of anhydrous magnesium perchlorate.

The furnace assembly was pivoted about its centre on a rigid frame. Movement through 45° was effected by a connecting rod from the furnace to a circular cam which was driven through gears by an

electric motor. The cam rotated 9 cycles per hour.

The dimensions of the second furnace were identical to the first. The heating element was 18 s.w.g. kanthal wire wound on a tube of impervious mullite and insulated with aluminous firebrick. The method of temperature control and the condenser arrangement were similar to that just described, but the position chosen for equilibration was 8" above the base of the furnace. Tilting was done manually.

2.5. EXPERIMENTAL PROCEDURE FOR SOLUBILITY MEASUREMENTS

Equilibrations of aluminium with cryolite were performed in TiB_2/TiC crucibles whose design has already been shown in figure 6. Because of the appreciable sodium partial pressure as tight a fit as possible between lid and crucible was required. TiB_2 and TiC are two of the hardest substances know (Vickers hardness numbers 3400 and 3200 respectively[115]) and a polished finish could not be obtained with the standard silicon carbide or corundum abrasives. Polishing with 7μ diamond paste on a prepared "paxolin" surface was an extremely tedious operation and the degree of improvement in the fit which could be achieved was not commensurate with the effort involved.

Instead it was considered sufficiently satisfactory to grind lid and crucible top on plate glass using 3F (20 - 25μ) "carborundum" (SiC) powder, which was found to give a mean gap of 10 - 15μ.

This figure was estimated from the rate of vaporisation of an equimolar mixture of ethyl alcohol and diethyl ether from a closed crucible. The solution was assumed to be ideal (the total vapour pressure = 300 mm Hg at 25°C) and the mean gap was calculated from the equation

$$\dot{m} = \frac{\pi . d . \delta}{L} (D_1 \Delta C_1 + D_2 \Delta C_2)$$

where $\dot{m}$ = mass flux

D = vapour diffusivity

ΔC = concentration of vapour inside the crucible in $g.cm^{-3}$

d = diameter of crucible

L = wall thickness

and δ = mean gap between crucible and lid

(a pure volatile liquid of known vapour pressure and diffusitivity could not be used because of condensation between lid and crucible).

Crucibles were treated with a strong acid solution of aluminium chloride which dissolved residual cryolite and aluminium from the previous run. The inside walls

were then ground with carborundum paste and, after drying, brushed to remove a surface coating of ground particles. The crucibles were finally rinsed in a jet of warm distilled water and dried for 30 minutes at 120°C. The charge consisted of 0.4-0.6 g. of metal and 3.6-3.9 g. of salt (the actual weights depended on the volume of the wells which varied slightly from one crucible to another).

In all runs (except those mentioned in Chapter 3) the boride-carbide crucible was contained in a graphite envelope. The lid was lightly compressed in position by a steel washer inserted between it and the graphite cap, which was attached to the envelope by means of a slot into which a carbon pin was fitted. Tight compression of the lid was liable to cause cracking of the envelope. This was taken as evidence that the crucible had a higher coefficient of expansion than graphite, and therefore that during equilibration the lid adhered to the crucible.

The assembly was supported by 18 s.w.g. nicroalloy wire (Hall and Pickles Ltd.) threaded through the graphite cap and protected from it by an alumina sheath. This precaution was necessary since the wire was rapidly attacked when in contact with

graphite, leading to early brittle fracture. The length in the hottest part of the furnace was wound double to improve its strength, and had a satisfactory life up to 1250°C.

After making up, the assembly was inserted a small distance into the reaction tube whilst the furnace was vertical. The furnace was then tilted back 45°, and, whilst a flow of nitrogen was sweeping out residual air, the charge was lowered $\frac{1}{2}$" every two minutes. Thermal stresses in the tube were therby reduced to a minmum. The assembly was held in its chosen position by tightening the grub screw in the sleeve of the 3" pulley, which rested on the brass washer through which a small hole had been drilled to take the wire. The pulley was connected by a rubber band to a reduction pulley system driven by an electric motor and was rotated three times per minute.

When the crucible had been in the furnace for the required length of time, the furnace was brought back to the vertical, the screw holding the supporting wire in position loosened, and the assembly lifted smartly into the condenser. It was estmated that solidification of the melt took several seconds. Faster cooling, although desirable, was not possible

because of the poor thermal shock resistance of the crucible material (the average crucible life was 20 runs). The tube was flushed out with nitrogen for 15 minutes before removal and dismantling of the assembly.

The crucible lid was detached by hand, or if necessary by gentle tapping in a vice. The solidified salt was relatively soft (and was readily crumbled even when alumina was present) and the small well sample (weighing about 1g.) was extracted by drilling and scraping out with a sharpened high carbon steel rod. It was then carefully ground in an agate mortar, and loaded and sealed into a gelatin capsule for excess metal analysis.

Samples for NaF/AlF_3 ratio determination were taken from the large well. Here caution was necessary to avoid contamination by aluminium. The metal bead did not solidify in a fixed spot within the well and could be located only by persistent removal of salt.

2.6 ANALYSIS OF EXCESS METAL IN THE QUENCHED SALT

Gas volumetric techniques have been used successfully in this laboratory[116] for direct determination of a metal in the presence of soluble salt. Here however it was found that samples contained aluminium

carbide
~~metal~~, and the analysis was performed in two stages - (i) measurement of the total gas volume on immersion in HCl and (ii) determination of the hydrogen content of the evolved gas.

Discussion of the technique and of the origin of Al_4C_3 is included in Chapter 3.

2.6.1 Determination of Total Gas Volume on Immersion of Sample in N HCl

Description of Apparatus

A diagram of the gas volumetric flask (50 ml capacity) is shown in figure 10. The arm (B) could be attached to a horizontal capillary tube, of 2.17 mm mean dia. and 150 cm long, containing a mercury bead which enabled gas volumes of up to 5 ml to be read off. The end of the capillary protruded into a water thermostat which was kept at 25°C by a "Tecam" contact controller operated by a bi-metallic strip. At this temperature the vapour pressure of water over the N.HCl solution (22.7 mm) was below the saturated value for room temperature ($>$ 24°C) and so condensation of moisture in the capillary tube was avoided. A lead coil, through which cold tap water was passed, was placed in the bath. This had the object of balancing the heating and cooling cycles and thus of improving

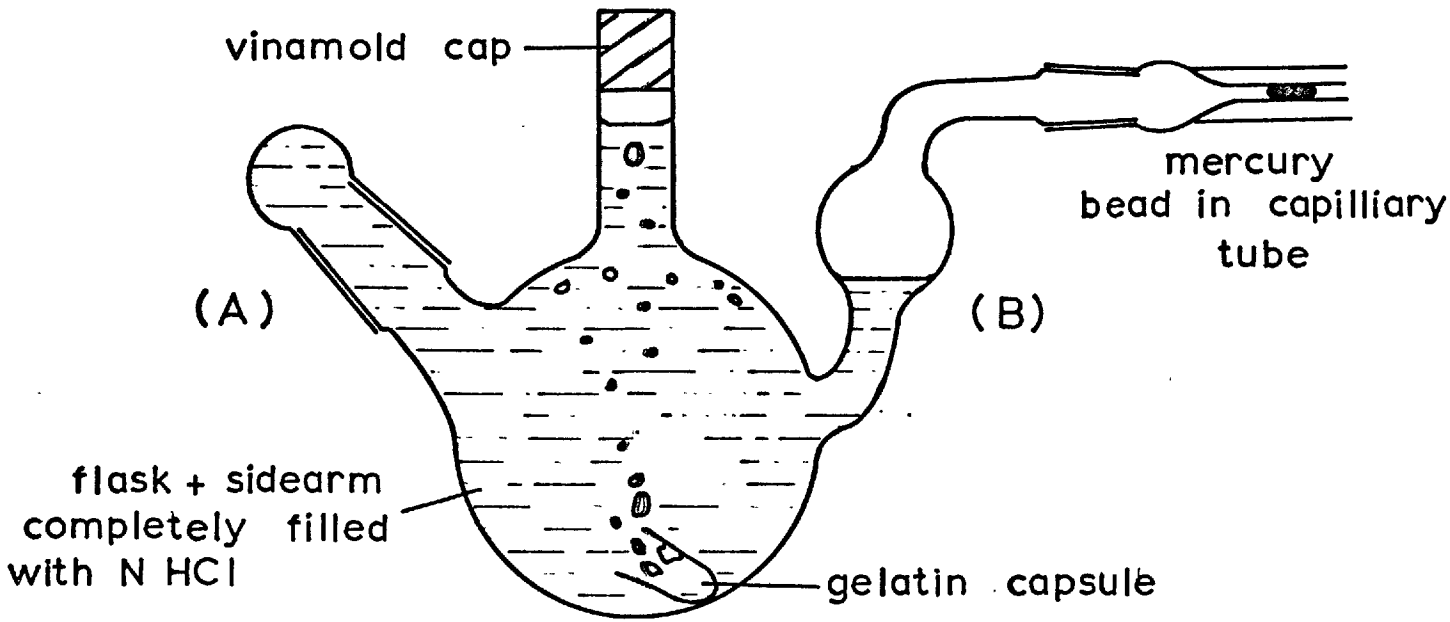

FIG. 10 GAS VOLUMETRIC APPARATUS

the degree of temperature control (which was $\pm$ 0.1°C).

A few drops of chloroplatinic acid were added to the acid solution in order to reduce the hydrogen overvoltage and thus to increase the rate of solution of metal.

Procedure

The flask was completely filled with acid and the capsule (20 mm long, 8 mm dia: suppliers Parke, Davis & Co.) containing the powdered sample was introduced via the arm (A), which was immediately stoppered off. A small amount of trapped air, together with excess acid, was removed by tilting, so that the acid level was in the lower section of the arm (B). The flask was connected to the capillary tube with the bath half empty, and which was then topped up over the "vinamold" cap. A few minutes elapsed before acid penetrated the capsule and gas evolution began, by which time the system had attained thermal equilibrium and the bead a steady position. The contents were stirred occasionally by means of a magnetic follower encased in glass, and the distance of travel of the bead noted after $2\frac{1}{2}$ hours, when dissolution was complete.

Nearly all the evolved gas was trapped in the neck (C) from which samples could be extracted by a syringe.

2.6.2 Chromatographic Gas Analysis: Instrument

Gas samples were analysed in a Model 25V Fischer Gas Partitioner containing two chromatographic columns. The first (30" long, ¼" o.d.) was filled with 60/80 mesh 30% hexamethylphosphoramide (HMPA), and the second (6½ feet long, 3/16" o.d.) with activated molecular sieve (30/60 mesh). The temperature was stabilized by an air thermostat at 60°C.

The thermal conductivity cell contained four thermistors forming the arms of a bridge circuit, one pair of which acted as references and the other as detectors. Since the instrument is most sensitive when the thermal conductivity of the carrier gas is considerably different from the components of the sample, hydrogen was determined against argon whilst methane and air were determined against helium. The cell currents were 7 ma and 5 ma respectively, and the inert gas flowrate was 80 ml/min in both cases. At the maximum sensitivity setting, deflections of up to 5 mv could be recorded by an AEI potentiometric recorder Type 10S on a 10 inch chart (speed 1" per minute).

Procedure

Calibration curves for hydrogen at 25% maximum sensitivity, and methane and oxygen at 10% maximum

sensitivity were determined on standard 0.4 ml gas samples. For all three gases the peak height-composition relationship was non-linear for deflections of less than two inches.

Because the "dead" space of the syringe was an appreciable percentage of the sample volume, the syringe was flushed with a portion of sample gas before injecting into the partitioner.

2.6.3 Determination of Final Melt Composition

Aluminium in the fluoride mixture was determined by a modification of the gravimetric 8-hydroxyquinoline method described by Hilldebrand and Lundell.[117]

Its accuracy is adversely affected by varying amounts of excess precipitant. For this reason a technique was adopted in which the pH was adjusted after adding a constant excess of 8-hydroxyquinoline to the solution containing aluminium ions.

The following reagent solutions were used:

50% H_2SO_4

2.5% 8-hydroxyquinoline in 2N acetic acid

40% ammonium acetate

50% ammonia

A 15% excess was chosen in standardisation experiments on 1% ammonium alum solution (table 6)

TABLE 6

Standardisation of Technique

No.	wt. of precipitate (g.) calculated	experimental	difference %
1	0.2030	0.2026	-0.2
2	"	0.2021	-0.4
3	"	0.2022	-0.4
4	"	0.2027	-0.1
5	"	0.2019	-0.5
6	"	0.2024	-0.3

The mean of the six determinations, 99.7%, was within 0.2% of the minimum specification (99.5%) of "analar" ammonium alum. Thus agreement was very good and this excess was adopted for all following analyses.

Procedure

Well ground samples of 0.1-0.15 g. (containing 0.02 g. Al) were fumed with 1 ml of 50% H_2SO_4 in a platinum basin. After fuming ceased, 5 ml of 6N HCl was added and the mixture heated gently until the caked material became dislodged. The contents were then transferred to a 600 ml beaker containing 100 ml of distilled water, and boiled gently for 10 minutes or until the solution became completely clear. An estimated 15% excess of the 8-hydroxyquinoline solution

was then added from a burette, followed by 10 ml of 40% ammonium acetate, drop by drop, with stirring. Precipitation was made complete by slowly adding 50% ammonia solution until the pH rose to the required value of 7.0. The precipitate was then digested on a steam bath for 30 minutes before being retained on a no. 4 sintered glass suction pad. After washing with warm distilled water it was dried at 120° to constant weight.

Analyses were performed in duplicate. The difference between the two single figures was consistently less than 0.5% of the total aluminium.

CHAPTER 3 PART A

PRELIMINARY RESULTS

3.1. Preliminary Solubility Measurements

Because of the unavailability of an inert container material at the start of this project, preliminary measurements were made in alumina, graphite and nickel containers. In this way it was hoped to gain some useful information on the behaviour of the aluminium + cryolite system.

The charge consisted of 1 g. of 99.99% pure aluminium foil (Hopkin and Williams Ltd.) and 2g. of laboratory prepared cryolite, which were equilibrated for 6 hours at 1050°C in a dry forming gas atmosphere. The melt was prepared by fusion of the stoichiometric proportions of purified NaF and AlF_3 (see Chapter 2). The first runs, with alumina saturated cryolite, were performed in crucibles of "Purox" recrystallised alumina (Morganite Refractories Ltd.), as this material had been used with some success by previous workers. However the crucibles of 1.5 mm wall thickness and 10 mm internal diameter were found to be pervious to the molten system after less than two hours equilibration. Graphite (EY9 grade) was then tried but to a lesser extent suffered from the same disadvantage, and extraction of clean samples of the solidified salt was found to be impossible.

Nickel crucibles were also tried. From the Al-Ni

phase diagram at 1050°C, a solid alloy would be formed in the presence of excess nickel. However as the rate of formation of such an alloy would be diffusion controlled, it was anticipated than an aluminium rich liquid alloy, in which the aluminium activity could be calculated, would still be present after several hours (the solubility using pure aluminium could then be derived from the activity data). This supposition proved to be correct, but again it was found to be impossible to remove uncontaminated samples. Altogether ten experments were attempted in different crucibles.

A technique which appeared to be more promising involved pinch sealing of 1 g. of cryolite and 1 g. of aluminium in a $1\frac{1}{2}$" length of $\frac{1}{4}$" diameter nickel tubing, and equilibrating in a rocking furnace (in which a dry nitrogen atmosphere was maintained) for 2 - 10 hours at 1050°C. On removal and quenching, the ampoules were sawn open and the cryolite and alloy bead scraped out. The per cent Ni in the alloy was determined gravimetrically by precipitation as nickel dimethylglyoxime. The quenched melt was screened to remove fine metallic particles and the coarse fraction analysed for aluminium by grinding under 5.0 ml of N/2 HCl solution and comparing the subsequent Na_2CO_3 titre with a standard. This analytical method was chosen because

of its simplicity and because possible oxidation of aluminium by the atmosphere was prevented.

Table P1 shows that reproducible results were not obtained. Samples of synthetic cryolite had slightly alkaline properties, and the solubility was calculated assuming that the increase in basicity after equilibration was due to oxidation of H^+ ions by the metal.

TABLE P1

Solubility of Aluminium in Cryolite at 1050°C

Run No.	Cryolite Sample	Time at 1050°C (hours)	Solubility of Al (wt %)	Atom % Ni in Alloy
1	A	2.5	0.174	30.3
2	A	2.6	0.102	27.7
3	A	2.5	0.445	30.5
4	A	2.5	0.157	30.6
5	A	9.5	0.012	34.1
6	A	9.5	0.118	36.4
7	A	9.6	0.118	43.3
8	B	2.7	0.156	29.7
9	B	2.5	0.132	30.1
10	B	3.1	0.091	29.7
11	B	2.6	0.212	30.4
12	B	2.6	0.307	30.1
13	B	4.4	0.032	30.9

CRYOLITE A:- initial NaF/AlF_3 ratio = 1.500

wt. loss on fusion = 9.5% of initial charge

alkaline reaction (mean of seven determinations) = 0.515 $\pm$ 0.05 ml. N/2 HCl per g.

CRYOLITE B:- initial NaF/AlF_3 ratio = 1.476

wt. loss on fusion = 26.3% of initial charge

alkaline reaction (mean of three determinations) = 1.64 $\pm$ .10 m. N/2 HCl per g.

There were intrinsic disadvantages in the method which could not be overcome. It was never certain that the salt phase was completely free from nickel contamination and that the coarse fraction analysed was representative of the whole sample.

The analytical technique which was found later to be unsatisfactory is discussed in the next section.

3.2 Preliminary Solubility Measurements in TiB_2/TiC Crucibles

The method of equilibration chosen was to rock the crucible containing 3 g. of molten cryolite and 0.8 g. of aluminium in the large well 45° from the vertical and back nine timesper hour. The temperature was maintained at 1050°C and the furnace tube flushed in a slow stream of dry forming gas. Samples of the quenched

melt were scraped from the small well in a dry box under argon. The results using the same analytical technique as before are shown in Table P2.

TABLE P2

Aluminium Solubility in Cryolite at 1050°C

Run No.	Cryolite Sample	Time at 1050°C (hours)	Wt. Sample (g.)	ml.of N/2 HCl neutralised per g.sample
1	C	14min.	0.3027	2.10
			0.3349	1.87
2	C	2.6	0.4827	0.87
3	C	2.8	0.4765	1.27
			0.4158	1.32
4	C	3.2	0.4478	0.62
			0.5332	0.61
5	D	4.0	0.2948	0.49
			0.3937	0.47
6	D	3.4	0.4942	0.27

CRYOLITE C:- initial NaF/AlF_3 ratio = 1.507

wt. loss on fusion = 17.5% of initial charge

alkaline reaction (mean of six determinations) = 1.54 $\pm$ 0.05 ml N/2 HCl per g.

CRYOLITE D:- initial NaF/AlF_3 ratio = 1.50

wt. loss on fusion = 6.9% of initial charge

alkaline reaction (mean of seven determinations) = 0.60 $\pm$ 0.03 ml N/2 HCl per g.

With the exception of the first run, the alkaline reaction was greater for the original cryolite samples, showing that the analytical technique was inapplicable.

Despite precautions, the weight loss on fusing sodium and aluminium fluorides was substantial, and in view of the significant vapour pressure of solid AlF_3, and of $NaAlF_4$ over liquid cryolite at about 1000°C, the product was likely to be enriched in sodium fluoride. If a small impurity of alumina were present then the alkaline reaction of the quenched salt could have arisen from a reaction described by the equation

$$NaAlO_2 + 4HCl = NaCl + AlCl_3 + 2H_2O$$

Because of further composition change during equilibration, subtraction of the basicity values of the originally prepared samples was not valid. For this reason the analytical technique was abandoned in favour of a gas-volumetric method, and the fusion of stoichiometric proportions of NaF and AlF_3 was discontinued.

3.3 Gas Volumetric Analysis

It was assumed that the gas evolved was hydrogen. A diagram of the apparatus is shown in figure 11.

3.3.1 Calibration

Weighed specimens of aluminium foil from which the

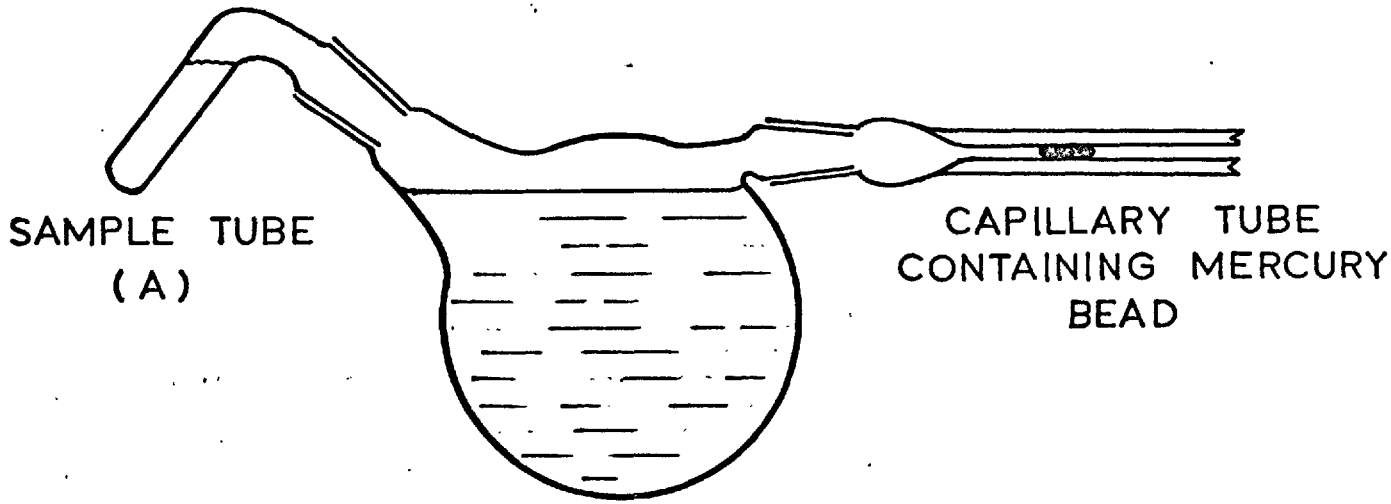

PRELIMINIARY

FIG.11 GAS VOLUMETRIC APPARATUS

oxide layer had been removed were dissolved in hydrogen saturated HCl in order to establish how closely the volume corresponded to the formula

$$2Al + 6HCl = 2AlCl_3 + 3H_2$$

The reproducibility was found to be $\pm$ .5%.

Previous workers[93] measuring the amount of metal phase in a metal + salt mixture found that dissolution of salt gave rise to a small constant positive volume change. Here however, this solubility was very small and no zero shift was detected on immersion of pure cryolite in the acid solution.

3.4 Results using Gas Volumetric Analysis

Table P3 shows the results of ten runs. In the first two synthetic cryolite D was charged, and in the remainder natural cryolite. The high temperature procedure was similar to that described earlier. Analytical samples were ground and stoppered under dry argon and immersed in hydrogen saturated N HCl solution by rotating the container (A) (figure 11). 0.7 g. of aluminium was added initially, and the cryolite deficit replenished after each run.

TABLE P3

Solubility of Aluminium in Cryolite at 1050°C

Run No.	Time at 1050°C (hours)	Wt. Loss (g.)	Solubility (wt.% Al)
1	3.2	-	0.076
2	7.0	-	0.085
3	3.4	-	0.039
4	2.1	0.0941	0.060
5	5.0	0.0645	0.140
6	2.2	0.0469	0.096
7	2.2	0.0501	0.065
8	2.4	0.0739	0.075
9	2.1	0.0677	0.083
10	2.0	0.0858	0.081

Nelgecting runs 3 and 5 the mean solubility figure was 0.078 ± 0.012 and the technique was considered to be promising.

However in subsequent runs a number of experimental difficulties arose. In run 11 (not shown) very little gas evolution occurred and on cleaning out the crucible no aluminium was found in the large well.

The alumina reaction tube fractured and was replaced by one of impervious mullite as this material was cheaper and had better resistance to thermal shock.

Because it is slightly attacked by hydrogen, forming gaseous silicon monoxide, argon was passed through the furnace. The wetting properties of aluminium on the crucible were then found to be affected. The metal either formed a thin film extending over the ridge between the two wells and into the small well itself, or else escaped from the crucible altogether. Great difficulty was experienced in separating lid and crucible after a run, which was achieved only by using a diamond saw. Contamination of analytical samples could not therefore be avoided.

For a reason which was not clearly understood no creep of aluminium occurred under an atmosphere of forming gas which was used (with recrystallised alumina tubes) for all later experiments. The lid was also readily removed, either by hand or by gentle tapping in a vice.

Comparison of weight losses and solubilities under argon and forming gas respectively are given in Table P4.

Because of a fault which developed in the rocking mechanism of the furnace, the method of agitation was modified to that described in Chapter 2, and was found to be satisfactory for all subsequent runs.

TABLE P4

Solubility of Aluminium in Cryolite at 1050°C

Run No.	Furnace Atmosphere	Wt. Loss (g.)	Equilibration Time (hours)	Solubility (wt.% Al)
12	Argon	0.4277	3.0	0.18
13		0.3887	2.3	0.38
14		0.3368	2.5	0.75
15		0.3284	2.8	0.13
16		0.2506	2.2	0.18
17		0.3634	0.7	0.11
18		0.6409	0.6	0.079
19		0.5616	0.5	0.076
20	Forming Gas	neg.	0.5	0.057
21		0.0223	0.5	0.062
22		0.0250	0.5	0.060
23		0.0440	0.5	0.033
24		neg.	0.5	0.048
25		neg.	0.9	0.062
26		neg.	0.6	0.057

3.5 Preparation of Samples

The samples containing fine metal particles were prepared under argon as a precaution against oxidation. As this was a time consuming procedure an experiment was conducted to see if it was necessary. At the same time the possibility of incomplete solution of metal was investigated.

Quenched melt from both wells (run 25) was lightly crushed in the dry box and approximately one third removed and ground to -150 mesh in air before immersion in HCl. Of the remainder one portion was charged directly into the flask whilst the other was ground in the usual manner before analysis.

Figure 12 shows the rate of gas evolution from the three samples.

The volume of gas per g. was identical in each case, but dissolution of the unground sample was appreciably retarded.

Grinding under argon was therefore unnecessary, and incomplete dissolution of metal could be discounted. In all succeeding runs samples were ground in air and 150 minutes allowed for completion of gas evolution.

3.6 Short Time Experiments

It was thought at this stage that saturation of the melt could be reasonably expected to be reached in

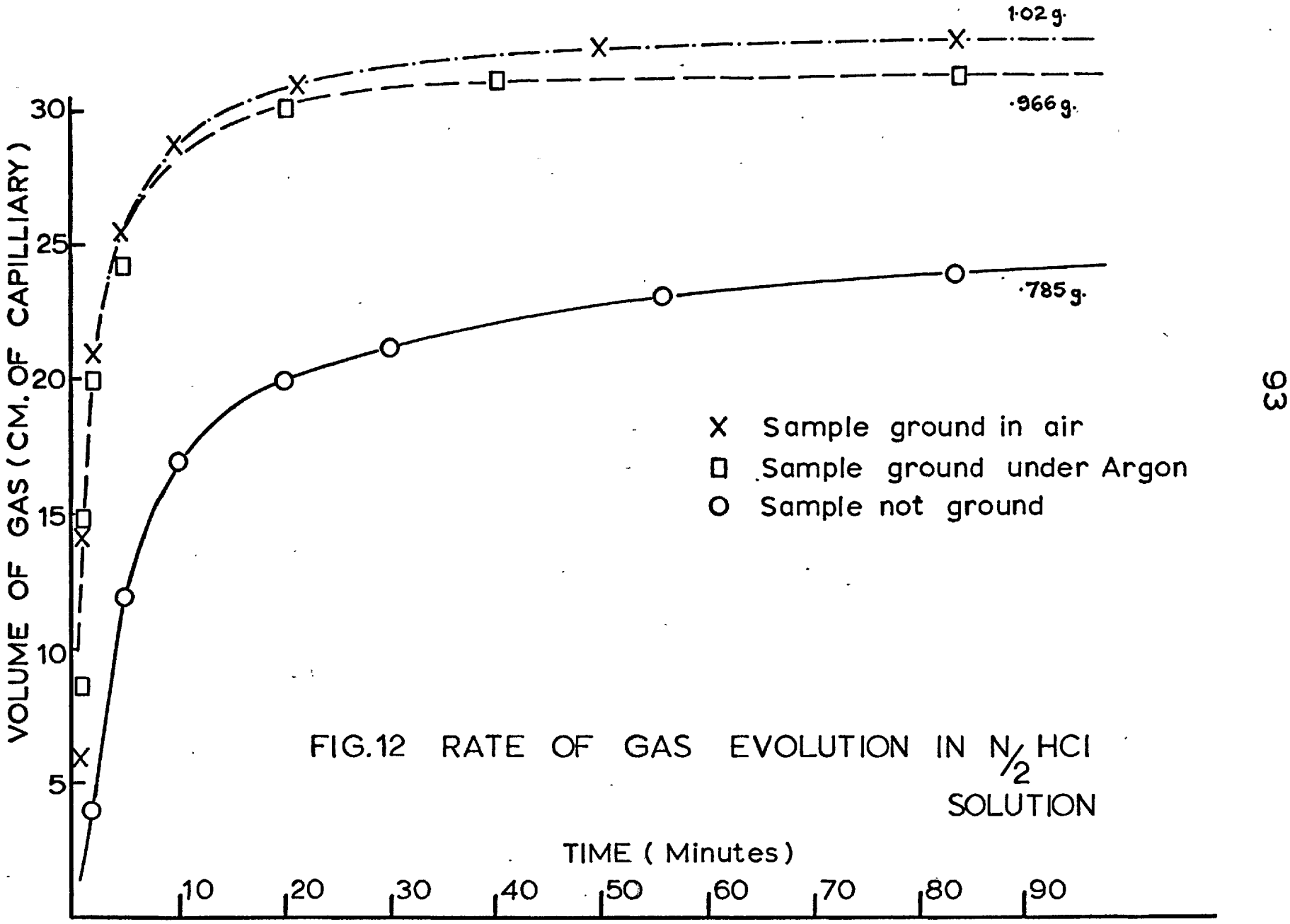

FIG.12 RATE OF GAS EVOLUTION IN N/2 HCl SOLUTION

a few minutes and no runs of greater than 40 minutes duration were attempted.

However reproducible results were still not obtained and it was found that cryolite samples equilibrated in the absence of aluminium gave off significant volumes of gas (see Table P5).

TABLE P5

Solubility of Aluminium in Cryolite at 1100°C

Run No.	Crucible	Wt.Loss (g.)	Time at 1100°(min)	Al Present	Solubility (wt.%Al)
1	C	0.0202	5		0.054
2	D	0.0150	5	No	0.011
3	D	0.0028	5	No	0.004
4	D	0.0003	5		0.053
5	D	0.0063	5	No	0.011
6	C	0.0132	10		0.106
7	C	0.0038	10	No	0.024
8	D	neg.	10		0.052
9	C	0.0146	10		0.050
10	C	0.0081	10	*	0.040
11	C	0.0066	10	*	0.040
12	D	neg.	20		0.055
13	C	0.0356	40		0.069
14	C	0.0138	40	No	0.046

*Al/Ag alloy containing 14.0 atomic % Ag.

This gas was considered to arise from insufficient cleaning of the crucible which thus contained residual aluminium metal (immersion in a warm solution of acid aluminium chloride for a few days was required for complete removal of salt).

It was then decided to extend the equilibration times to see if a constant solubility value was attained.

3.7 Determination of Time to Reach Saturation

Despite careful efforts to ensure reproducible conditions, no consistent pattern of behaviour was observed (Table P6).

TABLE P6

Solubility of Aluminium in Cryolite at 1100°C

Run No.	Crucible	Wt. Loss (g.)	Time at 1100° (hours)	Solubility (wt.% Al)
15	D	0.2808	14.5*	0.002
16	D	0.0608	6	0.107
17	D	0.0813	6	0.176
18	A	0.0667	12	0.169
19	A	-	12	0.167
20	D	0.1149	12	0.226
21	A	0.2220	12	0.163
22	D	0.0475	12	0.172
23	C	0.1930	26	0.248
24	D	0.3489	36	0.262
25	A	0.4436	36	0.288
26	D	0.3958	44	0.232
27	D	0.4945	45	0.209
28	D	0.4243	49	0.338

*no aluminium charged

A negligible volume of gas was evolved from the material from the blank run (no. 15) in a thoroughly cleaned crucible, which was taken as confirmation that the previous samples were contaminated with aluminium.

It appeared that the melts were unsaturated even after 26 hours equilibration. At this point it was thought that either a fine dispersion of aluminium was formed mechanically or from thermal fluctuations, or else that the solubility was markedly dependent on the melt composition and, as enrichment in AlF_3 occurred, so the solubility limit increased with time.

In order to test the first hypothesis experiments were performed using an Al/Ag alloy containing 86.0 atom% aluminium (39.4 wt.% Ag) which had a density of 3.60 $g.cm.^{-3}$ at room temperature compared with 2.70 for pure Al. Silver was chosen because of its unreactivity and high density (10.5), and because the thermodynamic properties of liquid Al - Ag alloys have been established.[118] The Ag content of the alloy was analysed gravimetrically by dissolution in nitric acid and precipitation as chloride. The results are shown in Table P7.

TABLE P7

Solubility of Aluminium in Cryolite at 1100°C
(in equilibrium with an Al/Ag alloy)

Run No.	Crucible	Time at 1100°C (hours)	Wt.Loss (g.)	Final Alloy Comp. (atom %Al)	a_{Al}	Measured Soly. (wt.%Al)	Solubility $a_{Al}=1$
29	D	6	0.0946	(83.0)	(0.83)	0.136	(0.164)
30	D	26	0.1832	70.0	0.70	0.115	0.164
31	A	26	0.1697	66.0	0.66	0.215	0.325

The high result of no. 31 indicated that the possibility of formation of a metallic dispersion in previous runs could be ruled out.

Since the final activity of aluminium in the alloy was apparently not related to the solubility value, the possibility of the melt never becoming saturated with respect to aluminium because of vaporisation losses was investigated (although hermetic sealing of the crucibles was highly desirable there appeared to be no convenient way of achieving it). However mass transfer calculations showed that this situation was extremely unlikely.

Alternatively a marked dependence of the saturation limit on the $NaF-AlF_3$ ratio was a possible explanation for the data obtained and large well material from runs at three different temperatures was retained for analysis.

3.8 Melt Analyses

Table P8 shows the Na, Al and F compositions of five samples. Since titanium forms the stable anion TiF_6^{2-} the melt Ti content of two runs was also determined. The analyses were kindly performed by the Electrochemical Research Group of the British Aluminium Company, Kinlochleven.

TABLE P8

Melt Compositions after Equilibration

Run No. Temp.°C	32 1020	33 1020	34 1020	35 1100	36 1140
Elementary Analysis					
Al	13.9	14.8	18.4	14.0	13.6
Na	31.0	29.8	24.5	30.8	32.0
F	54.8	55.4	56.3	55.0	54.5
Total	99.7	100.0	99.2	99.8	100.7
Rational Composition					
Na_3AlF_6	94.5	90.7	74.4	93.7	97.3
excess AlF_3	5.4	9.0	23.5	6.1	2.5
Al_2O_3	0.1	0.5	2.4	0.1	0.6
Total	99.8	100.2	100.3	99.9	100.4

Titanium Analyses:	Run No.	Temp.	Wt.% Ti
	37	1100	0.006
	34	1020	< 0.001

Aluminium and sodium were determined on 0.2 g. sample by fuming with sulphuric acid, precipitating the aluminium as hydroxide and weighing as oxide, and estimating the sodium in the filtrate gravimetrically as sodium sulphate. Fluorine was determined on 0.1 g. sample by the Willard and Winter method of distillation with sulphuric acid and titration of the distillate with thorium nitrate solution.

Titanium was determined on 0.2 g. sample by bringing into solution with sulphuric acid and potassium bisulphate, followed by a photometric estimation using peroxide.

The results show that Ti pick up by the melt was negligible.

The excess AlF_3 could be calculated directly from the aluminium percentage, and the values so derived and those from the Na and F analyses (rational composition) are compared in Table P9 (p. 100).

The discrepancy between the two sets of figures was attributed at the time to insufficient care in collection of samples, which were liable to contamination by aluminium metal. This would have accounted for the apparent appreciable alumina composition, since the equilibration technique precluded the gradual

pick-up of oxygen by the melt.

TABLE 9

Melt Composition after Equilibration: estimation of excess aluminium fluoride from aluminium analysis

Run No.	32	33	34	35	36
Al	13.9	14.8	18.4	14.0	13.6
AlF_3	43.3	46.1	57.3	43.6	42.3
$100-AlF_3=NaF$	56.7	53.9	42.7	56.4	57.7
Na_3AlF_6	94.5	89.8	71.2	94.0	96.2
Excess AlF_3	5.5	10.2	28.8	6.0	3.8
" *	5.4	9.0	23.5	6.1	2.5
" †	5.5	9.3	25.6	6.3	2.7

*from rational composition †from ($100-Na_3AlF_6$) Table P8

As the error involved in estimating the excess AlF_3 from the single aluminium analysis was no greater than that from the sodium and fluorine compositions, in later runs melt samples were analysed only for aluminium.

The results at 1020°C indicated that the solubility limit was highly dependent on composition, increasing with increase in AlF_3 content.

TABLE P10

Solubility of Aluminium in $NaF-AlF_3$ at 1020°C Melt as a Function of Composition

Run No.	Crucible	Time (hours)	Final Melt Composition (mol fraction AlF_3)	Solubility wt. % Al
32	D	5.0	0.275	0.052
33	A	15.2	0.299	0.075
34	A	45.0	0.403	0.150

Runs at 1100°C were continued in order to check the validity of this relationship.

3.9 Composition Dependence of Solubility

As a minimum solubility at the cryolite composition had recently been mentioned in the literature,(119) runs with NaF enriched melts were carried out and, in order to find the time required to reach saturation, an attempt was made to terminate runs of different weighed in mol ratio of NaF to AlF_3 at a constant composition (28.0 mol % AlF_3).

The results (Tables P11 and P12) were widely discrepant. A trend of decreasing solubility with increase in NaF content was however observed for each crucible (Table P11).

3.10 Gas Analysis

Up to this stage it had been assumed that the gas evolved on immersion of the quenched melt in HCl was

TABLE P11

Solubility of Aluminium in Cryolite at 1100°C
As a Function of Composition

Run No.	Crucible	Equilibration Time (hours)	Wt.Loss (g.)	Melt Composition mol % AlF_3 Initial	Final	Solubility wt.% Al
38	B	14.0	.1581	0.250	0.311	0.176
39	B	20.0	.1276	0.250	0.307	0.180
40	B	44.2	.2464	0.250	0.318	0.213
41	B	50.7	.2046	0.250	0.337	0.258
42	B	55.3	.2971	0.250	0.358	0.316
43	G	21.0	.2486	0.250	0.288	0.229
44	G	24.2	.0888	0.250	0.288	0.216
45	G	29.5	.1323	0.250	0.294	0.283
46	G	34.8	.1258	0.250	0.296	0.307
47	G	43.5	.1628	0.250	0.311	0.313
48	G	45.2	.1607	0.250	0.311	0.315
49	J	5.0	.0188	0.184	0.211	0.141
50	J	5.0	.0473	0.184	0.206	0.109
51	J	4.0	.0736	0.230	0.251	0.054
52	J	2.5	neg.	0.332	0.348	0.182
53	J	15.0	.2094	0.332	0.369	0.292
54	H	5.0	.0681	0.163	0.186	0.120
55	H	20.0	.1924	0.184	0.246	0.140
56	H	12.0	.1472	0.206	0.249	0.111
57	H	12.6	.1482	0.206	0.241	0.166
58	H	16.0	.1708	0.206	0.244	0.099

TABLE P12

Solubility of Aluminium in an $NaF-AlF_3$ Melt Containing 28.0 mol% AlF_3 at 1100°C

Run No.	Crucible	Equilibration Time (hours)	Wt.Loss (g.)	Melt Composition mol % AlF_3 Initial	Melt Composition mol % AlF_3 Final	Solubility wt.% Al
59	H	1.0	.0095	0.273	0.286	0.057
60	H	1.0	.0206	0.268	0.279	0.132
61	K	1.0	.0198	0.268	0.281	0.142
62	K	1.0	.0013	0.266	0.286	0.087
63	H	2.0	.0125	0.268	0.281	0.111
64	H	2.0	.0339	0.266	0.279	0.105
65	K	2.1	.0525	0.266	0.281	0.101
66	H	4.0	.0292	0.266	0.288	0.095
67	K	4.1	.0606	0.255	0.279	0.155
68	K	12.0	.1645	0.213	0.279	0.211
69	K	16.0	.1698	0.206	0.255	0.172
70	K	28.0	.3017	0.206	0.294	0.255

100% hydrogen. To verify this some gas samples were collected and analysed on the gas partitioner (see Chapter 2 p. 77). The presence of methane, which was identified from the sequence of peaks on the chromatogram and by its combustion with a bluish yellow flame, was quite unexpected. Al_4C_3 is more unstable than TiC by 20 kcal per g. atom C at 1000°C and its formation and dissolution had thus been discounted. Furthermore, with the sole exception of Haupin[56] who used graphite crucibles, no reference to carbide dissolution in NaF-AlF_3 melts had been published.

Because of the need to analyse the gas mixture for hydrogen, the simple arrangement of figure 11 was inadequate and the method described in Chapter 2 p. 74 was developed. The evolved gas was found to be entirely methane + hydrogen.

The results of ensuing runs are presented in part B of this chapter.

3.11 Correction to Data: Melt Composition

The earlier estimation of the excess AlF_3 content of the melts, from the aluminium analyses alone, were in error due to carbide reporting as fluoride. This also partly accounted for the discrepancy between the data of Table 9. Corrected analyses are given in Appendix B (Tables I-VI).

3.12 Determination of Methane Solubility in N HCl at 25°C

The original purpose of saturating the acid solution with hydrogen was to ensure that the measured gas volume on dissolution of a sample represented the true volume evolved. Once it was appreciated that a considerable quantity of methane was present the acid was left untreated and the measured volume had to be corrected for gas dissolution.

It was assumed that the acid was saturated with respect to each gas and that the solubilities were proportional to the respective partial pressures (Henry's law). The first assumption was considered to be valid since a dense cloud of tiny bubbles were produced immediately on immersion of samples and 150 minutes were allowed for completion of gas evolution.

The solubility of hydrogen in N HCl has been measured[94], but as no corresponding data for methane was found in the literature, an apparatus was devised in which the solubility at 25°C and at various partial pressures could be determined.

A 50 ml gas bulb was necked at opposite ends, one of which was sealed with a "Vinamold" plug and the other with a rubber bung connected to a length of calibrated capillary. The flask was filled with air

free acid solution and immersed in a thermostat at 25°C. 2.0 ml of a known methane/nitrogen mixture from a syringe was introduced through the plug, and the bulb shaken at intervals until the capillary meniscus reached a steady position. The solubility could then be calculated from the methane content of the final mixture (which was analysed on the chromatograph).

The results are shown in figure 13. By extrapolation 100 ml of N HCl would dissolve 3.20 ml of methane at 25°C and 1 atmosphere pressure.

3.13 Dummy Runs

Two possible sources of error in the analytical technique were investigated. The first arose from reference in the literature to the evolution of a small quantity of hydrogen from the reaction between aluminium carbide and water,[95] and the second from contamination of samples in the removal operation by the high carbon steel drill or rod (p. 73).

To examine the two questions dummy equilibrations at 1100° in (i) and unused and (ii) previously used crucible were carried out. The results are shown on the following page.

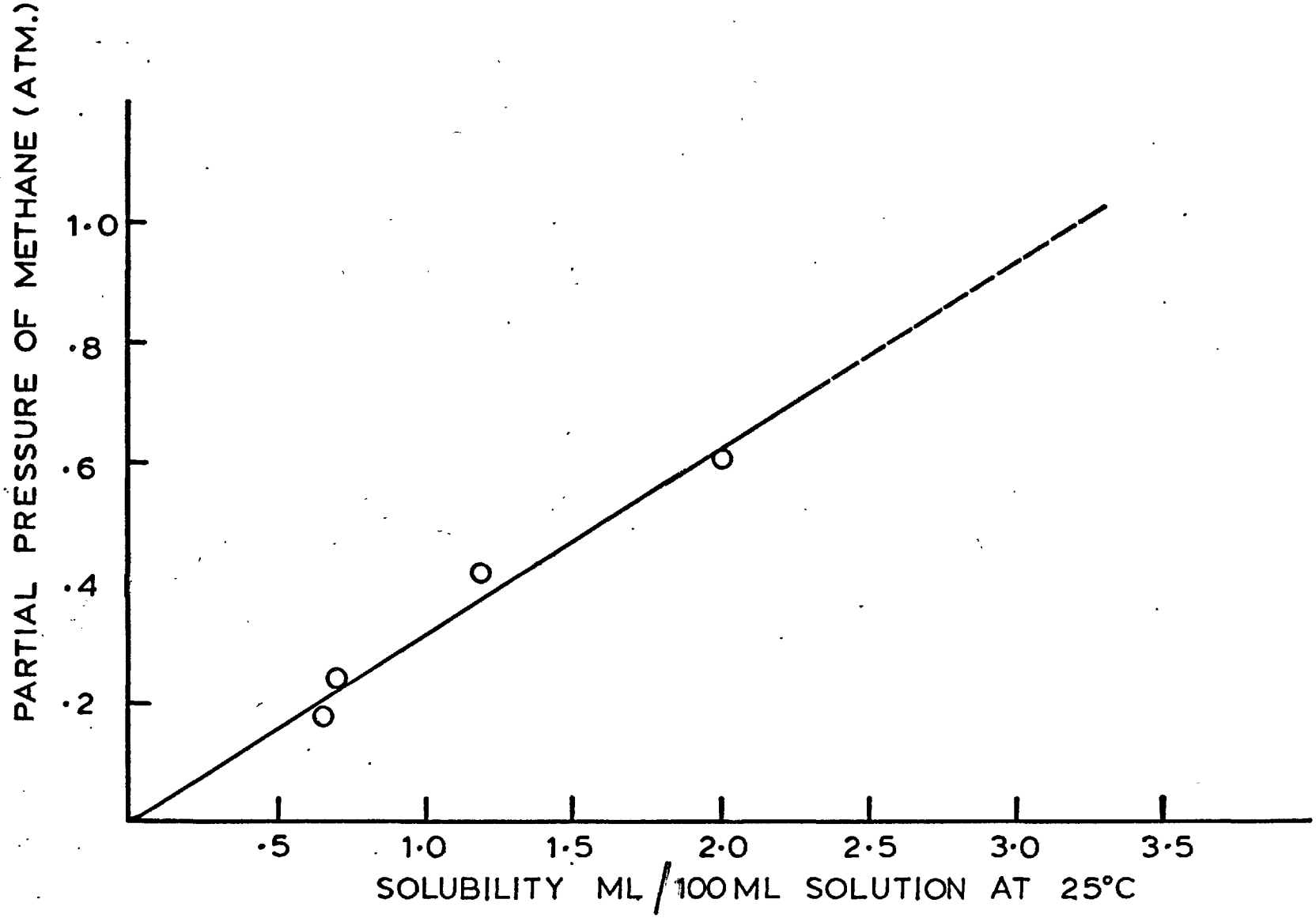

FIG .13 SOLUBILITY OF METHANE IN N HCl SOLUTION AT 25°C

TABLE 13

Dummy Experiments at 1100°C

Run No.	Crucible	Time (hrs.)	Final Comp. mol fraction AlF_3	Wt.Loss (g.)	Gas Composition %H_2	%CH_4	%air	Al_4C_3 wt.%
71	L	19.5	0.251	0.0392	neg.		100	-
72	H	12.5	0.261	0.0655	nil.	20	80	0.13

A neligible volume of gas was given off from the sample from the new crucible and the gas evolved from the sample in the second experiment was 100% methane.

It was thus concluded that the occurrence of contamination in the removal procedure was insignificant and that no error was incurred in assuming hydrogen to be derived solely from aluminium metal.

The previous explanation of gas from dummy runs (p. 96) was incorrect. The absence of gas in the earlier run (no. 15 Table P6) was possibly due to complete vaporisation of sodium from the reaction

$$Al_4C_3 + 24\ NaF = 4Na_3AlF_6 = 12Na + 3C \text{ (solid solution in TiC)}$$

CHAPTER 3 PART B

FINAL RESULTS

3.14 Time to Reach Saturation

Equilibrations were repeated for different periods of time at 1020°C in order to establish that saturation had been reached. Equilibrium with respect to aluminium was in fact attained in less than two hours but carbide dissolution increased steadily with time up to 20 hours (figures 14 and 15). The metal solubility appeared to be independent of composition over the experimental range (1.2-22.5 wt.% excess AlF_3).

Figure 14 also shows the results of measurements at 1100, 1180 and 1240°C. Full tables of data with their method of derivation is given in Appendix B.

3.15 Origin of Carbide

The reason for the presence of dissolved aluminium carbide was not immediately obvious. Two possible causes were considered: (i) diffusion of methane (formed from the attack of hydrogen on the graphite envelope) into the crucible where a reaction producing Al_4C_3 occurred and (ii) diffusion of carbon from the envelope through the crucible wall.

The partial pressure of methane in equilibrium with H_2 at 0.1 atm and carbon is about 0.6 mm Hg at 1020°C (ammonia formation from N_2 and H_2 at this temperature is very slight). Assuming the diffusion

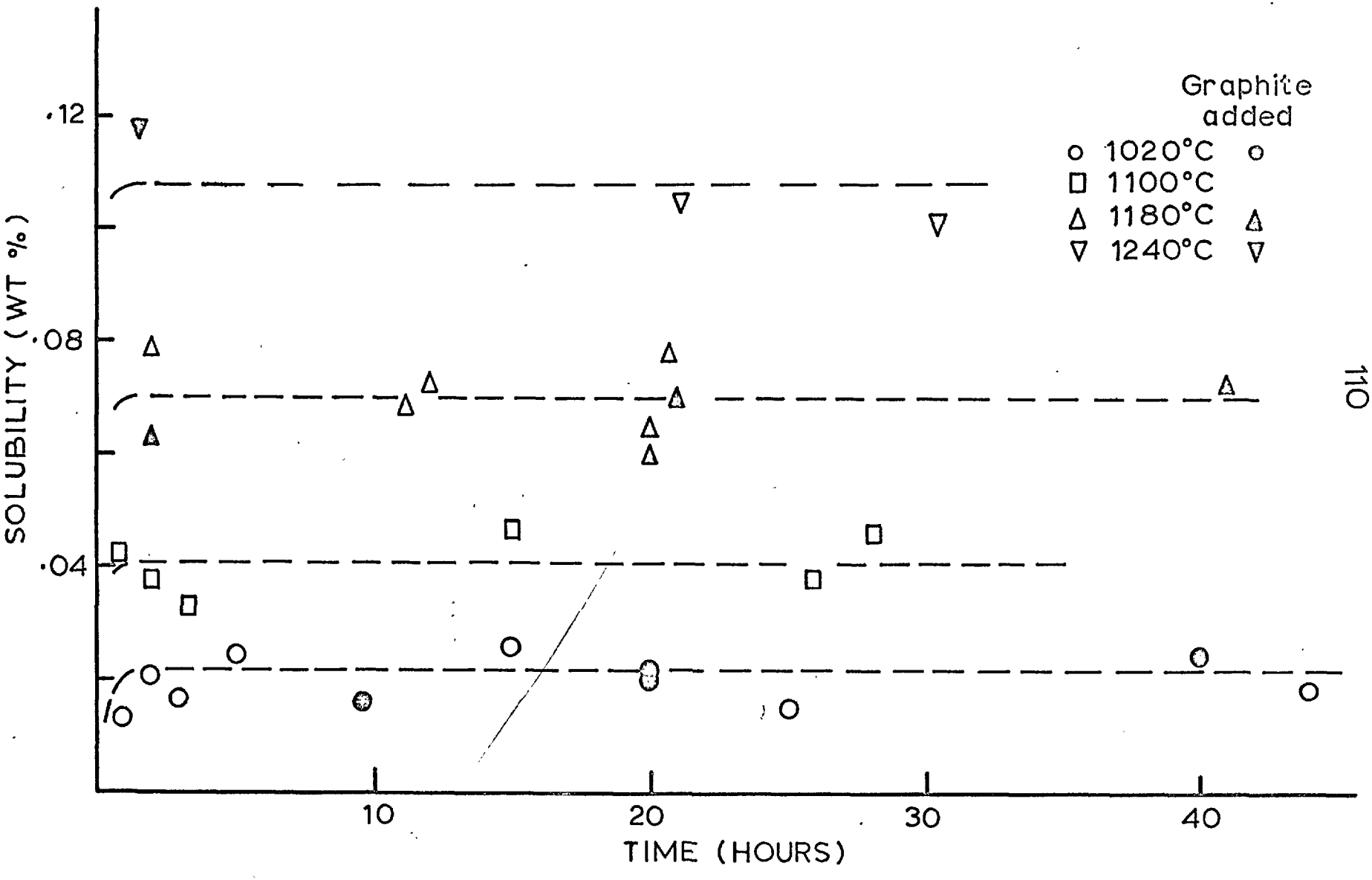

FIG.14 SOLUBILITY OF ALUMINIUM IN $NaF-AlF_3$ MELT

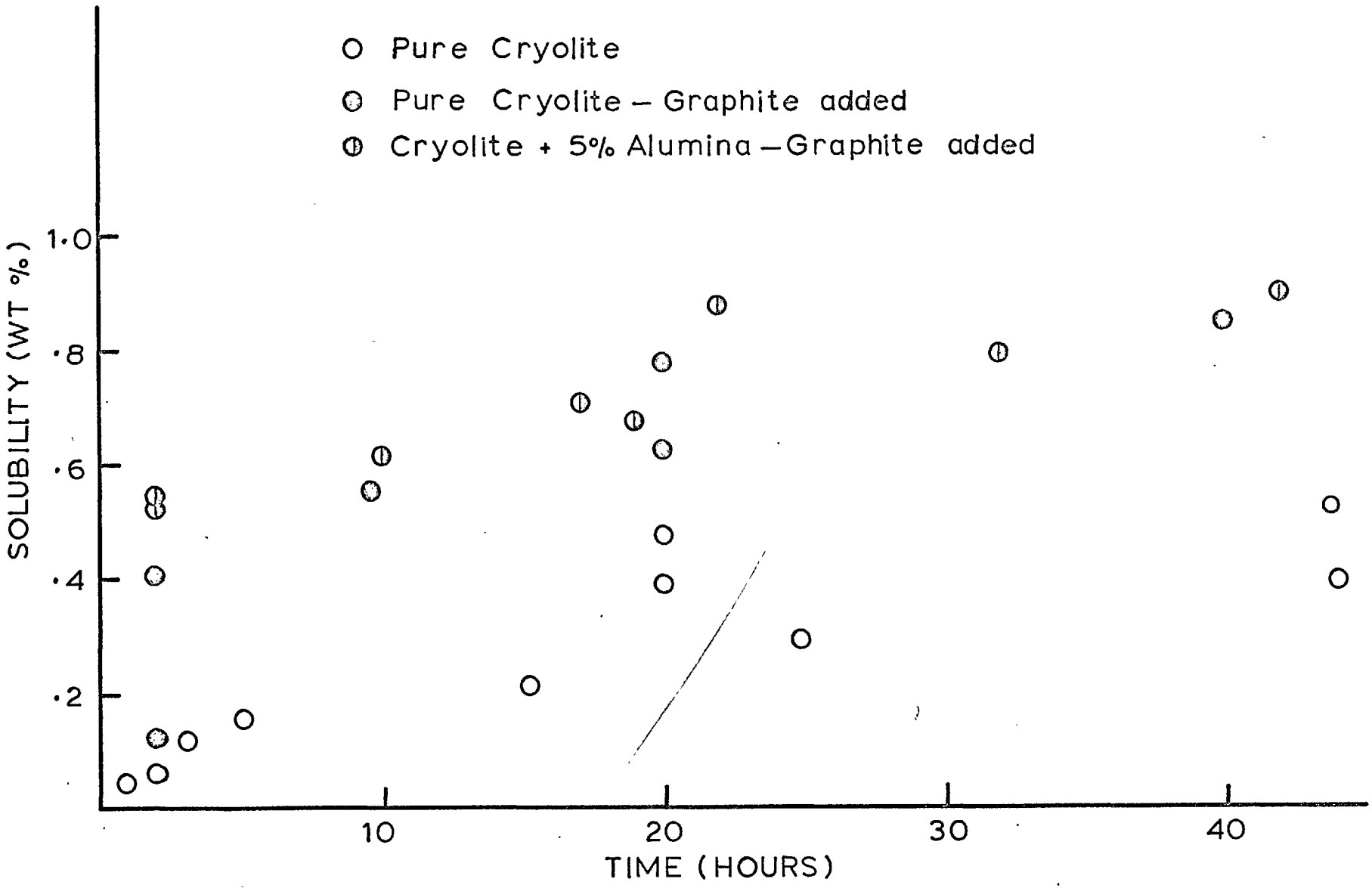

FIG. 15 SOLUBILITY OF ALUMINIUM CARBIDE IN $NaF-AlF_3$ MELT AT 1020°C

of methane into the crucible to be the rate controlling step in the dissolution of carbide and by assigning a reasonable value to the diffusivity, the rate of pick-up was calculated to be somewhat lower than that observed, but of the same order of magnitude. At 1180°C the formation of carbide would have been slower since the partial pressure of CH_4 was smaller (about 0.3 mm). However the opposite was the case (figure 16), showing that methane was unlikely to be the cause of the presence of carbide. This was confirmed by an experiment conducted in an atmosphere of nitrogen, in which the rate of carbide formation was unaffected (run 96 Table II).

Calculations to assess the significance of the second possibility were inconclusive, due to difficulty in estimating reasonable values of the variables involved. But it appeared that graphite acting as a source of carbide was not out of the question if a grain boundary diffusion mechanism and a substantial solid solubility of carbon in the crucible were assumed.

However in a run (no. 98 Table II) in which the graphite envelope was replaced by one of mild steel ($a_c < 0.1$) no significant reduction in the rate of carbide formation was detected, and it was concluded that the carbide originated from the crucible material

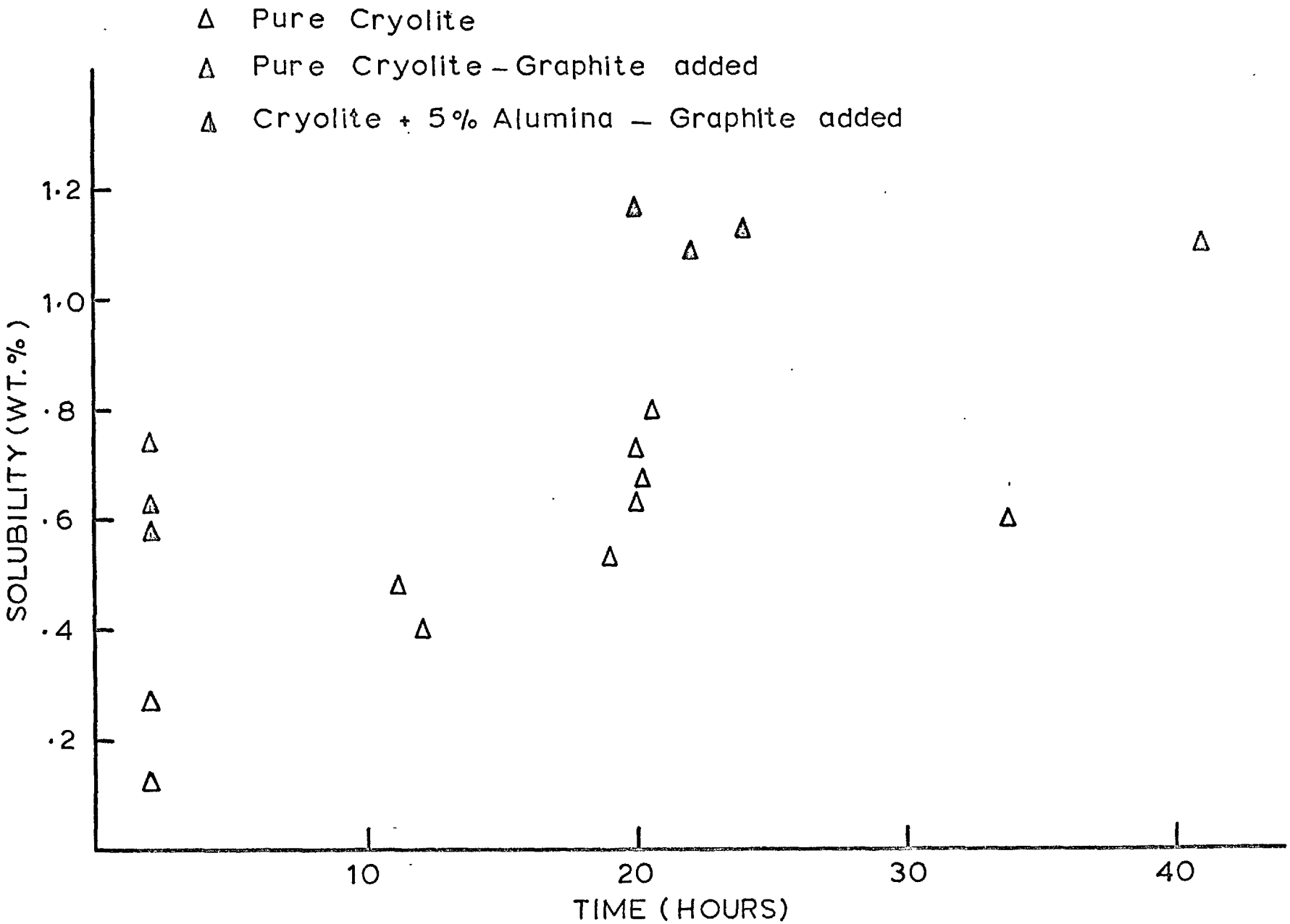

FIG.16 SOLUBILITY OF ALUMINIUM CARBIDE IN $NaF-AlF_3$ MELT AT 1180°C

itself. This matter is further discussed in Chapter 4.

3.16 Solubility Measurements in the Presence of Graphite

The metal solubility appeared not to be significantly affected by varying concentrations of carbide in the melt. This was verified in experiments in which 0.05 g of small lumps of graphite was added to the large well (figure 14).

However the carbide solubility was higher, and increased with increasing time and thus with increasing AlF_3 content of the melt (figures 15 and 16: Tables I-II Appendix B).

3.17 Solubility Measurements on Melts containing added 5% Alumina

This composition was chosen because it is near the maximum normally encountered in the industrial process. Graphite was added in all runs in order to see if the presence of dissolved alumina affected the solubility limit of Al_4C_3.

The results of these experiments are shown in Table III, Appendix B and in figures 17 and 15. The solubility of aluminium was markedly higher than in corresponding pure fluoride melts, but the saturation

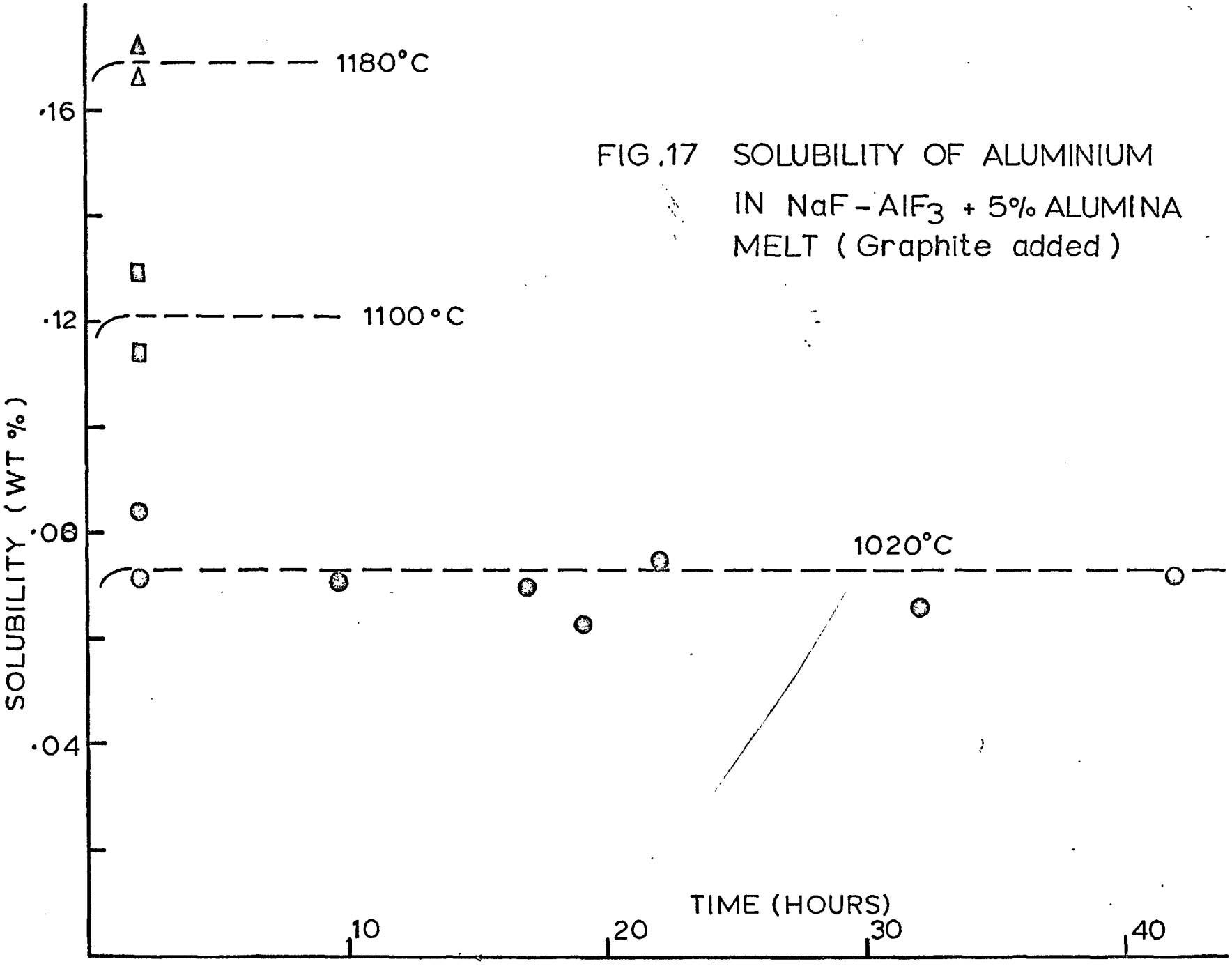

FIG. 17 SOLUBILITY OF ALUMINIUM IN $NaF-AlF_3$ + 5% ALUMINA MELT (Graphite added)

limit of aluminium carbide was similar.

Analyses of the final melt compositions, which were carried out at the B.A. Electrochemical Research Laboratories, Kinlochleven, are shown in Table 14.

3.18 Errors in Solubility Figures

The standard deviations of the solubilities at 1020, 1100, 1180 and 1020° (5% alumina melts) are shown in Table 15 (the results at 1240° were too few to be statistically treated).

TABLE 15

Temp. °C	No. of Determinations	Mean Solubility (wt.% Al)	Standard Deviation
1020	11	0.022	± 0.004
1100	6	0.041	± 0.006
1180	9	0.072	± 0.009
1020	8	0.073	± 0.006

The standard deviation was greater for the higher temperature measurements, but the relative error amounted to 20% of the solubility figure at 1020°C.

The major contribution to the final error arose from the error in the gas analysis. The measured percentage of hydrogen+methane+air varied between 95 and 105%. The uncertainty in the hydrogen analysis

TABLE 14

Analysis of Cryolite + 5% Alumina Melts

Run No.	Elements				Rational Composition		
	Al	Na	F	Total	Na_3AlF_6	Exc.AlF_3	Al_2O_3
107	15.2	30.4	51.8	97.4	92.5	2.4	3.9
108	15.2	30.5	51.6	97.3	92.8	1.8	4.4
109	16.1	29.0	52.7	97.8	88.3	7.0	3.6
110	16.2	28.5	53.0	97.7	86.6	8.8	3.1
111	16.6	28.5	52.6	97.7	86.6	8.2	4.3
112	17.8	27.1	53.0	97.9	82.5	12.1	4.9
113	17.7	27.1	53.6	98.4	82.5	13.0	4.3
114	18.2	25.5	52.8	96.5	77.6	15.8	4.5
115	15.4	30.1	52.4	97.9	91.6	3.8	3.5
116	15.3	30.3	51.6	97.2	92.1	2.4	4.0
117	16.0	29.5	52.0	97.5	89.7	4.9	4.3
118	15.9	29.5	51.5	96.9	89.7	4.1	4.6

was especially accentuated in the case of experiments at 1020°, since either the volume of gas evolved only permitted single determinations of the concentration of the components, or else the hydrogen percentage in the gas was less than 10%.

In comparison errors arising from the method of temperature measurement and control were likely to be insignificant. The temperature coefficient of solubility was 0.0002 wt.% per C° at 1020° and 0.0005 wt.% per C° at 1240°. An estimated error of $\pm$ 5° in measuring the melt temperature would have caused errors in the solubility figures of $\pm$ 0.001 wt.% at 1020° and $\pm$ 0.003 wt % at 1240°C.

3.19 Segregation of Al_4C_3

This could give rise to serious errors in estimating the final melt composition if the carbide content of the large well sample was different from that determined on the small well.

The results of duplicate analyses of a number of runs are presented in Table 16 and show that segregation of carbide was small enough to be ignored.

TABLE 16

Segregation of Aluminium Carbide

Run No.	Small Well wt.% Al_4C_3	Large Well wt.% Al_4C_3
84	0.13	0.14
86	0.63	0.57
96	0.27	0.24
102	1.08	1.01
103	1.10	1.13
107	0.55	0.55

3.20 Relation between Melt Composition and Weight Loss

Figure 18 shows that up to 1180°C vaporisation losses at the cryolite composition correspond almost entirely to sodium.

The curve was constructed in the following manner. A composition of 10 wt % Al (18.4 mol.% AlF_3) was taken as the origin and the first points were plotted for melts which started at this composition. Coincidence with the sodium vaporisation line (derived for a 3.8 g. melt: Appendix B) was found up to the cryolite composition and this gave a fresh origin for melts starting as pure cryolite. AlF_3 enriched melts were included in the graph by estimating an origin from the curve already drawn. Because of the uncertainties of

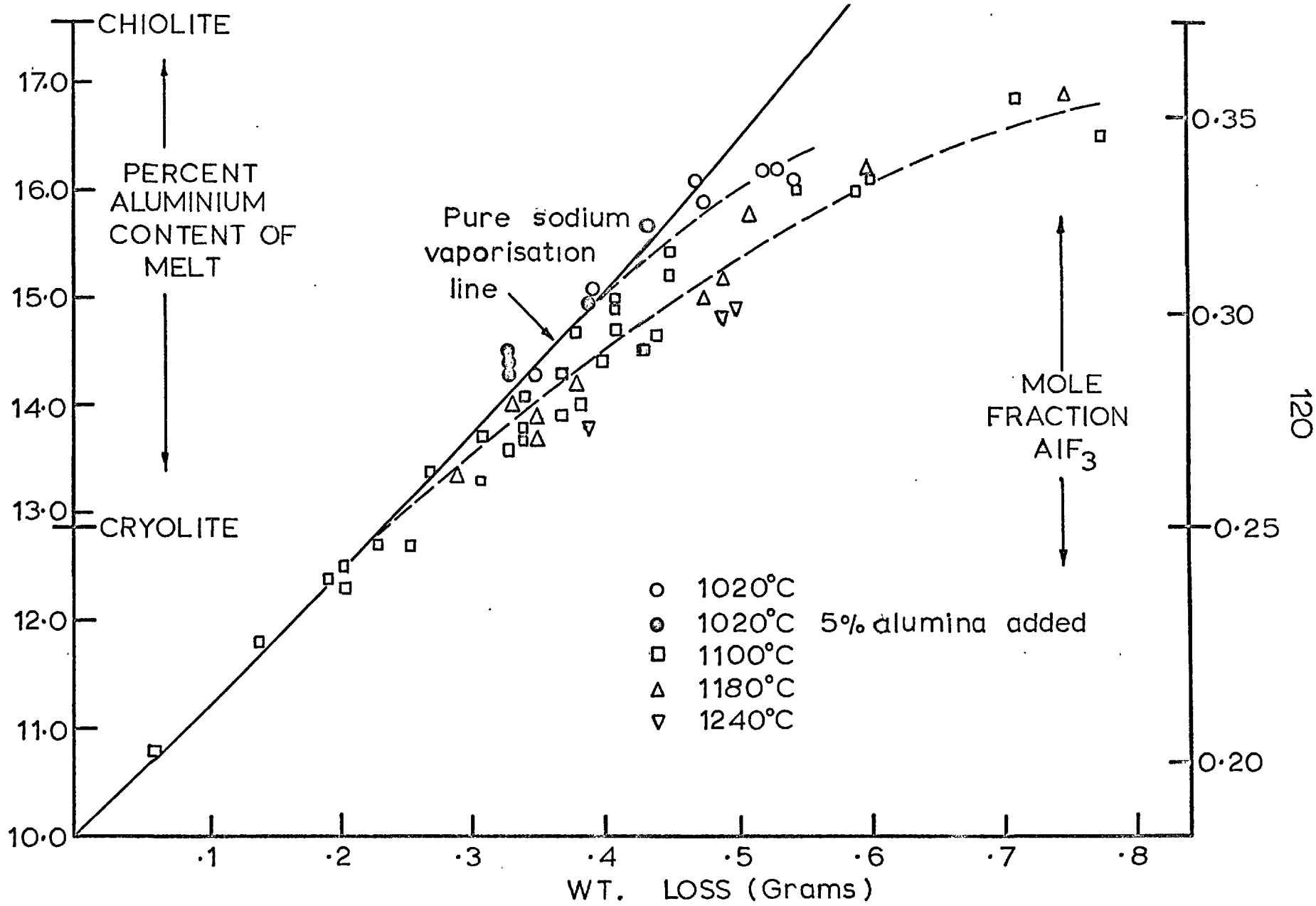

FIG.18 MELT COMPOSITION CHANGE AGAINST WT. LOSS

of the weight loss data, points were plotted only for runs in which this was 0.1 g. or higher.

At a given composition, the vapour pressure over the melt contained a higher percentage of an aluminium containing species at 1180° than at 1020°C.

CHAPTER 4

DISCUSSION

4.1 Comparison with Previous Investigations

This work has confirmed that the solubility figures for aluminium dissolution in cryolite reported by previous workers who determined the metal weight loss, are much too high (Table 5 p. 47), since the essential condition of attainment of equilibrium without material losses from the system was not fulfilled.

It has also shown that, because of carbide formation, gas volumetric analysis in the case of measurements in graphite or carbon containing crucibles is invalid, unless the hydrogen content of the evolved gas is determined. For this reason the results of Mashovets and Svoboda[55] and Zhurin[52] can be discounted. Mashovets and Svoboda's attempt to find the relationship between solubility and composition at 1060°C merely indicated that the rate of solution of Al_4C_3 increases with increase in the AlF_3 content of the melt.

Haupin[56] determined the percent hydrogen and methane and found up to 0.24 wt % Al_4C_3 to be present in the melt after 72 hours. In his experiments a large graphite crucible held 100 g. of metal and 750 g. of an $NaF-AlF_3$ melt containing 5% alumina and 8% CaF_2. The reported solubility figures of 0.09, 0.10 and 0.11 wt. % at 980° applied to melts whose final NaF/AlF_3

weight ratios were 1.14, 1.34 and 1.31 respectively (these figures are equivalent to excess AlF_3 contents of 11.5, 4.5 and 5.5 wt % in a pure NaF-AlF_3 melt).

These compare with a value of 0.056 wt.% obtained by extrapolation from the results of this work on melts containing an added 5% alumina and 1.8-15.8 wt.% excess AlF_3.

4.2. Mechanism of Solubility

Three types of mechanism describing aluminium solution in cryolite have been suggested in the literature and can be summarised as follows

(i) aluminium atoms

(ii) an aluminium compound in which the aluminium has a lower than normal valency

(iii) a dimerised form of sodium.

As there is no experimental evidence for atomic dissolution of metals in molten salts, which would require the valence electron orbitals to be unaffected by the surrounding solvent species, this possibility is of academic interest only and can be ignored.

The second mechanism has a sounder chemical basis, since AlF is known in the gaseous state, and subsalts are known to account for the dissolution of some metals in their molten halides (see p. 17). AlF would indeed

have a real activity in the melt, and in view of the highly polar nature of the electrolyte would most probably be present as Al^{+} and F^{-} ions.

A form of the third mechanism has been proposed by Bredig[11] in interpreting freezing point depression and conductivity data for the alkali metal - alkali metal halide systems and could originate in this case from the appreciable equilibrium partial pressure of sodium.

Thus aluminium dissolution in cryolite can be most profitably considered from the viewpoint of the two independent equilibria.

$$2Al + AlF_3 = 3AlF \quad \ldots \quad \ldots \quad \ldots \quad 4.2(i)$$

and

$$Al + 3NaF = AlF_3 + 3Na \quad \ldots \quad \ldots \quad 4.2(ii)$$

4.3 Composition Dependence of Aluminium Solubility in $NaF-AlF_3$ Melts

4.3.1 Calculation of a_{NaF}, a_{AlF_3} with respect to Composition at the Melting Point of Cryolite

The composition dependence of the solubility by either reaction (i) or (ii) would depend on the relationship between melt composition and the activities of the components NaF and AlF_3.

No experimental determination of these activities has been made, but they can be calculated by a method which entails establishing values at the cryolite composition, and then deriving further values over a composition range by a modification of the method used by Grjotheim.[8]

Data from experiments in which the sodium content of liquid lead or aluminium in equilibrium with melts of varying $NaF-AlF_3$ ratio was determined[4,121] have been ignored in these calculations because of (i) the large scatter of the results (ii) uncertainties in extrapolation of activity data for the binary alloy systems Na-Pb[122] and Na-Al[83,123] and (iii) use of melts saturated with alumina.[121]

First, Stokes and Frank's[85] measured partial pressure of sodium over aluminium+solid cryolite+melt (23 mm Hg: figure 5 p. 43) was used together with thermodynamic data for the reaction

$$Al_{(l)} + Na_3AlF_{6(s)} = 2AlF_{3(s)} + 3Na_{(g)} \quad \ldots \quad \ldots \quad 4.3(i)$$

$$\Delta G^\circ_{1282} = +60.50 \text{ kcal}$$

to calculate a_{AlF_3}, which was found to be 1.32×10^{-3} with respect to the pure solid as standard state. This value was then substituted in the expression for the equilibrium

constant for the reaction.

$$3NaF_{(l)} + AlF_{3(s)} = Na_3AlF_{6(s)} \quad \ldots \quad \ldots \quad \ldots \quad 4.3(ii)$$

$$\Delta G^{\circ}_{1282} = -27.87 \text{ kcal}$$

from which $a_{NaF} = 0.238$.

Since the presence of the AlF_4^- ion in molten cryolite has been demonstrated by various investigators (Chapter 1 section 1.5) a simple model of the NaF-AlF_3 system is proposed, which states that the melt consists of an ideal Temkin mixture of the ions Na^+, Al^{3+}, F^-, AlF_6^{3-} and AlF_4^- existing in mutual equilibrium. If, therefore, the free energies of formation of AlF_6^{3-} and AlF_4^- are known, the activities of the components NaF, AlF_3, Na_3AlF_6 and $NaAlF_4$ can be calculated over the whole composition range from the simultaneous equilibria

$$Na_3AlF_6 = 2NaF + NaAlF_4 \quad \ldots \quad \ldots \quad \ldots \quad 4.3(iii)$$

$$(AlF_6^{3-} = AlF_4^- + 2F^-)$$

and $$3NaAlF_4 = 2AlF_3 + Na_3AlF_6 \quad \ldots \quad \ldots \quad \ldots \quad 4.3(iv)$$

$$(3AlF_4^- = 2Al^{3+} + AlF_6^{3-} + 6F^-)$$

This however would be an extremely tedious procedure; but in view of the high stability of the AlF_6^{3-} and AlF_4^- ions, approximations can be made which simplify

the model of the molten mixture. At the cryolite composition for instance the activity of AlF_3 would be so small that its presence can be disregarded. The melt then consists essentially of Na^+, AlF_6^{3-}, AlF_4^- and F^- ions (this is the basic assumption made by Grjotheim[8, 61] and Rolin[62, 64] in their interpretation of the liquidus curve around the cryolite peak). In NaF enriched melts the model is further simplified because of the small AlF_4^- activity, and reduces to a mixture of Na^+, F^- and AlF_6^{3-} ions.

However the composition range of interest here is between cryolite and chiolite, as this covers the range of experimental measurements as well as the electrolyte compositions normally maintained in the reduction cell. It is also the most difficult part of the system to treat theoretically as all four component activities would be significant and would have to be taken into consideration.

The following simplified procedure was therefore adopted, in which the equilibrium constant K_1 for reaction (iii) was calculated, and from it the equilibrium constant K_2 for reaction (iv).

The degree of dissociation of cryolite, α_1, according to equilibrium 4.3(iii) was calculated to be 0.156 from the relation

$$a_{NaF} = \frac{2\alpha_1}{1+2\alpha_1}$$

$a_{Na_3AlF_6}$ and a_{NaAlF_4} (with respect to the pure hypothetical liquids) were then found from the expressions

$$a_{Na_3AlF_6} = \frac{1 - \alpha_1}{1+2\ \alpha_1} = 0.644$$

$$a_{NaAlF_4} = \frac{\alpha_1}{1+2\alpha_1} = 0.119$$

The value of α_1 is rather smaller than that reported by Grjotheim (0.25) and Rolin (0.204) and corresponds to a value of $K_1 = 0.0102$ for equilibrium 4.3(iii) ($\Delta G^\circ_{1282} = +\ 11.7$ kcal).

The equilibrium constant derived from the activity data for the reaction

$$3NaF_{(l)} + AlF_{3(s)} = Na_3AlF_{6(l)} \quad \ldots \quad \ldots \quad 4.3(v)$$

is 2.76×10^{-5} ($\Delta G^\circ_{1282} = -\ 26.8$ kcal)

This shows, as expected, that the pure hypothetical liquid cryolite is less stable than the pure solid at the actual melting point.

The degree of dissociation of sodium tetrafluoroaluminate was then estimated on the basis of the scheme 4.3(iv), in the following manner. The equilibrium

constant for the reaction

$$3NaAlF_{4(l)} = Na_3AlF_{6(l)} + 2AlF_{3(s)} \quad \ldots \quad \ldots \quad 4.3(vi)$$

obtained from the data on reactions (iii) and (v) was found to be 6.9×10^{-4} ($\Delta G^\circ = +18.6$ kcal), from which the equilibrium constant for reaction (iv), K_2, can be derived if the free energy change for the reaction

$$AlF_{3(s)} \rightarrow AlF_{3(l)} \quad \ldots \quad \ldots \quad \ldots \quad 4.3(vii)$$

at 1282°K is known. Neither the melting point nor the heat of fusion of AlF_3 has been reported, but the relative instability of the super-cooled liquid can be estimated by assigning a reasonable value to the melting point (1580°K compared to the sublimation temperature of 1554°K) and the entropy of fusion (8 eu). Neglecting differences in heat capacity between solid and liquid, ΔG° for reaction (vii) = + 2.4 kcal; from which K_2 [reaction (iv)] was found to be 2.63×10^{-4} ($\Delta G^\circ_{1282} = +21.0$ kcal).

The expression

$$K_2 = \frac{32.6^3 . \alpha_2^9}{(3+2\alpha_2)^2 (1-\alpha_2)^3 (3+4\alpha_2)^4}$$

which relates the activities of the components $NaAlF_4$, Na_3AlF_6 and AlF_3 (in terms of their ionic

fractions) to the degree of dissociation, α_2, of $NaAlF_4$, enabled α_2 to be calculated (0.335); from which $a_{AlF_3} = 1.8 \times 10^{-2}$ with respect to the supercooled liquid. a_{AlF_3} with respect to the pure solid as standard state is thus 4.5×10^{-2}, and using the data of equilibrium 4.3(v) $a_{NaF} = 3 \times 10^{-2}$.

Thus between cryolite and sodium tetrafluoroaluminate, the activity of AlF_3 rises from 1.32×10^{-3} to 4.5×10^{-2} whilst that of NaF falls from 0.238 to 3×10^{-2}. The activity values at the $NaAlF_4$ composition were then used as a check on the validity of the expression

$$K_1 = \frac{(2\alpha_i - \frac{n_2}{n_o})^2(\alpha_i + \frac{n_2}{n_o})}{(1+2\alpha_i)^2(1-\alpha_i)} \quad \text{[after Grjotheim}^{(8)}\text{]}$$

for equilibrium (iii) for calculating activities up to the chiolite composition (n_2, n_o are the respective weighed in mol fractions of cryolite and aluminium fluoride). It was found that the sodium fluoride activity would not have been significantly different had dissociation (iv) been taken into account, but a_{AlF_3} [derived from equilibrium 4.3(v)] values were too high. An arbitrary correction was made by drawing a smooth curve between the point for pure cryolite and $NaAlF_4$ (figure 19).

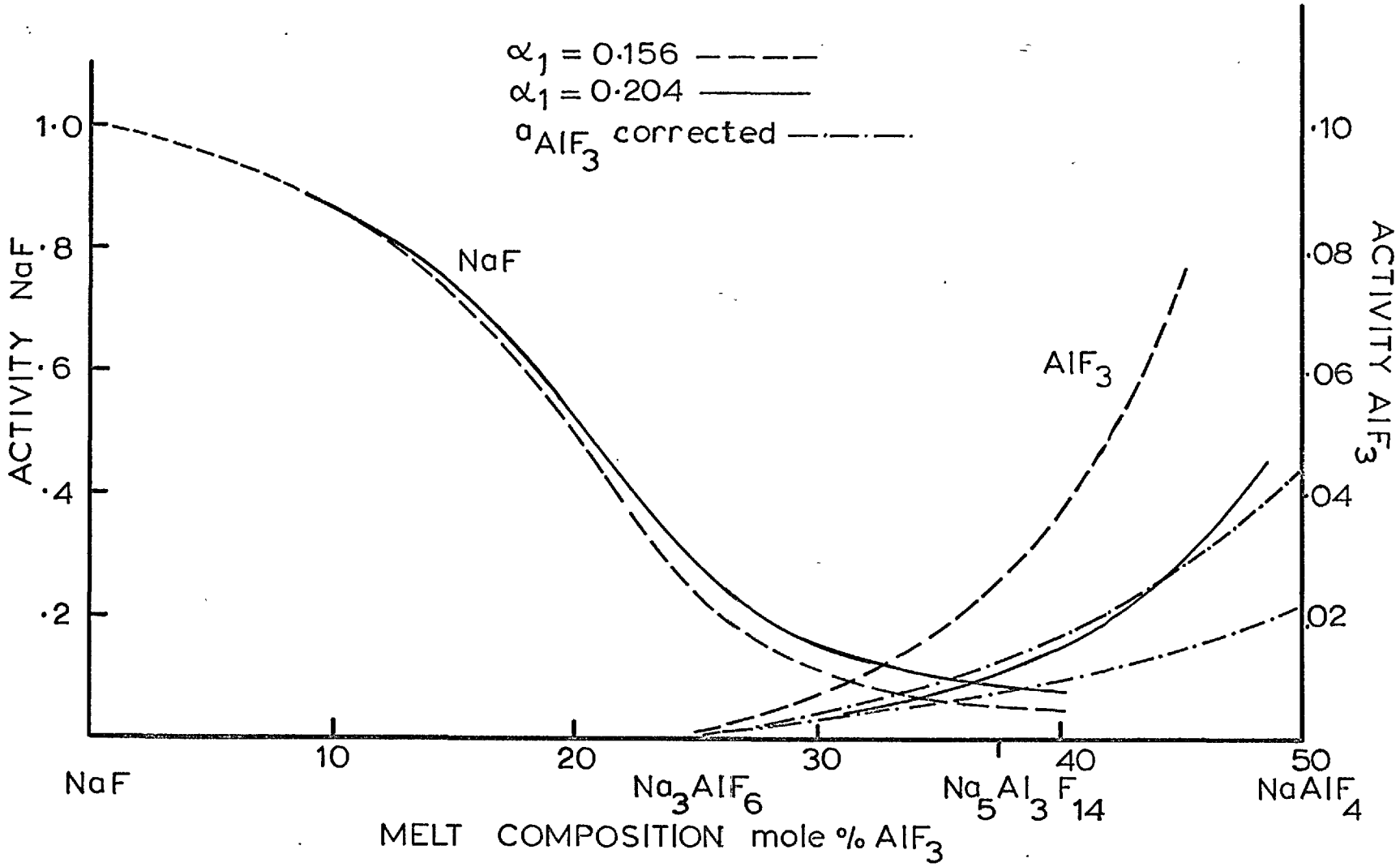

FIG. 19 ACTIVITY OF NaF AND AlF_3 IN NaF-AlF_3 SYSTEM AT 1009°C

4.3.2 Calculation of Na and AlF Partial Pressures with Respect to Composition

The partial pressures of sodium and aluminium sub-fluoride calculated from the activity data of figure 19 and from the thermodynamic data for reactions 4.2(i) and 4.2(ii) have been plotted in figure 20. P_{Na} falls from 23 mm at $3NaF.AlF_3$ to 2.5 mm at $5NaF.3AlF_3$. P_{AlF} is less highly dependent on composition and rises over the same range from 3.6 to 7.5 mm.

The high composition dependence of the sodium partial pressure (a 1 wt.% excess AlF_3 in cryolite causes a reduction from 23 to 20.5 mm) throws doubt on the accuracy of the measurements of Stokes and Frank, which have been briefly described in p. 42.

These authors attributed the discrepancy between the observed pressures and the values calculated from the dissociation (iii) using an $\alpha = 0.35$[66] to uncertainties in the thermodynamic data. However if this were so, the error in $\Delta G°$ for the reaction

$$Al + 6NaF = Na_3AlF_6 + 3Na \quad \ldots \quad \ldots \quad \ldots \quad 4.3(viii)$$

would be 9.5 kcal which, in view of the good agreement between recent heat of formation data (Appendix A) is unreasonable. It is more likely that the degree of dissociation (0.35) is exaggerated and that the

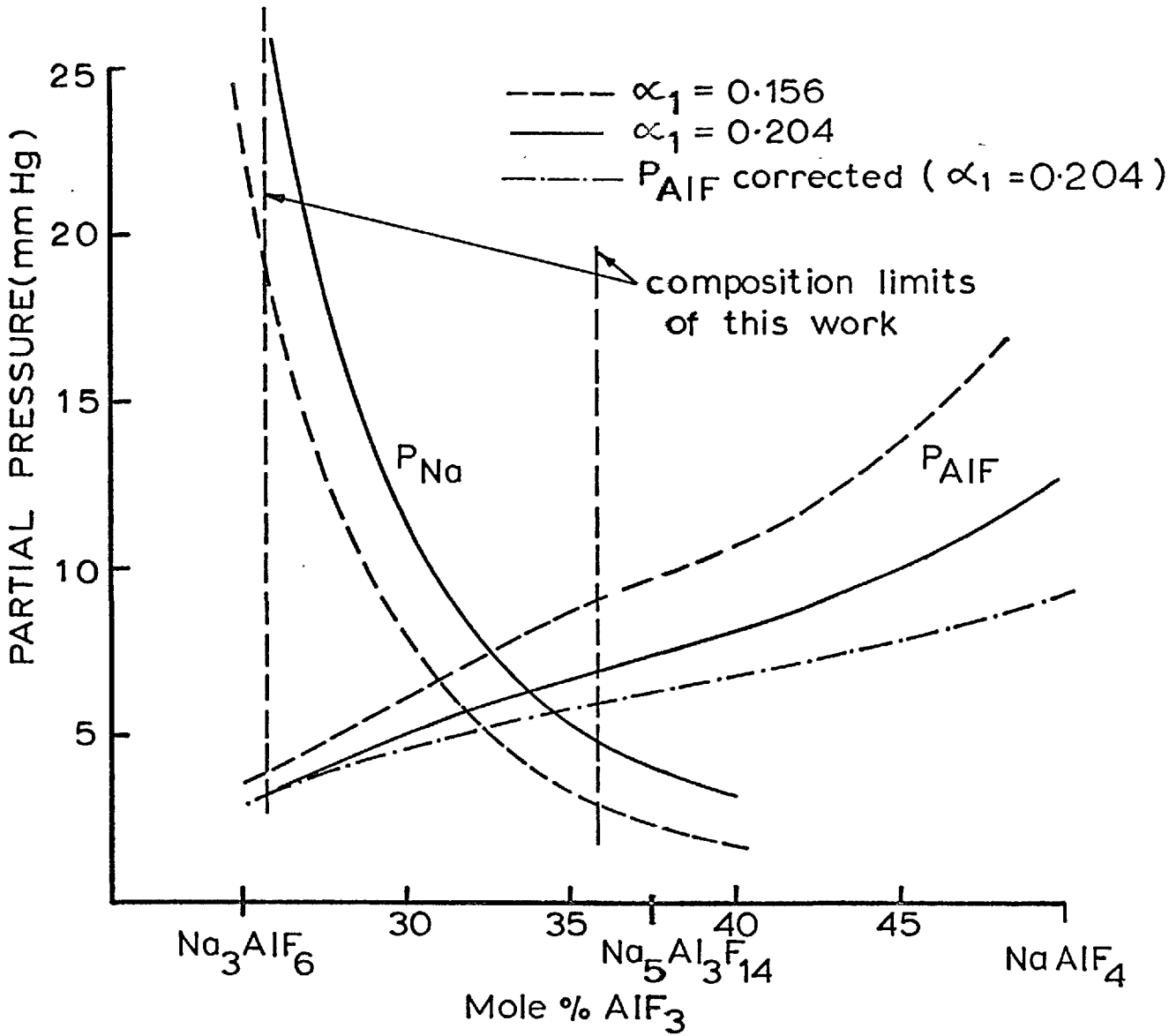

FIG. 20 P_{Na} AND P_{AlF_3} (mm Hg) AS A FUNCTION OF MELT COMPOSITION

measured pressures are low.

Escape of sodium gas at 1100°C (the reported pressure was 74.5 mm Hg) from the open-ended graphite cell would have been appreciable, and significant changes in composition would have occurred by the time the temperature of the system had been reduced to the melting point of cryolite. Since there is no solid solubility of AlF_3 in cryolite, the pure compound would crystallise as the liquidus temperature was reached, leaving a liquid phase which would become increasingly enriched in AlF_3 as the temperature continued to fall (figure 3 p. 26). The measured pressures below the melting point would therefore apply to AlF_3 rich melts and not pure solid cryolite

[the sodium partial pressure in equilibrium with pure solid cryolite and aluminium fluoride at 1009°C (reaction 4.3(i) is 0.28 mm Hg].

The low pressures recorded below 800°C, when the amount of liquid present was small, could have been due in part to non-attainment of equilibrium and in part to the change in liquid composition (figure 5 p. 43).

Although the authors stated that the change in composition was negligibly small, this would not be unexpected since the solidified contents of the cell

would have consisted mainly of pure cryolite and a small amount of a peritectic mixture of cryolite and chiolite.

For this reason the sodium and aluminium sub-fluoride pressures have been replotted using Rolin's α_1 of 0.204 (figure 20). The respective partial pressures of Na and AlF at the cryolite composition are then 35 and 2.9 mm, which are probably nearer the equilibrium pressures than those measured by Stokes and Frank.

It is now possible, by making certain assumptions, to interpret the results of this investigation in which no composition dependence of the solubility was detected, in terms of the equilibria 4.2(i) and 4.2(ii).

4.3.3 Dissolution through an Na-NaF Equilibrium

The phase diagram for the Na-NaF system has been established by Bredig and co-workers and is shown in figure 1 (page 12). At 1009°C a salt rich liquid containing 2.5 atom % Na is in equilibrium with a metal rich liquid containing 18 mol % salt. This type of diagram is invariably associated with positive deviations from Raoult's law, and thus a_{Na} is likely to be greater than 0.82 and $a_{NaF} > 0.975$. For the purpose of this discussion it is sufficient to assign

a_{Na} = 0.85 (with respect to the pure superheated liquid) and $a_{NaF} \approx 1$. The system can then be summarised by stating that a salt rich solution containing 2.5 atom % Na is in equilibrium with a metal rich solution, in which the metal activity = 0.85. As a_{Na} is also known for the molten aluminium+cryolite system (at the melting point of cryolite) it is possible to estimate a corresponding atom fraction of dissolved sodium, assuming it to be proportional to the NaF activity (which is not affected by the presence of metal). The pressure of sodium gas over the pure superheated liquid at 1009°C is 2.9 atm.,[120] and taking 35 mm as the equilibrium partial pressure of sodium over cryolite, N_{Na} = 0.00014.

The solubility at 1009°C obtained by extrapolation from the data of the present work is 0.019 wt.% Al. Assuming this metal to have originated from the quantitative displacement of equilibrium 4.2(ii) to the left on cooling, the solubility : = 0.048 wt.% Na. Expressing this figure in terms of the number of mols of solvent, N_{Na} = 0.0043, which is more than a factor of ten higher than that calculated from considerations of the Na-NaF equilibrium alone.

However, the postulated mechanisms for sodium dissolutions in sodium halides involve an interaction between the metal atoms and the Na^+ cations. In both

sodium fluoride and cryolite this cationic fraction is unity. Expression of the magnitude of solubility would thus have a better theoretical basis in terms of the cation activity rather than the activity of NaF. The expected atom fraction of sodium in the salt phase would then be 0.00048. Again this estimate may be misleading since the activity of Na^+ in an Na^+ F^- melt with respect to the activity of Na^+ in an Na^+-AlF_6^{3-} or Na^+-AlF_6^{3-}-AlF_4^- melt would not be unity. The presence of the AlF_6^{3-} anion might allow a greater number of Na° - Na^+ interactions and thus enhance the solubility of metal. This process has a parallel in the depression of the solubility of cadmium in $CdCl_2$ by $CeCl_3$ (Chapter 1 p. 24) in which the molar ratio of cadmium to cadmium chloride actually increases on addition of the second cation. This was related by Ukshe[36] to the polarising powers of the cations. Here, because of the highly polarisible nature of the AlF_6^{3-} anion, addition of cryolite to sodium fluoride might cause an overall increase in the metal solubility (assuming that the sodium partial pressure was maintained below that capable of displacing aluminium metal as a separate phase).

However it is unlikely that a sodium-sodium fluoride equilibrium accounts for the major part of

metal dissolution, since this would involve a high composition dependence which was not observed in this work. On the other hand, in a system of aluminium+ cryolite containing a 10 wt.% excess NaF, the equilibrium sodium partial pressure, 210 mm Hg, corresponds to an N_{Na} of 0.0029 which is of the same order of magnitude as the calculated figure.

4.3.4 Dissolution through an Al-AlF_3 Equilibrium

Since no measurements have been made on this system, and because the condensed sub-fluoride is unknown, the magnitude of aluminium solubility by a mechanism involving sub-compound formation can be estimated with even less certainty.

The method adopted was to calculate a lattice energy of the hypothetical ionic solid AlF and then by means of the Born-Haber thermochemical cycle to derive its standard heat of formation. The heat of sublimation can be estimated subtracting this value from ΔH°_{f298} AlF(gas) of - 62.5 kcal. By assigning an entropy of sublimation of 27 eu, the sublimation point can be determined, and from it the temperature relationship of the vapour pressure of the solid. Neglecting the error involved in considering the liquid to be the same as the solid, and by making the final assumption that

AlF is dissolved ideally in molten cryolite, so that N_{AlF} is equal to $\frac{P_{AlF}}{P^{\circ}_{AlF}}$ where P° is the vapour pressure of the pure liquid, the magnitude of the solubility can be obtained.

The lattice energy is given by the expression

$$U = \frac{N.A.e^2}{r_o} (1 - \frac{1}{n})$$

where n is the repulsion exponent, r_o the shortest distance between the centres of the ions, and A the Madelung constant. The ions are assumed to be point charges at the lattice positions with values + e and - e, where e is the electronic charge.

Ukshe[36] calculated U to be - 187.7 kcal. However this value is much too small, since the cationic radius (Al^+) was taken to be equal to that of the Na atom, 1.60Å. Furthermore the reported $\Delta H^{\circ}_{f298}{}^{AlF}{}_{(c)}$ of - 34 kcal is less negative than the corresponding heat for the gas. The value of U can thus be discounted.

Irmann[125] estimated the Al^+ radius to be 0.75Å from the ratio of the radii Na^+ and Na, and calculated the lattice energy to be - 247 kcal. It was assumed that the crystal structure was the same as that of NaCl and therefore that the Madelung constant was 1.748. A correction of +4 kcal was made by comparing

measured and calculated lattice energies of the alkali metal fluorides.

The heat of formation of the solid was found to be - 103 kcal from the expression

$$\Delta H = U - \tfrac{1}{2}D + E - S - I$$

where D, E, S and I are respectively the dissociation energy of fluorine (46 kcal), electron affinity of fluorine (98 kcal), sublimation energy of aluminium (75 kcal) and first ionization potential for aluminium (140 kcal). This figure is probably only accurate to $\pm$ 10 kcal but makes sense chemically. It is sufficiently small to explain the spontaneous disproportionation to AlF_3 and Al, and yet large enough to give a heat of sublimation of 40 kcal, corresponding to a sublimation point of 1480°K. Accepting this temperature as reasonable, the vapour pressure of the pure solid at 1282°K would be 92 mm Hg, which gives N_{AlF} in pure cryolite as 0.03. This figure is compatible with the fact that the vapour pressure of Al over a mixture of Al and AlF_3 is 32.4 mm Hg at 1282°K (Table 4 p. 46) and that the standard free energy change for the reaction

$$2Al_{(l)} + AlF_{3(s)} = 3AlF \text{ (solid or liquid)}$$

calculated from $a_{AlF_3} = 7.31 \times 10^{-4}$ (in cryolite)

is + 8 kcal.

If the metal present in the solidified salt originated from displacement of equilibrium 4.2(i) to the left, the mol fraction of AlF in pure cryolite at 1009° would be 0.0002.

Reversing the procedure, a value of 95 kcal for $\Delta H^{\circ}_{f298}{}^{AlF}{}_{(s)}$ is derived from this solubility figure which again is compatible with the chemistry of the $Al+AlF_3$ system.

Summary

Of the two mechanisms of solubility it therefore seems more probably that reaction 4.2(i) is of greater significance at the cryolite composition.

However, the total solubility in terms of the contributions from the two equilibria 4.2(i) and 4.2(ii) would be expected to change from x+y to 1.9x+0.14y over the composition range of this work. To interpret the results obtained, it is thus necessary to assume that both equilibria are of approximately equal importance at the cryolite composition, and therefore that the influence of the sodium-sodium fluoride mechanism is greater than indicated from a comparison with the pure Na-NaF system.

4.4 Aluminium Solubility in $NaF-AlF_3$+5% Al_2O_3 Melts

The solubility in melts containing an added 5% alumina was found to be a factor of 3.3 higher than in the pure $NaF-AlF_3$ system at 1020°C. In these melts a third mechanism of dissolution is possible, through formation of the suboxide, Al_2O, from the equilibrium

$$4Al_{(l)} + Al_2O_{3(l)} = 3Al_2O_{(l)} \quad \ldots \quad \ldots \quad \ldots \quad 4.4(i)$$

As in the case of AlF, the compound Al_2O is unstable in the condensed state and has only been reported as a gas at high temperatures. However Cochran[126] observed freezing point depressions of up to 85° when molten Al_2O_3 was cooled in the presence of aluminium, but the results were not reproducible enough to indicate the position of a liquidus curve. A very rough estimate of the stability of Al_2O (liq.) can however be made. Assuming that Al_2O_3 and Al_2O form an ideal solution and using the accepted heat of fusion of Al_2O_3 of 28.3 kcal,[97] then by making use of an equation of the type 1.5(vii) p. 29, it may be shown that a monotectic 50° below the melting point of pure Al_2O_3 would correspond to a solubility of 13 mol % Al_2O and a $\Delta G°$ for reaction 4.4(i) of +27.4 kcal at 2000°C. Assuming that $S°_{298}$ for Al_2O is roughly 16 eu which gives

a ΔS°_{298} for reaction 4.4(i) of 8 eu the value of ΔG° at 1282°K is then +35 kcal. Since the activity of alumina in the cryolite melt is about 0.3[128] the equilibrium mol fraction of Al_2O is approximately 0.007. This corresponds to an aluminium solubility of about 0.12 wt.% which is close to the experimentally observed value of 0.067 wt.% in view of the large errors in the calculation.

The enhanced dissolution of metal in the presence of alumina can thus be ascribed to equilibrium 4.4(i). The composition independence is not unexpected since the activity of alumina remains approximately constant over the composition range of the measurements (1.8 - 15.8 wt.% excess AlF_3).

4.5 Temperature Dependence of Solubility

A plot of log solubility against $\frac{1}{T}$ is shown in figure 21. The derived partial molar heats of solution are 30 and 21 kcal for pure $NaF-AlF_3$ and $NaF-AlF_3$+ 5%Al_2O_3 melts respectively. These values clearly indicate that a different mechanism of solubility must operate in the case of Al_2O_3 containing melts as outlined in the previous section.

The heats are associated with partial molar entropies of solution of 23 eu and 16 eu respectively.

FIG. 21 PARTIAL MOLAR HEAT OF SOLUTION OF ALUMINIUM IN CRYOLITE.

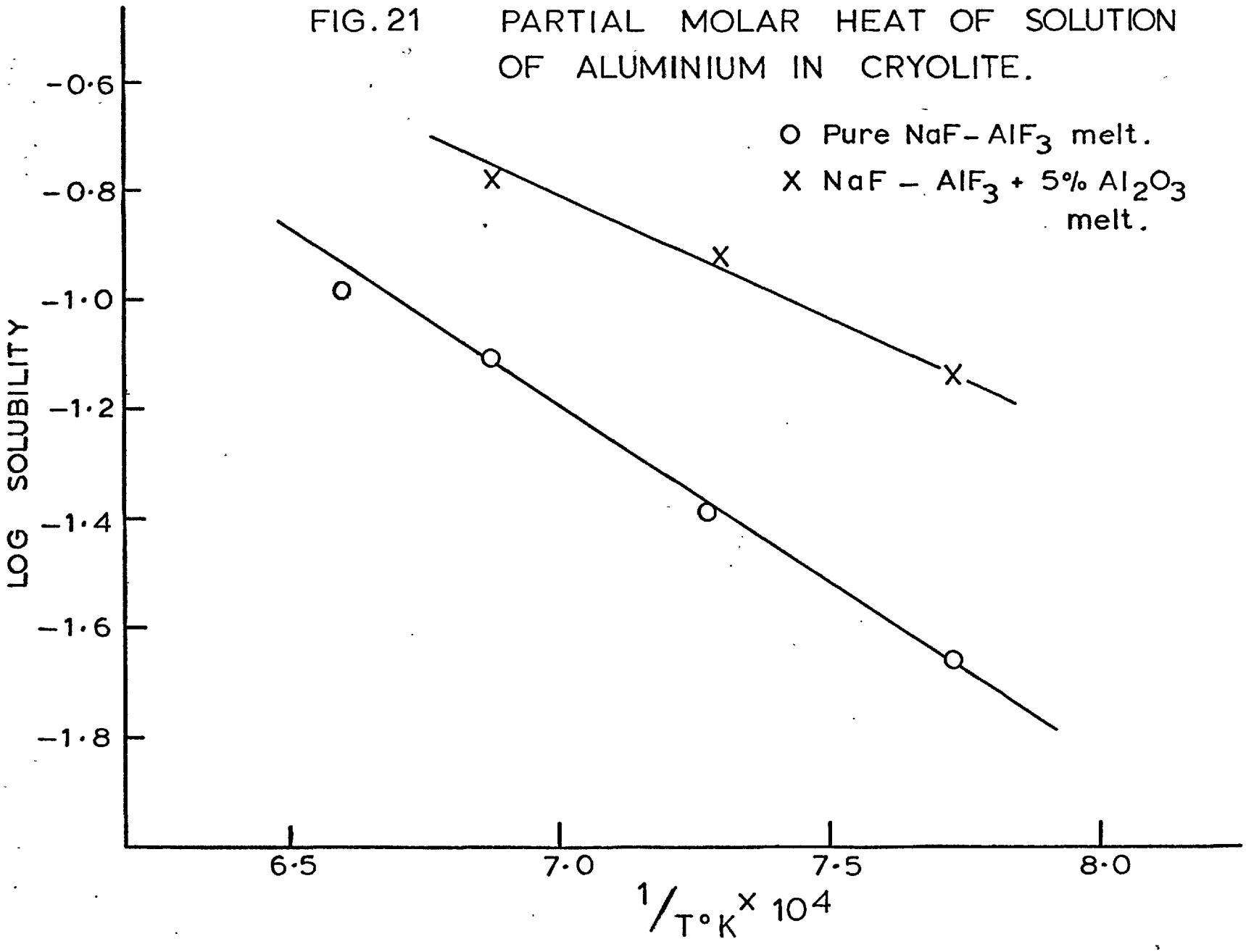

It would be of interest to make a comparison with estimates obtained by considering the mechanisms 4.2(i), 4.2(ii) and 4.4(i). Unfortunately it is not possible to do this with meaningful accuracy, but it may be noted that the entropy change for the process

$$Al_{(l)} + AlF_{3(s)} \rightarrow 3AlF \text{ (soln. N = 0.002)}$$

obtained from the thermodynamic data in Appendix A (Table III) and using an ideal partial molar entropy of solution for $AlF_{(l)}$, is approximately 20 eu.

Similarly for the process

$$4\ Al_{(l)} + Al_2O_{3(l)} = 3Al_2O \text{ (soln. N = 0.004)}$$

the partial molar entropy of solution for $Al_2O_{(l)}$ is about 22 eu.

4.6 Presence of Aluminium Carbide

4.6.1 Origin

Two possible causes of carbide formation in the molten system have been discounted in Chapter 3 p. 109 where it was concluded that carbon originated from the crucible itself.

This can only be explained in terms of a reaction involving TiC. Of the possible processes it is considered that the most likely is described by the equation

$$TiC + N_2 = 2TiN + 2C \qquad \Delta G^{\circ}_{1400^{\circ}K} = -16.8 kcal$$

Carbon could be produced by this reaction at a low partial pressure of nitrogen since complete solid solution is shown by the system TiC-TiN.(129)

Attack by aluminium can be disregarded because the standard free energy of the reaction

$$4Al + 3TiC = Al_4C_3 + 3Ti$$

is + 82.8 kcal at 1400°K.

Since the carbon would be formed in a finely divided form, the question arises as to whether the figures reported in graphs 15 and 16 represent a true solubility of Al_4C_3 or whether this is present as a fine dispersion in the melt (or bath).

4.6.2 Solubility

In view of the structure of Al_4C_3 in which the carbon exists as atoms ~~and~~ or C^{4-} ions, dissolution in a pure NaF-AlF melt would be expected to be slight. However in the presence of alumina the oxycarbides Al_4O_4C and Al_2OC can be formed,(138) which would be more likely to form stable complex ions in the fluoride melt. These compounds react with water to produce soluble alumina and a volume of methane corresponding to the stoichiometric proportion of carbide, and would therefore be indistinguishable from the pure compound in the

quenched salt.

However no detectable increase in the amount of Al_4C_3 present was observed in the 5% alumina melts (graph 15 p. 111). It is therefore considered that of the carbide present in the pure molten fluoride, the greater part was not dissolved, and also that the reported solubility in melts containing alumina is not reliable.

4.7 Considerations of Current Efficiency in the Reduction Cell

Current efficiency in the reduction cell can arise from two sources

(i) electronic conduction

and (ii) reoxidation of metal.

4.7.1 Electronic Conduction

It is evident that electronic conduction through an Na-NaF solution mechanism can contribute to current inefficiency. The fall in metal yield with rise in operating temperature is consistent with the observed positive temperature coefficient of conductance of alkali metal-alkali metal halide systems.

A current inefficiency of 10% by this means would entail increasing the specific conductance of the electrolyte from 2.5 $ohm^{-1}cm^{-1}$ at 1000°C[127] by 0.25 $ohm^{-1}cm^{-1}$. In comparison with sodium-sodium halide

systems for which data is available this would correspond to a sodium mol fraction of 0.0025. Although in the light of the foregoing discussion this magnitude of solubility could be expected in NaF enriched melts, in AlF_3 enriched electrolytes, which are commonly favoured in commercial operation it would be much lower, and electronic conduction can be discounted as a major source of current inefficiency.

4.7.2 Reoxidation of Metal

This process entails transfer of species in the electrolyte and the overall reaction may be written

$$2Al + 3CO_2 = Al_2O_3 + 3CO \quad \ldots \quad \ldots \quad \ldots \quad \ldots \quad 4.7(i)$$

The rate at which reoxidation occurs, relative to the rate of metal deposition, defines the current efficiency and thus it can be considered in terms of a rate controlling step involving (a) dissolved CO_2 or (b) dissolved metal. In the case of an unstirred melt this would be steady state diffusion, and in the presence of stirring, boundary diffusion into the bulk of the electrolyte.

4.7.3 CO_2 Dissolution as a Cause of Current Inefficiency

Haupin reported that 21 μg of CO_2 dissolved in 10 g. of molten electrolyte. However this figure

is certainly low since his technique of quenching a sample of melt to room temperature and measuring the quantity of evolved gas on reheating to 500°C would mean that most of the dissolved gas was expelled on solidification. Grjotheim et al[132] suggested that CO_2 dissolution could be a cause of current inefficiency, and as a preliminary step measured the solubility of CO_2 in molten sodium and potassium chlorides. The reported figure at 970°C in KCl was 200 times greater than that given by Haupin for the industrial fluoride electrolyte, and it was suggested that dissolution in a melt containing alumina would be even greater due to chemical interaction. However it is possible that the results are too high since a small oxygen impurity in the CO_2 could produce $NiCO_3$ in a concentration of the same order of magnitude as the observed solubility. Grimes et al[133] using a similar technique reported argon solubilities in fluoride melts a factor of 100 lower.

The importance of CO_2 as a cause of current inefficiency cannot therefore be assessed until reliable values of its solubility in cryolite-alumina melts are available.

4.7.4 Previous Mass Transfer Work

The kinetics of reaction 4.7(i) in the presence of molten cryolite were investigated independently by Revazyan[130] and Gjerstad and Welch.[131] Both workers introduced CO_2 gas by means of a refractory hood over the surface of a layer of molten cryolite covering another layer of aluminium.

Revazyan used a container of pure sintered alumina and the melts were therefore alumina saturated. The temperature was maintained at 1035°C. It was found that the amount of carbon dioxide reacted after a given period of time was independent of its flow rate and of the depth of electrolyte. A reduction in the speed of reoxidation was observed when the aluminium activity was lowered by alloying with copper. The rate of transfer of CO_2 was thus ruled out as the slow step which was considered to be the rate of metal dissolution at the metal-melt interface.

Gjerstad and Welch confirmed Revazyan's findings with regard to the CO_2 feed rate and partial pressure, and the aluminium activity; but observed a definite dependence on the depth of electrolyte. The rate of metal oxidation was reduced by a factor of three when the height of the melt layer was increased from 1 to 4 cm. A positive temperature gradient was maintained

up the crucible containing the molten system, and it was stated that mass transfer occurred by steady state diffusion. The rate of reaction for a 2 cm layer of bath was 7.6×10^{-6} mol $cm^{-2} min.^{-1}$ The experiments were performed at 980° in a boron nitride container in which the melt was initially not quite saturated with respect to alumina. When this happened a sharp falling off in oxidation rate was noted, which was attributed to a fine suspension of alumina particles near the surface of the melt.

Using the above figure for the reaction rate and the solubility of 0.056 wt.% Al extrapolated from the measurements of this work at higher temperatures, an unreasonably high diffusion coefficient of dissolved metal, $3.9 \times 10^{-3} cm^2 sec^{-1}$, is obtained, which indicates that convection currents were present in the bath. This is supported by the observed increase in reaction

rate of only a factor of four, to 33×10^{-6} mol $CO_2 cm^{-2} min^{-1}$, by deliberately reversing the thermal gradient and thereby introducing strong convection currents. Furthermore the materials were not dried and it is possible that a considerable amount of moisture was initially present. If this were so the metal "fog" reaction (oxidation of hydroxyl ions in the melt to form hydrogen bubbles) would occur for a considerable period of time (Haupin[56] reported that hydrogen evolution reached a maximum after 30 minutes using materials which were dried at 200°C for 12 hours), and could account for a certain amount of convection.

The apparent conflict on the effect of bath depth between the two workers can be resolved if it is assumed that strong convection currents existed in Revazyvan's system. This is indicated by the reaction rate of 28×10^{-6} mol CO_2 $cm^{-2} min^{-1}$, which is close to Gjerstad and Welch's figure, and by the fact that no build up of alumina at the melt surface in the alumina saturated bath was reported.

Both workers stated that the results of their laboratory investigation were applicable to the industrial cell during electrolysis. Gjerstad and Welch quoted the results of the industrial measurements of Pruvot[134] and of Nozaki[135] and Miyanchi as evidence supporting

their conclusions on the rate controlling step of metal reoxidation. Pruvot observed that the current efficiency increased as the separation of anode and cathode

increased from 1 to 4 cm. However Schmitt[137] has recently shown that the current efficiency is independent of interelectrode distance if this is between 4 and 7 cm.

Nozaki and Miyanchi analysed electrolyte layers between the anode and cathode in a reduction cell that had been suddenly closed down. It was found that the concentration of free metal near the anode was zero, but increased gradually to a maximum at the metal-bath interface. However use of this data as a basis for interpretation of mass transfer conditions during electrolysis is unjustified. On switching off the current, gas evolution would cease and CO_2 would be carried away from the furnace, thereby altering the conditions of aluminium oxidation.

It is thus concluded that the rate controlling step in the reoxidation reaction depends on the degree of stirring in the bath during electrolysis, but diffusion of metal in the boundary layer at the cathode is favoured if Schmitt's observation on the effect of interelectrode distance is valid.

4.7.5 Estimation of the Mass Transfer Coefficient for Metal Transfer to the Electrolyte

Taking a cathode current density of 1.0 amp cm^{-2}, the rate of metal deposition calculated from Faraday's law is 0.336 $g.hr^{-1}cm.^{-2}$ To account for an assumed current inefficiency of 15% entirely by metal transfer across the metal-electrolyte interface, and using the solubility value of 0.056 wt.% from this investigation, the aluminium transfer coefficient in the electrolyte would have to be 0.012 cm $sec.^{-1}$ Although the meaning of this figure is uncertain, as no values have been published for similar systems under similar conditions, it is of interest to note that values derived from the data of Revazyan and Gjerstad and Welch are 0.007 and 0.0084 respectively.

4.7.6 Effect of Electrolysis on Rate of Metal Dissolution

As the saturation solubility of aluminium in cryolite is much higher in the case of melts containing alumina, an increase in current efficiency with decrease in alumina content as electrolysis proceeds might be expected. However, this is not observed in practice, as the kinetics of the back reaction depend on the conditions in the electrolyte boundary layer at the cathode surface rather than on the equilibrium properties of the system.

Because most of the current is carried by the Na^+ cation, there will be an activity gradient of sodium ions in the region adjacent to the cathode surface. Arising from this there will be an activity gradient of alumina in the reverse direction due to the aluminium depositing from a species which diffuses into the boundary layer. The effective partial pressure of sodium generated at the interface would thus be considerably higher than the equilibrium value; consequently the rate of metal reoxidation could arise from a sodium-sodium fluoride rather than an $Al_{(l)}$-Al_2O_3 reaction, which would be expected in the absence of electrolysis.

CONCLUSIONS AND SUGGESTIONS FOR FUTURE WORK

The results of this investigation indicate that two mechanisms of aluminium dissolution in $NaF-AlF_3$ melts are possible and are of approximately equal significance at the cryolite composition. These are defined by the equilibria

$$2Al + AlF_3 = 3AlF_{(l)} \quad \ldots \quad \ldots \quad \ldots \quad (i)$$

$$Al + 3NaF = AlF_3 + 3Na_{(diss.)} \quad \ldots \quad (ii)$$

As the AlF_3 content is increased, equilibrium (ii) is displaced to the left and the contribution therefrom falls sharply. At the same time the concentration of AlF rises and the total solubility remains roughly constant until the effect of equilibrium (ii) becomes negligible, when a steady increase with further addition of AlF_3 would be expected. In NaF enriched melts on the other hand the contribution from equilibrium (ii) predominates and the solubility would be expected to rise rapidly with further increase in NaF content. The solubility thus shows a minimum in melts containing between 25 and 35 mol per cent AlF_3.

The relative effect of the equilibria does not appear to be changed significantly up to 150° above the melting point of cryolite.

In the presence of alumina a third mechanism applies - described by the following equation - which accounts for the greater solubility observed

$$4Al + Al_2O_3 = 3Al_2O_{(l)}$$

and is approximately independent of the NaF/AlF_3 mol ratio.

The amount of aluminium carbide reported in all runs including those in which graphite was added does not represent its true solubility in $NaF-AlF_3$ and $NaF-AlF_3$+5% alumina melts.

With regard to the industrial process, the observed decrease in current efficiency with increase in temperature is consistent with the positive temperature coefficient of solubility found in this work.

The balance of evidence favours diffusion of dissolved metal across the cathode boundary layer in a well stirred bath as the rate controlling step in the metal loss reaction, rather than steady state diffusion in an unstirred electrolyte or diffusion across an anode boundary layer. This involves accepting that the inter-electrode distance has no effect on the current efficiency, as was found by Schmitt.

The effect of electrolysis is to produce non-equilibrium conditions at the cathode and in view of the

activity gradients set up through the current being carried almost exclusively by the Na^+ ion, it is suggested that reaction (ii) controls the kinetics of dissolution. This is in agreement with the lower current efficiencies experienced with NaF enriched electrolytes, but assumes that current efficiency is independent of alumina concentration, which contradicts the findings of Schmitt. The actual mechanism may not therefore be as simple as that proposed, and the metal loss may be influenced by processes occurring at the anode.

In view of the evidence for the high dependence of the sodium partial pressure on composition, it would be of interest to extend aluminium solubility measurements to sodium fluoride enriched melts. A sharply increasing solubility with increase in NaF content would be expected, arising from the Na-NaF dissolution mechanism.

It would also be of interest to study the effect of alumina concentration on the solubility. If the proposed mechanism is correct, then an increase approximately proportional to $N_{Al_2O_3}^{1/3}$ would be expected.

APPENDIX A

THERMOCHEMICAL DATA

The heat of formation, heat content and entropy data for the reactions

$$Al_{(l)}+Na_3AlF_{6(s)} = 2AlF_{3(s)}+3Na_{(g)} \quad \ldots \quad \ldots \quad 1.$$

$$Al_{(l)}+3NaF_{(s,l)} = AlF_{3(s)}+3Na_{(g)} \quad \ldots \quad \ldots \quad 2.$$

and $$2Al_{(l)}+AlF_{3(s)} = 3AlF_{(g)} \quad \ldots \quad \ldots \quad 3.$$

(Tables I-III) have been taken from the J.A.N.A.F. Interim Thermochemical Tables[97] revised up to Dec. 31st 1964. From these equations thermodynamic functions for the reactions

$$AlF_{3(s)}+3NaF_{(s,l)} = Na_3AlF_{6(s)} \quad \ldots \quad \ldots \quad 4.$$

$$Al_{(l)}+6NaF_{(s,l)} = Na_3Al_{6(s)}+3Na(g) \quad \ldots \quad 5.$$

$$Al_{(l)}+3NaF_{(s,l)} = AlF_{(g)}+Na_{(g)} \quad \ldots \quad \ldots \quad 6.$$

can be derived.

A Heat of Formation Data at 298°K

1. Aluminium Trifluoride

The old value of -323 kcal[98] has long been known to be much too low, although it has still been used in some recent work.[99]

Gross, Hayman and Levi[88] found the heat of reaction

$$2Al + 3PbF_2 = 3Pb + 2AlF_3 \quad \ldots \quad \ldots \quad 7.$$

to be -237.2 kcal,[100] which gave -356.3 kcal for the standard heat of formation of AlF_3, based on a ΔH_f° PbF_2 of -158.5 kcal. This latter value was in turn based on ΔH_f° HF(g) of - 64.2 kcal[101] which has since been shown to be too low.[102] Using the value of -64.8 kcal,[97] ΔH_f° $AlF_{3(c)}$ becomes -358.1 kcal. Mashovets and Yudin,[68] from measurements of the P_{HF}/P_{H_2O} ratio over an $AlF_3 + Al_2O_3$ mixture derived -355.3 ± 0.5 kcal using old heat capacity data, which was later revised to -356.6 ± 0.5 kcal.[97] Domalski[103] determined the heat of formation directly from combination of the elements in a bomb calorimeter and reported -356.3 ± 0.3 kcal. The value used here, -358.0 ± 0.5 kcal is a weighted mean of the three independently measured figures.

2. Sodium Fluoride

Coughlin[104] studied the reaction

$$NaCl_{(l)} + HF_{(soln.)} = NaF_{(l)} + HCl_{(soln.)} \quad \ldots \quad 8.$$

and calculated -136.3 kcal for the heat of formation of NaF therefrom. Armstrong[105] subsequently reported a revision to the value of ΔH_f° HF(aq.) which was employed in the calculation and which increased the above value to

-137.1 ± 0.3 kcal. This was in excellent agreement with a value obtained from a study of the reaction[106]

$$NaOH.\infty H_2O + HF \infty H_2O = NaF.\infty H_2O + H_2O(l) \quad \ldots 9.$$

3. Cryolite

Coughlin[104] derived a $\Delta H°f$ cryolite = -784.8 kcal from measurements on the reaction

$$Al(c)+3NaCl(c)+6HF(sol^{n}\cdot) = Na_3AlF_6(c)+3HCl(sol^{n}\cdot)+\tfrac{3}{2}H_2(g) \quad \ldots 10.$$

which when corrected (as above) gave a value of -789.8 kcal. Gross Hayman and Levi[100] from the reaction

$$3PbF_2 + 6NaF + 2Al = 2Na_3AlF_6 + 3Pb \quad \ldots \quad \ldots \quad 11.$$

obtained -784.9 kcal, from which a revised heat of -789.0 kcal was calculated. Baud[107] reported ΔH°_r = -40.7 kcal for the reaction

$$Al_2F_6(c) = 2Na_3AlF_6(c) \quad \ldots \quad \ldots \quad \ldots \quad 12.$$

which corresponded to ΔH°_f cryolite = -789.7 kcal. The mean of the three determinations, -789.5 ± 1.7 kcal is the value adopted.

4. Aluminium Monofluoride

The accepted heat, -62.5 ± 1.5 kcal, is based upon the values determined by Witt and Barrow (-60.9)[108] Mashovets and Yudin (-61.2)[68] and Gross, Hayman and Levi (-61.4)[100] from vapour pressure measurements,

taking into account the revision to ΔH_f° $AlF_3(c)$.

B. Heat Capacity and Entropy Data

1. AlF_3, NaF, Na_3AlF_6

These are based on a graphical interpolation of the low temperature measurements of King[109] and the high temperature measurements of O'Brien and Kelley[60] whose data were corrected by Frank[74] (see below).

2. AlF(g)

The vibrational and rotational constants reported in a spectroscopic study by Naude and Hugo[110] were in fair agreement with those of Witt and Barrow[108] and the heat capacity data derived therefrom have been accepted.

C. Heat of Fusion of Cryolite

Because of partial dissociation of cryolite on melting, calorimetrically determined heats of fusion include a heat of dissociation.

Two old calorimetric values 16.64 kcal[63] and 20.85 kcal[59] have since been discounted. Four recent determinations show very good agreement; O'Brien and Kelly[60] 27.64 kcal, Albright[111] 27.91 kcal, Grjotheim[61] 27.58 kcal and Rolin[64] 27.70 kcal.

However Frank[74] pointed out that the melting points of NaF and Na_3AlF_6 as reported by O'Brien and

Kelley (1012° and 1027°C respectively) were about 20° higher than other literature values, and so corrected their heat capacity measurements for an assumed 20° temperature error. The recalculated heat of fusion of cryolite was 26.71 kcal, which in view of the close agreement of the other three independently measured figures tends to throw some doubt on the validity of the method of correction.

From careful observations of the freezing point depression by various salts Rolin[64] obtained 26.6 ± 0.2 kcal.

The value adopted here, 27.7 kcal, is a mean of the four calorimetric determinations.

In Tables I-III 1009°C has been chosen as the melting point. This is 3° higher than the value accepted by Frank[74] from an assessment of the data which did not include the figure of 1010.8°C subsequently reported by Grjotheim et al.[73] The small discrepancy arising from the use of Frank's heat capacity data based on the lower melting point has been ignored.

TABLE I

$Al_{(l)} + Na_3AlF_{6(s)} = 2AlF_{3(s)} + 3Na_{(g)}$

$H_T - H_{298}$(cal.mol^{-1}) ΔH°_{r298} = +73.5 kcal ΔS°_r = 4.880 cal.deg^{-1}mol^{-1}

Temp°K	Al	Na_3AlF_6	Total	AlF_3	$2AlF_3$	Na	3Na	Total	Difference	ΔH°_r
1000	7313	47,237	54,550	16,276	32,552	29,249	87,726	120,278	65,728	139,228
1100	8013	54,478	62,491	18,740	37,480	29,739	89,217	126,697	64,206	137,706
1200	8713	62,065	70,778	21,237	42,474	30,236	90,708	133,182	62,404	135,904
1282	9287	68,585	77,872	23,317	46,634	30,644	91,932	138,566	60,694	134,194

$S_T - S_{298}$(cal.deg^{-1}mol^{-1}) ΔS°_r

1000	10.734	78.021	88.755	27.285	54.570	30.430	91.290	145.860	57.105	61.985
1100	11.403	84.920	96.323	29.634	59.268	30.904	92.712	151.980	55.657	60.537
1200	12.012	91.519	103.531	31.807	63.614	31.336	94.008	157.622	54.091	58.971
1282	12.460	96.789	109.249	33.447	66.894	31.655	94.965	161.859	52.610	57.490

TABLE II

$Al_{(l)} + 3NaF_{(s,l)} = AlF_{3(s)} + 3Na_{(g)}$

$H_T - H_{298}$(cal.mol^{-1}) $\quad \Delta H^\circ_{r298^\circ} = +53.3$ kcal $\quad \Delta S^\circ_{r298} = 9.219$ cal.deg^{-1}mol^{-1}

Temp°K	Al	NaF	3NaF	Total	AlF_3	Na	3Na	Total	Difference	ΔH°_r
1000	7313	9220	27,660	34,973	16,276	29,242	87,726	104,002	69,029	122,329
1100	8013	10,733	32,199	40.212	17,740	29,739	89,217	107,957	67,745	121,045
1200	8713	12,296	36,888	45,601	21,237	30,236	90,708	111,945	66,344	119,644
1282	9287	21,543	64,629	73,916	23,317	30,644	91,932	115,249	41,333	94,633
1300	9413	21,847	65,541	74,954	23,767	30,732	92,196	115,963	41,009	94,309
1400	10,113	23,534	70,602	80,715	26,329	31,230	93,690	120,019	39,304	92,604
1500	10,813	25,220	75,660	86,473	28,924	31,726	95,178	124,102	37,629	90,929

$S_T - S_{298}$(cal.deg^{-1}mol^{-1}) $\quad \Delta S^\circ_r$

1000	10.734	15.473	46.419	57.153	27.285	30.430	91.290	118.575	61.422	70.641
1100	11.403	16.915	50.745	62.148	29.634	30.904	92.712	122.346	60.198	69.417
1200	12.012	18.275	54.825	66.837	31.807	31.336	94.008	125.815	58.978	68.197
1282	12.460	26.000	76.800	89.260	33.447	31.655	94.965	128.412	39.152	48.371
1300	12.573	25.839	77.517	90.090	33.831	31.734	95.202	129.033	38.943	48.162
1400	13.091	27.089	81.267	94.350	35.730	32.102	96.306	132.036	37.678	46.897
1500	13.574	28.253	84.759	98.333	37.520	32.444	97.332	134.852	36,519	45.738

TABLE III

$2Al_{(l)} + AlF_{3(s)} = 3AlF_{(g)}$

$H_T - H_{298}$(cal. mol^{-1}) $\quad \Delta H^\circ_{r298^\circ} = +172.9$ kcal $\quad \Delta S^\circ_{r298^\circ} = 124.776$ cal.$deg^{-1}mol^{-1}$

Temp°K	Al	2Al	AlF_3	Total	AlF	3AlF	Difference	ΔH°_r
1000	7313	14,626	16,276	30,902	5,932	17,796	13,106	159,794
1100	8013	16,026	18,740	34,766	6,817	20,451	14,315	158,585
1200	8713	17,426	21,237	38,663	7,706	23,118	15,545	157,355
1282	9287	18,574	23,317	41,891	8,436	25,308	16,583	156,317
1300	9413	18,826	23,767	42,593	8,598	25,794	16,799	156,101
1400	10,113	20,226	26,329	46,555	9,492	28,476	18,079	154,821
1500	10,813	21,626	28,924	50,550	10,390	31,170	19,380	153,520
$S_T - S_{298}$(cal.$deg^{-1}mol^{-1}$)								ΔS°_r
1000	10.734	21.468	27.285	48.753	10.087	30.261	18.492	106.284
1100	11.403	22.806	29.634	52.440	10.931	32.793	19.647	105.129
1200	12.012	24.024	31.807	55.831	11.704	35.112	20.719	104.057
1282	12.460	24.920	33.447	58.367	12.274	36.822	21.545	103.231
1300	12.573	25.146	33.831	58.977	12.418	37.254	21.723	103.053
1400	13.091	26.182	35.730	61.912	13.081	39.243	22.669	102.107
1500	13.574	27.148	37.520	64.668	13.700	41.100	23.568	101.208

APPENDIX B

CALCULATION OF SOLUBILITY VALUES FROM GAS ANALYSIS

1. ALUMINIUM

The aluminium solubility in weight % was calculated from the expression

$$\frac{V_T.1.8}{22.4.W}$$

where W = weight of sample (g.)

and $V_T = V_o + V_s$

= ml of hydrogen evolved + ml of hydrogen dissolved at N.T.P.

$$= \frac{P_{H_2}.L.A.(P_o-P_1).273}{760.T_r.y} + \frac{P_{H_2}.v.0.0179.273}{T}$$

where L = distance of travel of bead (cm)

A = mean cross sectional area of capillary (cm^2)

P_o = atmospheric pressure in mm Hg

P_1 = vapour pressure of N HCl solution at 25°C

= 22.7 mm Hg

T_r = room temperature (°K)

y = % of H_2+CH_4 in analysed gas

P_{H_2} = per cent hydrogen in the analysed gas

v = volume of acid solution in flask

= 50 ml

0.0179 = solubility (Ostwald expression) of hydrogen in N HCl solution at 25°C

and T = temperature of thermostat

= 25°C

2. ALUMINIUM CARBIDE

The aluminium carbide solubility in weight % was calculated from the expression

$$\frac{V_T \cdot 4.8}{22.4 \cdot W}$$

where $V_T = V_o + V_s$

= ml of methane evolved + ml of methane dissolved at N.T.P.

$$= \frac{P_{CH_4} \cdot L.A.(P_o - P_1).273}{760.T_r.y} + \frac{P_{CH_4} \cdot v.0.032.273}{T}$$

where P_{CH_4} = per cent methane in analysed gas

0.032 = methane solubility (Ostwald expression) in N HCl at 25°C

3. WEIGHT LOSS - COMPOSITION CHANGE RELATIONSHIP

The sodium vaporisation line (figure 18 p. 120) was calculated from the expression

$$W = \frac{23w(y_2 - y_1)}{9 + 14y_2}$$

which was derived from the stoichiometry of the reaction

$$Al + 3NaF = AlF_3 + 3Na$$

where W = weight loss of sodium

w = initial weight of salt (3.8 g.)

y_1 = initial Al percent of salt

y_2 = final Al percent of salt

The points on the graph were taken from runs in Tables P11 and P12 and I-III (this Appendix). In the former, the correction for carbide reporting as fluoride was calculated from the total gas evolved and the metal solubilities shown in figure 14. The composition change was expressed throughout per an initial 3.8 g. of salt.

TABLE I

Aluminium and Aluminium Carbide Solubilities in $NaF-AlF_3$ Melts at 1020°C

Run No.	Time (hours)	Comp.(mol.fration AlF_3) original	Comp.(mol.fration AlF_3) final	Wt.Loss (g)	Gas Analysis %H_2	Gas Analysis %CH_4	Gas Analysis %air	Wt.Sample (g)	Total Gas Vol.(ml)	Wt.%Al	Wt.% Al_4C_3
73	1.0	0.250	0.256	0.0327	19	11	70	1.1182	1.02	0.014	0.050
74	2.0	"	0.264	0.0271	13	11	76	1.2373	2.31	0.021	0.068
75	3.0	"	0.273	0.0828	18	22	60	1.1023	1.49	0.018	0.12
76	5.0	"	0.273	0.0475	12	22	66	1.1977	2.84	0.026	0.16
77	15.2	"	0.293	0.1203	14	30	56	0.9856	2.07	0.027	0.22
78	20.0	"	0.309	0.1750				1.0301			0.48†
79	20.2	"	0.283	-				1.0672			0.40†
80	24.9	"	0.338	0.2708	8	41	51	1.0810	2.28	0.015	0.29
81	44.2	"	0.346	0.3177	9	67	24	1.0101	2.46	0.018	0.53
82	45.0	"	0.390	0.3819				0.9929			0.40†
83*	2.0	"	0.263	0.0777				1.3213			0.41†
84*	2.0	"	0.260	0.0314				1.0909			0.13†
85*	9.7	"	0.295	0.1144	5	58	37	0.9454	2.97	0.017	0.56
86*	20.0	"	0.287	0.1053	7	63	30	1.0943	3.15	0.021	0.63
87*	20.0	"	0.299	0.1496	6	70	24	0.9468	3.76	0.022	0.78
88*	40.0	"	0.351	0.3590	9	69	22	0.9112	4.13	0.024	0.85

*graphite added

†estimated from gas evolved

TABLE II

Aluminium and Aluminium Carbide Solubilities in $NaF-AlF_3$ Melts

1100°C

Run No.	Time (hours)	Comp.mol fraction AlF_3		Wt.Loss (g.)	Gas Analysis			Wt.Sample (g.)	Total Gas vol (ml)	Wt.%Al	Wt.% Al_4C_3
		original	final		$\%H_2$	$\%CH_4$	%air				
89	1.0	0.273	0.278	0.1930	19	22	59	0.5401	1.49	0.044	0.11
90	2.0	0.266	0.273	0.0339	16	21	63	0.8795	3.02	0.038	0.18
91	3.7	0.250	0.261	0.0167	15	23	62	0.8437	2.71	0.033	0.19
92	15.0	0.332	0.346	0.2094	18	33	49	0.5411	1.90	0.047	0.42
93	26.0	0.250	0.288	0.1970	14	31	55	0.4521	1.65	0.038	0.44
94	28.0	0.206	0.280	0.3017	26	47	27	0.9810	3.02	0.046	0.39

1180°C

95*	2.0	0.250	0.266	0.0386	16	64	20	1.2312	5.69	0.063	0.74
96	2.0	"	0.261	0.0165	30	30	40	1.1043	3.46	0.079	0.27
97	11.1	"	0.271	0.1050	18	40	42	0.9411	4.09	0.069	0.47
98	12.0	"	0.283	0.0761	30	50	20	0.9033	2.07	0.072	0.40
99	20.0	"	0.309	0.2385	12	48	40	0.9820	5.99	0.065	0.73
100	20.2	"	0.283	0.1335	15	57	28	1.0229	4.64	0.060	0.68
101	20.7	"	0.366	0.5035	9	32	59	0.7603	8.10	0.078	0.80
102*	21.0	"	0.337	0.2632	10	76	14	1.0281	5.57	0.072	1.08
103*	41.1	"	0.337	0.2852	16	69	15	1.0780	6.98	0.082	1.10

TABLE III

Aluminium and Aluminium Carbide Solubilities in $NaF-AlF_3+5\%Al_2O_3$ Melts

Run No.	Time (hours)	Comp.mol fraction AlF_3 original	Comp.mol fraction AlF_3 final	Wt.Loss (g.)	Gas Analysis %H_2	Gas Analysis %CH_4	Gas Analysis %air	Wt.Sample (g.)	Total Gas vol (ml)	Wt.%Al	Wt.% Al_4C_3
1020°											
107*	2.0	0.250	0.260	neg.	24	52	24	1.1810	4.59	0.084	0.55
108*	2.0	"	0.258	-	20	50	30	1.0400	4.22	0.072	0.55
109*	10.0	"	0.283	-	16	46	38	0.8636	4.34	0.070	0.62
110*	17.1	"	0.292	0.0957	16	52	32	0.8472	4.32	0.070	0.71
111*	19.0	"	0.288	0.0924	12	48	40	1.0672	6.62	0.063	0.68
112*	22.1	"	0.309	0.0933	15	60	25	1.1717	7.17	0.075	0.88
113*	32.0	"	0.313	0.1617	13	53	34	0.9080	5.40	0.065	0.80
114*	42.0	"	0.329	0.1994	14	61	25	0.8769	5.20	0.072	0.90
1100°											
115*	2.0	"	0.268	0.0154	29	48	23	1.1073	5.88	0.129	0.55
116*	2.0	"	0.260	0.0064	25	45	30	1.0318	5.30	0.114	0.59
1180°											
117*	2.0	"	0.273	0.0801	34	36	30	1.1049	5.93	0.172	0.59
118*	2.0	"	0.269	0.0625	27	38	35	1.0715	7.40	0.165	0.63
1240° (no alumina)											
104*	1.5	"	0.282	0.1382	23	55	22	1.0372	6.17	0.118	0.81
105	21.2	"	0.299	0.2267	18	47	35	0.8850	6.01	0.104	0.79
106	31.0	"	0.315	0.2936	19	54	27	1.1258	6.82	0.098	0.79

ACKNOWLEDGMENTS

The author is indebted to the British Aluminium Company for sponsoring this research, to Professor F.D. Richardson for the provision of laboratory facilities, and to the Department of Scientific and Industrial Research for its award of a NATO Science Studentship.

In particular, he wishes to express his gratitude to his supervisor, Dr. J.W. Tomlinson, for his interest, guidance and encouragement throughout the course of this work.

Thanks are also due to Dr. P.S. Rogers for his useful criticisms and suggestions in connection with this thesis, and to Mr. P.F. Hart for checking parts of the manuscript.

In addition the author acknowledges his debt to the late Dr. T.G. Pearson, to Dr. C.E. Ransley and to Mr. J. Waddington of the British Aluminium Company, for making available company facilities without which this work would not have been possible. In this connection his thanks go to Mr. D. Ball of the Research Laboratories, Chalfont Park for supplying the titanium diboride crucibles and Mr. R. Smart of the Electrochemical Research Group, Kinlochleven, for performing some of the chemical analyses.

Finally the author thanks his colleagues in the Nuffield Research Group for many valuable discussions, and the permanent laboratory staff for their co-operation.

J. D. Uher

Royal School of Mines,
London, S.W.7.

REFERENCES

1. Smart R. "Extractive Metallurgy of Aluminium" Vol. 2, Ed. Gerard G., Interscience, New York (1963)
2. Hiraoko T. et al. ibid.
3. Beletskii M., Mashovets V.P. Tsvetn. Metal., 28 (1955) 51
4. Pearson T.G., Waddington J. Disc. Faraday Soc. 1 (1947) 307
5. Beck T.R. J. Electrochem. Soc. 106 (1959) 710
6. Hamlin J.D., Richards N.E. "Extractive Metallurgy of Aluminium" Vol. 2 Ed. Gerard G. Interscience New York (1963)
7. Pearson T.G. "Chemical Background of the Aluminium Industry" Roy. Inst. Chem. Lect. Mons. Repts., No. 3 (1955)
8. Grjotheim K. "Contribution to the Theory of Aluminium Electrolysis" Kgl. Norske Videnskabers Selskabs Skrifter No. 5 (1956)
9. Førland T., Storegraven H., Urnes S. Alluminio 22 (1953) 631
10. Mellors G.W., Senderoff S., J. Phys. Chem. 63 (1959) 1111
11. Bredig M.A., Johnson J.W., Smith W.T. J.A.C.S. 77 (1955) 307
12. Bredig M.A., Bronstein H.R. J. Phys. Chem. 64 (1960) 64
13. Bredig M.A., Bronstein H.R., Smith W.T. J.A.C.S. 77 (1955) 1454
14. Johnson J.W., Bredig M.A. J.Phys. Chem. 62 (1958) 604
15. Bredig M.A., Johnson J.W., J. Phys. Chem. 64 (1960)1899

16. Schäfer H., Niklas A. Angew. Chem. 64 (1952) 611

17. Rogers P.S., Tomlinson J.W., Richardson F.D. "Physical Chemistry of Process Metallurgy" Part 2 Interscience New York (1961)

18. Staffanson L.I. Ph.D. Thesis, Imperial College, London (1960)

19. Topol L.E., Landis A.L., J.A.C.S. 82 (1960) 6291

20. Grjotheim K.B. Grönvold F., Krogh-Moe J. J.A.C.S. 77 (1955) 5824

21. Hedger R.E., Terrey H. Trans. Faraday Soc. 32 (1936) 1614

22. Yosim S.J., Darnell A.J., Gehman W.G., Mayer S.W., J. Phys. Chem. 63 (1959) 230

23. Yosim S.J., Ranson L.D., Sallach R.W., Topol L.E. J. Phys. Chem. 66 (1962) 28

24. Corbett J.D., von Winbush S. J.A.C.S. 77 (1955) 3964

25. Yosim S.J., Mayer S.W., J. Phys. Chem. 64 (1960) 909

26. Bredig M.A. "Molten Salt Chemistry" ed. Blander M. Interscience New York (1964)

27. Corbett J.D. "Fused Salts" ed. Sundheim B.R. McGraw-Hill New York (1964)

28. Bronstein H.R., Dworkin A.S., Bredig M.A. J. Phys. Chem. 66 (1962) 44

29. Corbett J.D., von Winbush S., Albers F.C. J.A.C.S. 79 (1957) 3020

30. Keneshea F.J. jr., Cubicciotti D., J. Chem Eng. Data 6 (1961) 507

31. Foster L.M., Russel A.S., Cochran C.N. J.A.C.S. 72 (1950) 2596

32. Bell M.C.E., Ph.D. Thesis, University of Toronto (1964)

33. Druding L.F., Corbett J.D. J.A.C.S. 83 (1961) 2462

34. Bronstein H.R., Bredig M.A. J.A.C.S. 80 (1958) 2077

35. Cubicciotti D. J.A.C.S. 74 (1952) 1198

36. Ukshe E.A. Bukun N.G. Uspekii Khim. 30 (1961) 248

37. Cubicciotti D., Cleary G. J.A.C.S. 74 (1952) 557

38. Corbett J.D., Druding L.F., Burkhard W.J., Lindahl C.B. Disc. Faraday Soc. 32 (1961) 79

39. Farquharson J., Heymann E. Trans Faraday Soc. 31 (1935) 1004

40. Nachtrieb N.H. J. Phys. Chem. 66 (1962) 1163

41. Rolin M. Bull. Soc. Chim. France (1960) 671

42. Phillips N.W.F., Singleton R.H., Hollingshead E.A. J. Electrochem. Soc. 102 (1955) 690

43. Peterson D.T., Hinkebein J.A. J. Phys. Chem. 63 (1959) 1360

44. Frank W.B., Foster L.M. J. Phys. Chem. 61 (1957) 1531

45. Bell M.C. Ph.D. Thesis University of Toronto (1964)

46. Phillips N.W.F., Singleton R.H., Hollingshead E.A. J. Electrochem. Soc. 102 (1955) 648

47. Weill D.F., Fyffe W.S. J. Electrochem. Soc. 111 (1964) 582

48. Rolin M. Bull. Soc. Chim. France (1960) 1201

49. Foster P.A. J. Am. Ceram. Soc. 43 (1960) 66

50. Fedotiev P.P., Iljinsky W. Z. Anorg. Chem. 80 (1913) 113

51. Pruvot E. Alluminio 22 (1953)

52. Zhurin A.I. Legkie Metall. 5 (1937) 27

53. Noguchi T. J. Electrochem Assoc. Japan 15 (1947) 72

54. Abramov G.A. et al. "Theoretical Basis of Electrometallurgy of Aluminium" Moscow, 1953

55. Mashovets V.P., Svoboda R.V. Zhur. Priklad. Khim. 32 (1959) 2157

56. Haupin W.E. J. Electrochem Soc. 107 (1960) 232

57. Ferber M. Metallurgia ital 52 (1960) 510

58. Firsanova L.A., Belyaev A.I. Izv. V.U.Z. Tsvetn. Metall. 4 (1961) No. 6

59. Kelley K.K. U.S. Bureau Mines Bull. 476 (1949)

60. O'Brien C.J., Kelley K.K. J.A.C.S. 79 (1957) 5616

61. Grjotheim K. Metallurgia ital. 52 (1960) 510

62. Rolin M. Bull Soc. Chim. France (1960) 677

63. Roth W.A., Bertram W., Z Electrochem 35 (1929) 305

64. Rolin M., Bernard M. Bull Soc. Chim.France (1962) 423

65. Howard E.H. J.A.C.S. 76 (1954) 2041

66. Frank W.B., Foster L.M. J. Phys. Chem. 64 (1960) 95

67. Foster P.A., Frank W.B. J. Electrochem. Soc. 107 (1960) 997

68. Mashovets V.P., Yudin B.F. Izv. V.U.Z. Tsvetn. Metall. 5 (1962) 95

69. Treadwell W.D. Schweiz Arch. angew. Wiss. Tech. 6 (1940) 69

70. Grünert E. Z. Electrochem 48 (1942) 393

71. Boner J.E. Helv. Chim. Acta. 33 (1950) 1137

72. Rolin M. Ann Phys. Ser. 6 (1951) 970

73. Brynestad J., Grjotheim K., Grönvold F., Holm J.L., Urnes S., Disc. Faraday Soc. 32 (1961) 90

74. Frank W.B. J. Phys. Chem. 65 (1961) 2081

75. Dewing E.W. J. Electrochem. Soc. 108 (1961) 611

76. Ivanova L. Izv. V.U.Z. Tsvetn. Metall. 2 (1959) 67

77. Kostiukov A.A. Thesis, Leningrad (1949)

78. Førland T. "Fused Salts" Chapter 2 see ref. 27

79. Holm J.L., Trans. Faraday Soc. 58 (1962) 1104

80. Holm J.L., Tidsskr. Kjemi Bergvesen Met. 22 (1962) 200

81. Piontelli R., Chimica e industria 22 (1940) 501

82. Jander W., Herrmann H., Z. anorg. allgem. Chem. 239 (1938) 65

83. Ransley C.E., Neufeld H., J. Inst. Metals 78 (1950) 25

84. Grube G., Hantchmann P. "The Reactions of Al with $NaF-AlF_3$ and $NaF-AlF_3-Al_2O_3$ Systems", Kaiser Wilhelm Institut für Metallforschung, Feb. 1945

85. Stokes J.J., Frank W.B., "Extractive Metallurgy of Aluminium " Vol. 2. Ed. Gerard G. Interscience, New York (1963)

86. Makansi M., Muendel C.H., Selke W., J. Phys. Chem. 59 (1955) 40

87. Yudin B.F., Mashovets V.P., Zhur. Priklad. Khim 36 (1963) 1244

88. Gross P., Hayman C., Levi D.L., Trans. Faraday Soc. 50 (1954) 477

89. Belyaev A.I., Zhemchuzhina E.A., Izv. V.U.Z. Tsvetn. Metall. 6 (1963) 49

90. Vetyukov M.M., Trudy Leningrad Politkhn. Inst. no. 239 (1964) 39

91. Stokes J.J. private communication to Dell M.B. "Extractive Metallurgy of Aluminium" Vol. 2 p. 409 Ed. Gerard G. Interscience New York (1963)

92. Grjotheim, K., Alluminio 22 (1953) 679

93. Rogers P.S., Bevan D.J.M., Tomlinson J.W., Mikrochimica Acta (1956) 1839

94. Geffkren K., Z. physik. Chem. 49 (1904) 268

95. Moeller T., "Inorganic Chemistry" Wiley New York (1952)

96. Ransley C.E. "Extractive Metallurgy of Aluminium" Vol. II Ed. Gerard G. Interscience, New York (1963)

97. J.A.N.A.F. Interim Thermochemical Tables, Thermal Research Laboratory, Dow Chemical Corpn. Midland, Michigan

98. Glassner A., "Thermochemical Properties of Oxides, Fluorides and Chlorides to 2500°K" U.S. Atomic Energy Commission Publication ANL 5750

99. Aylen P.E.J., M.A.Sc. Thesis, University of British Columbia, 1962

100. Gross P., Hayman C., Levi D.L., "Physical Chemistry of Process Metallurgy" Part 2 Interscience, New York (1961)

101. "Selected Values of Chemical Thermodynamic Properties" National Bureau of Standards circular 500 Washington (1952)

102. Skinner H.A. I.U.P.A.C. "Thermodynamics and Thermochemistry" Symposium Lund 1963, Butterworths, London (1964)

103. Domalski E.G., Natl. Bur. Standards Report 7587 (1962)

104. Coughlin J.P., J.A.C.S. 80 (1958) 1802

105. Armstrong G. Private Communication Natl. Bur. Standards Nov. 1963

106. Vanderzee C.E., Swanson J.A., J. Phys. Chem. 67 (1963) 285

107. Baud E., Ann. Chim. Phys. 1 (1904) 8

108. Witt W.P., Barrow R.F., Trans. Faraday Soc. 55 (1959) 730

109. King E.G., J.A.C.S. 79 (1957) 2056

110. Naude S.M., Hugo T.J., Can. J. Phys. 35 (1957) 64

111. Albright D.M., Thesis, Carnegie Institute of Technology (1956)

112. Cubicciotti D.D., Cleary G., J.A.C.S. 74 (1952) 557

113. Matiasovsky K., Malinovsky M. et al. Chem. Zvesti 15 (1961) 487

114. Henry J.L., Dreisbach S.H., J.A.C.S. 81 (1959) 5274

115. "Micro-Indentation Hardness Testing" Mott B.W. Butterworths, London (1956)

116. Angell C.A., Ph.D. Thesis, Imperial College, London (1962)

117. Hilldebrand W.F. and Lundell G.E.F. "Applied Inorganic Analysis"

118. Wilder T.C., Elliott J.F., J. Electrochem Soc. (1960) 107 628

119. Thonstad J. J. Electrochem. Soc. 111 (1964) 955

120. Hultgren R. et al. "Selected Values of Thermodynamic Properties of Metals and Alloys" Wiley, New York (1963)

121. Feinleib M., Porter B., J. Electrochem. Soc. 103 (1956) 231

122. Feinleib M., Porter B., ibid 300

123. Fink W.L., Willey L.A. Stumpf H.C. Trans. AIME, 175 (1948) 364

125. Irmann F., Helvetica Chimica Acta 33 (1950) 1449

126. Cochran C.N. J.A.C.S. 77 (1955) 2190

127. Yim E.W., Feinleib M., J. Electrochem Soc. 104 (1957) 626

128. Rolin M. Ducouret A. Bull Soc. Chim. France (1964) 790

129. Schwarzkopf and Kieffer "Refractory Hard Metals" MacMillan New York (1953)

130. Revazyan A.A. Tsvetn. Metall. 33, (1960) 51

131. Gjerstad S., Welch B.J., J. Electrochem. Soc. 111 (1964) 976

132. Grjotheim K., Higgelund P., Krohn C., Acta. Chim. Scand. 16 (1962) 689

133. Blander M., Grimes W.R., Smith N.V., Watson G.M. J. Phys. Chem. 63 (1959) 1164

134. Pruvot E. Alluminio 22 (1953) 721

135. Nozaki H., Miyanchi K., J. Chem. Soc. Japan (Ind. Chem. Sec.) 51 (1948) 3

137. Schmitt H. "Extractive Metallurgy of Aluminium" Ed. Gerard G. Vol II Interscience New York (1963)

138. Cox J.H., Pidgeon L.M., Can. J. Chem. 41 (1963) 671